

Implicit Regularization of Infinitesimally-perturbed Gradient Descent Toward Low-dimensional Solutions

Jianhao Ma¹, Geyu Liang¹, Salar Fattahi^{1*}

¹Department of Industrial and Operations Engineering, University of Michigan, Ann Arbor, 48109, MI, USA.

*Corresponding author(s). E-mail(s): fattahi@umich.edu;
Contributing authors: jianhao@umich.edu; lianggy@umich.edu;

Abstract

Implicit regularization refers to the phenomenon where local search algorithms converge to low-dimensional solutions, even when such structures are neither explicitly specified nor encoded in the optimization problem. While widely observed, this phenomenon remains theoretically underexplored, particularly in modern over-parameterized problems. In this paper, we study the conditions that enable implicit regularization by investigating when gradient-based methods converge to second-order stationary points (SOSPs) within an implicit low-dimensional region of a smooth, possibly nonconvex function. We show that successful implicit regularization hinges on two key conditions: **(i)** the ability to efficiently escape strict saddle points, while **(ii)** maintaining proximity to the implicit region. Existing analyses enabling the convergence of gradient descent (GD) to SOSPs often rely on injecting large perturbations to escape strict saddle points. However, this comes at the cost of deviating from the implicit region. The central premise of this paper is that it is possible to achieve the best of both worlds: efficiently escaping strict saddle points using *infinitesimal perturbations*, while controlling deviation from the implicit region via a small *deviation rate*. We show that *infinitesimally perturbed gradient descent* (IPGD), which can be interpreted as GD with inherent “round-off errors”, can provably satisfy both conditions. We apply our framework to the problem of over-parameterized matrix sensing, where we establish formal guarantees for the implicit regularization behavior of IPGD. We further demonstrate through extensive experiments that these insights extend to a broader class of learning problems.

Keywords: Nonconvex optimization, Gradient descent, Implicit regularization

1 Introduction

Over-parameterization, where the sheer number of variables surpasses what is essential for identifying the optimal solution, is a ubiquitous phenomenon in contemporary optimization problems in machine learning (ML). In the face of over-parameterization, gradient descent (GD) or its variants may encounter significant statistical gaps as they become prone to *overfitting*. However, recent research has postulated that these algorithms exhibit an *implicit regularization* in a wide range of optimization problems—spanning from the classical sparse recovery problem [1–4] to low-rank matrix and tensor optimization [5–9] to modern neural network training [10–15]—favoring solutions with *low dimensionality*, even when such low-dimensional structures are neither explicitly characterized nor encoded in the problem formulation. This property mitigates overfitting and enhances the interpretability of the solutions. Examples of implicit regularization of GD are pervasive across a wide range of learning problems:

- **Sparse recovery:** In sparse recovery problem, the goal is to obtain a sparse parameter vector $\theta^* \in \mathbb{R}^d$ with at most $s \ll d$ nonzero entries that minimizes an empirical loss function $L(\theta)$. Recent observations have revealed that, when the unknown parameter is represented as a two-layer model $\theta = \mathbf{u} \odot \mathbf{u} - \mathbf{v} \odot \mathbf{v}$ (where the notation \odot denotes the element-wise product), GD with a small initial point applied to the lifted objective $f(\mathbf{u}, \mathbf{v}) := L(\mathbf{u} \odot \mathbf{u} - \mathbf{v} \odot \mathbf{v})$ converges to the true s -sparse parameter θ^* [1, 4], even though denser solutions may lead to the same or smaller loss values. Remarkably, this result holds even when the sparsity parameter s is entirely unknown or unspecified.¹
- **Low-rank matrix recovery:** Another class of problems for which GD exhibits a natural implicit regularization is low-rank matrix recovery. A prominent example is the matrix sensing problem, where the goal is to recover an $n \times n$ positive semi-definite (PSD) matrix \mathbf{M}^* of rank r from a limited number of Gaussian measurements by minimizing a loss function $L(\mathbf{M}^*)$. A common approach involves factorizing \mathbf{M}^* as $\mathbf{X} = \mathbf{X}\mathbf{X}^\top$ and directly optimizing the lifted loss $f(\mathbf{X}) = L(\mathbf{X}\mathbf{X}^\top)$ over the $n \times r'$ factor matrix \mathbf{X} , where $r' \geq r$. Similar to the s -sparse recovery, GD with a small initial point applied to $L(\mathbf{X}\mathbf{X}^\top)$ converges to the rank- r matrix \mathbf{M}^* , even when r is unknown and severely over-estimated, up to $r' = n$ [5, 6, 16].
- **Models with sparse basis function decomposition:** A broader class of learning problems where the implicit regularization of GD toward low-dimensional solutions is empirically observed is those with *sparse basis function decomposition*, which encompasses both the sparse recovery and low-rank matrix recovery problems discussed above, as well as tensor decomposition and various types of nonlinear neural networks [17]. Further details on these models are provided later in the paper.

Despite these intriguing and promising findings, the theoretical foundations of the implicit regularization induced by GD in over-parameterized settings remain largely underexplored and are often limited to specific, idealized scenarios. In this paper, we aim to address this gap by presenting unified conditions that enable the implicit regularization in GD, potentially extending its applicability to broader classes of over-parameterized optimization problems.

¹A similar result has been established for a slightly different model, $\theta = \mathbf{u} \odot \mathbf{v}$ [2, 3].

More concretely, we consider a twice-differentiable, potentially nonconvex function $f : \mathbb{R}^d \rightarrow \mathbb{R}$ endowed with an *implicit region* $\mathcal{M} \subset \mathbb{R}^d$, presumed to possess a *low dimension*, specifically $\dim(\mathcal{M}) = k \ll d$, capturing the reduced dimensionality of the desired solution.

While the existence of a low-dimensional implicit region can often be justified and anticipated in various learning tasks, its explicit characterization is task-dependent and typically unknown *a priori*. For example, for the aforementioned sparse recovery problem, this implicit region can be defined as $\mathcal{M} = \{(\mathbf{u}, \mathbf{v}) : \mathbf{u}_i = \mathbf{v}_i = 0 \text{ if } \theta_i^* = 0\}$ with $\dim(\mathcal{M}) = 2s$, which depends on the unknown sparsity pattern of the s -sparse solution θ^* . Similarly, for the low-rank matrix recovery problem, a possible choice of the implicit region is $\mathcal{M} = \{\mathbf{X} \in \mathbb{R}^{n \times r'} : \text{rank}(\mathbf{X}) \leq r\}$ with $\dim(\mathcal{M}) = O(dr)$, which again depends on the unknown rank r . While conventional wisdom advocates for the use of explicit regularization or constraints to promote low-dimensional structure in the solution, recent findings suggest that, in both problems, GD with a small initialization tends to remain close to these (unknown) implicit regions.

Motivated by these intriguing observations, our goal is to identify general conditions on the loss function f and the implicit region \mathcal{M} under which GD converges to a second-order stationary point (SOSP) of f within \mathcal{M} , referred to as an \mathcal{M} -SOSP and mathematically characterized as:

$$\mathbf{x} \text{ is } \mathcal{M}\text{-SOSP} \quad \Longleftrightarrow \quad \mathbf{x} \in \mathcal{M}, \nabla f(\mathbf{x}) = 0, \nabla^2 f(\mathbf{x}) \succeq 0. \quad (1)$$

Our interest in an \mathcal{M} -SOSP is motivated by the key observation that, for generic functions, any \mathcal{M} -SOSP corresponds to a local minimum of f within \mathcal{M} [18, Theorem 2.9], which, by definition of \mathcal{M} , is low-dimensional. From a learning perspective, the low-dimensional nature of the local solutions within the implicit region \mathcal{M} promotes better generalization and enhances interpretability. In contrast, local solutions outside the implicit region \mathcal{M} tend to be less interpretable and more susceptible to overfitting.

Evidently, the successful convergence of GD to \mathcal{M} -SOSPs critically depends on both the structure of the implicit region \mathcal{M} and the properties of the loss function f . In this work, we identify two key factors governing this convergence: (i) the ability to efficiently escape strict saddle points, which are points that are first-order but not second-order stationary, while (ii) maintaining proximity to the implicit region \mathcal{M} . As will be explained next, the existing analyses that enables the convergence of GD to SOSPs often rely on applying large perturbations to the iterates to ensure an efficient escape from strict saddle points, but this typically comes at the cost of significantly deviating from \mathcal{M} . The main premise of this paper is that it is possible to achieve the best of both worlds: efficiently escaping from strict saddle points via *infinitesimal perturbations*, while controlling the deviation from \mathcal{M} by quantifying the *deviation rate* of f from \mathcal{M} . We prove that the implicit regularization of GD toward an \mathcal{M} -SOSP is achieved when the algorithm leverages both infinitesimal perturbations and a small deviation rate.

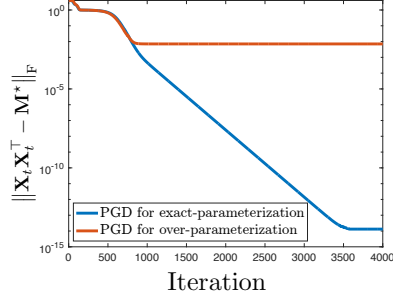


Fig. 1: PGD applied to matrix sensing converges at a linear rate under exact parameterization but fails to converge with over-parameterization. In this example, the true matrix \mathbf{M}^* is a 20×20 PSD matrix with rank $r = 3$. The search rank is set to $r' = 3$ and $r' = 4$ for exact- and over-parameterized settings.

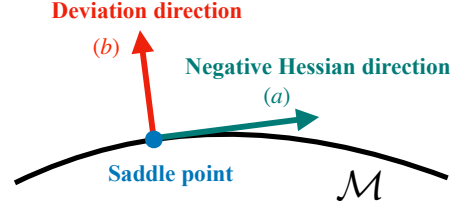


Fig. 2: When perturbation is added to the gradient, it contributes to two directions: deviation direction, which steers the iterations away from the implicit region \mathcal{M} , and the negative Hessian direction, which enables an escape from strict saddle points.

1.1 A Major Theoretical Hurdle in Over-parameterized Regime

It has been shown that various gradient-based algorithms—such as *perturbed gradient descent* (PGD) [19, 20] and *stochastic gradient descent* (SGD) [21]—can escape strict saddle points and converge to an approximate SOSP as effectively as their second-order counterparts.

To illustrate the underlying success mechanisms of these gradient-based algorithms, let us consider PGD. Starting from an initial point \mathbf{x}_0 , PGD iteratively updates the solution using the rule $\mathbf{x}_{t+1} = \mathbf{x}_t - \eta \nabla f(\mathbf{x}_t) + \boldsymbol{\xi}_t$, where $\boldsymbol{\xi}_t$ represents an isotropic perturbation uniformly drawn from the Euclidean ball with radius γ centered at zero, $\mathbb{B}(\gamma)$, when $\|\nabla f(\mathbf{x}_t)\|$ is sufficiently small; otherwise, $\boldsymbol{\xi}_t$ is set to zero [20, Algorithm 1]. The reasoning behind this episodal perturbation is natural: when $\|\nabla f(\mathbf{x}_t)\|$ is small, the iterate \mathbf{x}_t is either near a strict saddle point or an SOSP. Unlike SOSPs, strict saddle points are *unstable* fixed points of GD [22, Theorem III.7]. Consequently, an isotropic random perturbation of sufficient magnitude enables GD to escape from these strict saddle points efficiently [20, Theorem 3]. We note that a similar argument applies to a non-periodic variant of PGD [23, Theorem 4.1], and SGD under the *dispersive noise assumption* for the gradients [21, Assumption 4], as well as the earlier approaches such as *noisy stochastic GD* [19, Algorithm 1], and *saddle-normalized GD* [24, Algorithm 1]. Moreover, such additive perturbations appear necessary, as without them, vanilla GD may take exponential time to escape strict saddle points [25, Theorem 4.1].

Unfortunately, in over-parameterized settings, guaranteed escape from strict saddle points alone is insufficient to ensure convergence to an \mathcal{M} -SOSP. In fact, even a slight over-parameterization can disrupt the convergence of PGD, potentially causing it to fail. Figure 1 shows the performance of PGD on an instance of matrix sensing

(introduced in Section 1). When the rank r of the target matrix is known, PGD with a random initial point applied to $f(\mathbf{X}) = L(\mathbf{X}\mathbf{X}^\top)$ with $\mathbf{X} \in \mathbb{R}^{n \times r}$ converges to the ground truth matrix at a linear rate, without getting trapped at a strict saddle point. However, even a slight over-parameterization, with a search rank of $r' = r + 1$, causes PGD to converge to a solution with a rank strictly greater than r , thereby incurring significant errors.

The failure of PGD to converge to an \mathcal{M} -SOSP in the over-parameterized regime is precisely due to the impact of perturbations, as shown in Figure 2. When an isotropic random perturbation is applied, it inevitably affects two directions: a direction spanned by the eigenvectors corresponding to the negative eigenvalues of the Hessian, which pushes the iterate away from the strict saddle point (shown as (a)), and another direction that causes the iterate to deviate away from the implicit region \mathcal{M} (shown as (b)). When the perturbation is both isotropic and large, these directions become comparable, causing the PGD iterates to escape the saddle point but simultaneously drift away from \mathcal{M} , ultimately leading to the failure of the algorithm.

1.2 Overview of our Contributions

In this paper, our ultimate goal is to address the aforementioned failure mechanism of PGD in the over-parameterized models. At the core of our proposed framework lies a *signal-residual* decomposition: at each iteration, the current point \mathbf{x}_t is decomposed into $\mathbf{x}_t = \mathbf{x}_t^\sharp + \mathbf{x}_t^\perp$. Here, \mathbf{x}_t^\sharp represents the *signal*, defined as the projection of \mathbf{x}_t onto the implicit region \mathcal{M} . Conversely, $\mathbf{x}_t^\perp := \mathbf{x}_t - \mathbf{x}_t^\sharp$ is the *residual*. The key insight behind this decomposition is that \mathbf{x}_t^\sharp , by its definition, resides within the implicit domain \mathcal{M} . Therefore, to establish the convergence to an approximate \mathcal{M} -SOSP, it suffices to demonstrate the following: (1) the iterates \mathbf{x}_t converge to an approximate SOSP, and (2) the residual norm $\|\mathbf{x}_t^\perp\|$ remains small.

Efficient convergence to approximate SOSPs

In this work, we show that large perturbations are *unnecessary* for PGD to effectively escape strict saddle points. More specifically, we prove that, when GD encounters a strict saddle point, a single perturbation of arbitrarily small radius $\gamma > 0$, followed by $T = O(\text{poly} \log(1/\gamma))$ iterations of GD updates, escapes from this strict saddle point. This result is an improvement over the analysis of [20], revealing that the perturbation radius affects the convergence rate *only poly-logarithmically*, and hence, can be made arbitrarily small at the cost of only poly-logarithmic increase in the number of iterations (Theorem 2). More significantly, this result shows that the impact of an isotropic perturbation—necessary for efficiently escaping strict saddle points—on the residual norm $\|\mathbf{x}_t^\perp\|$ can be made arbitrarily small, effectively overcoming the fundamental bottleneck of PGD discussed earlier. We refer to this variant of GD as *infinitesimally-perturbed GD* (IPGD) (Algorithm 1).

Implicit regularization

Indeed, even if the infinitesimal perturbations of IPGD do not cause a significant increase in the residual norm $\|\mathbf{x}_t^\perp\|$, there remains the possibility that the iterates

may drift away from the implicit region during the standard GD updates, causing the residual norm $\|\mathbf{x}_t^\perp\|$ to grow. To analyze this behavior, we provide a fine-grained characterization of the dynamics of the residual norm, proving that, under reasonable assumptions, the growth or shrinkage of $\|\mathbf{x}_t^\perp\|$ is governed by a key quantity, which we call *deviation rate* (Definition 5). A positive deviation rate drives the shrinkage of the residual norm, while a negative deviation rate drives its growth (Proposition 4).

We combine this result with the saddle-escaping property of IPGD to establish its efficient convergence to an approximate SOSP within the implicit region \mathcal{M} (Theorem 5). In particular, we show that IPGD converges to an ϵ -neighborhood of an \mathcal{M} -SOSP within $\tilde{O}(1/\epsilon^2)$ iterations under three key conditions: (1) the closure of the implicit region \mathcal{M} under GD updates (Assumption 3); (2) the initial point being close to \mathcal{M} ; and (3) the deviation rate being sufficiently small. We argue that these conditions are satisfied—often provably—in a range of learning problems.

Improved convergence with additional structures

We show that the performance of IPGD can be improved (with a local refinement; see Algorithm 2) if the problem enjoys additional structures within the implicit region \mathcal{M} . First, we show that if the function satisfies the strict saddle property within \mathcal{M} (Definition 6), then convergence to an approximate \mathcal{M} -SOSP point translates into convergence to a local minimum within \mathcal{M} (Proposition 6). Additionally, if a certain regularity condition (Definition 7) holds within \mathcal{M} , the convergence rate can be improved to nearly-linear (Theorem 8). A key distinction of these results compared to the existing work is that, unlike existing work, which assumes these desirable structures hold globally, we only require them to hold within the implicit region \mathcal{M} , which is assumed to be low-dimensional. These are significantly milder conditions, as we will discuss.

Applications

We rigorously demonstrate the application of our general framework to a well-known and important learning problem: *over-parameterized matrix sensing*. This problem serves as an ideal test-bed for our approach for two key reasons. First, as discussed in Section 1.1, general-purpose saddle-escaping methods, such as PGD, are unable to converge to the true solution for this problem. Second, existing tailored analyses of GD for this problem typically involve intricate and lengthy derivations (see, e.g., [5, 6]). In contrast, we demonstrate that our proposed general conditions ensuring the near-linear convergence of IPGD can be established for this problem in a more straightforward manner, significantly simplifying the analysis while achieving near-optimal computational and sample complexities (Theorem 31).

Finally, through additional simulations, we demonstrate that the conditions required for the convergence of IPGD are satisfied across a broad range of over-parameterized problems, including sparse recovery, symmetric and asymmetric matrix completion, and symmetric and asymmetric one-bit matrix completion. Notably, we show that in practice, a perturbation radius of $\gamma = 1 \times 10^{-15}$ —which is close to the round-off error in double precision—is sufficient to ensure the efficient convergence of

IPGD. This underscores the insight that, while theoretically distinct, IPGD can be viewed as a practical implementation of GD under inexact arithmetic.

1.3 Related Work

While most results closely related to our work have already been discussed, there exists a substantial body of literature relevant to various aspects of our findings, which we review below.

Saddle-avoiding algorithms

Although second-order optimization methods—such as cubic regularization [26], trust region methods [27], and their efficient variants [28–30]—are well-known for their ability to efficiently escape saddle points, their applicability to modern large-scale optimization problems is limited by the computational burden of evaluating the full Hessian, Hessian-vector products, or suitable approximations. However, recent research has demonstrated that even first-order methods can escape saddle points under certain conditions. For instance, GD with random initialization avoids saddle points almost surely [31, 32], but it may do so in exponential time [25]. Moreover, under additional geometric assumptions—such as the invertibility of the Hessian—GD can escape strict saddle points at a linear rate [33, 34]. However, this invertibility condition is rarely satisfied in over-parameterized settings. To address this limitation, numerous GD variants have been developed with provable guarantees for efficient saddle-point escape. As discussed earlier, two such methods—perturbed GD and stochastic GD—leverage random perturbations to escape strict saddle points. In addition, more advanced techniques, such as Nesterov’s accelerated GD [35] and adaptive methods [36], achieve faster escape rates, but may still exhibit significant deviations from the implicit region in the over-parameterized settings.

Implicit regularization of local-search algorithms

As mentioned before, local-search algorithms in over-parameterized models often exhibit implicit regularization, converging to low-dimensional solutions (e.g. sparse or low-rank) despite the absence of explicit penalties. For example, training a factorized (over-parameterized) matrix model via alternating or greedy updates typically recovers a low-rank solution: it was conjectured in [37], with supporting evidence, that gradient-based optimization on a full-rank matrix factorization converges to the minimum nuclear norm (i.e., lowest-rank) solution, and it was later shown in [38] that increasing the depth of the factorization amplifies this bias toward low-rank solutions. In tandem, other work has connected this behavior to explicit algorithms: the work [39] proved that the continuous gradient flow with any commuting parametrization is equivalent to continuous mirror descent with a related Legendre function which acts as a regularizer, formalizing the intuition that such local methods perform implicit regularization on a transformed space. Coordinate descent methods likewise impart an implicit sparsity bias. Notably, in classification settings, coordinate-wise descent (analogous to a steepest descent under an ℓ_1 geometry) has been shown to converge to the maximum ℓ_1 -margin separator (the sparsest solution), whereas standard gradient descent finds the max- ℓ_2 -margin solution [40]. Across these studies, seemingly

unconstrained over-parameterized searches end up biased toward low-complexity (low-rank or sparse) solutions, a phenomenon observed empirically and proven in theory in certain applications.

However, prior analyses of implicit regularization have been largely instance-specific, limiting their applicability to broader settings. To the best of our knowledge, this work is the first to introduce a framework for studying the implicit regularization behavior of GD for general over-parameterized models.

Desirable landscape properties

In the literature, several favorable landscape properties have been identified that enable first-order methods to achieve strong convergence guarantees. A central example is the *strict saddle property*, which ensures that every saddle point possesses at least one direction of sufficiently negative curvature. This property allows common first-order methods—such as PGD [20]—not only to escape saddle points but also to converge to local minima. When combined with the *benign landscape property*, which guarantees the absence of sub-optimal local minima, this implies that any first-order method capable of escaping saddle points is ensured to converge to a global minimum.

Notably, both the strict saddle and benign landscape properties have been shown to hold in a wide range of problems, including matrix sensing and completion [41, 42], robust PCA [42], complete dictionary learning [43, 44], tensor decomposition [19], phase retrieval [45], and certain classes of neural networks [46–48]. More broadly, the strict saddle property holds generically in smooth optimization problems [18]. Specifically, for a smooth function f on \mathbb{R}^d and almost every perturbation vector $\mathbf{v} \in \mathbb{R}^d$, the perturbed function $f_{\mathbf{v}}(\mathbf{x}) = f(\mathbf{x}) - \langle \mathbf{v}, \mathbf{x} \rangle$ satisfies the strict saddle property, as guaranteed by Sard’s theorem. Additionally, many of these problems exhibit structural properties akin to local strong convexity, such as restricted strong convexity or the (α, β) -regularity condition. These properties are known to accelerate the convergence of GD, often yielding linear rates [49].

However, as we will demonstrate in this paper, assumptions such as the strict saddle property, benign landscape, or local strong convexity and regularity can be overly restrictive in over-parameterized regimes. In such settings, the presence of redundant dimensions can hinder convergence. Instead, we focus on a neighborhood of the implicit solution region, where the adverse effects of over-parameterization diminish and more favorable convergence behavior emerges.

1.4 Notations

For a twice-differentiable function $f : \mathbb{R}^d \rightarrow \mathbb{R}$, the gradient and Hessian at a point \mathbf{x} are denoted by $\nabla f(\mathbf{x})$ and $\nabla^2 f(\mathbf{x})$, respectively. For a vector \mathbf{x} , $\|\mathbf{x}\|$ denotes its usual Euclidean norm. The Euclidean distance of a vector $\mathbf{x} \in \mathbb{R}^d$ from a set $\mathcal{Y} \subseteq \mathbb{R}^d$ is denoted by $\text{dist}(\mathbf{x}, \mathcal{Y}) = \min_{\mathbf{y} \in \mathcal{Y}} \|\mathbf{x} - \mathbf{y}\|$. The projection of a vector \mathbf{x} onto a set \mathcal{Y} and its orthogonal complement are shown as $\mathcal{P}_{\mathcal{Y}}(\mathbf{x}) = \arg \min_{\mathbf{y} \in \mathcal{Y}} \|\mathbf{x} - \mathbf{y}\|$ and $\mathcal{P}_{\mathcal{Y}}^{\perp}(\mathbf{x}) = \mathbf{x} - \mathcal{P}_{\mathcal{Y}}(\mathbf{x})$, respectively². For a set $\mathcal{X} \subset \mathbb{R}^d$, its ϵ -neighborhood is defined as $\mathcal{N}_{\mathcal{X}}(\epsilon) = \{\mathbf{x} \in \mathbb{R}^d : \text{dist}(\mathbf{x}, \mathcal{X}) \leq \epsilon\}$. We also define $\mathbb{B}_{\mathbf{z}}(\xi)$ as the Euclidean ball with

²If the minimizer in $\arg \min_{\mathbf{y} \in \mathcal{Y}} \|\mathbf{x} - \mathbf{y}\|$ is not unique, we select an arbitrary one.

radius ξ centered at the point \mathbf{z} . For short, we use $\mathbb{B}(\xi) := \mathbb{B}_{\mathbf{0}}(\xi)$. Finally, $\text{Unif}(\mathbb{B}(\xi))$ denotes the uniform distribution over the Euclidean ball $\mathbb{B}(\xi)$.

For a matrix \mathbf{X} , we use $\|\mathbf{X}\|$, $\|\mathbf{X}\|_*$ and $\|\mathbf{X}\|_{\text{F}}$ to denote its operator norm, nuclear norm, and Frobenius norm, respectively. The identity matrix of size $d \times d$ is denoted as \mathbf{I}_d . The set of all $d_1 \times d_2$ orthonormal matrices with $d_1 \geq d_2$ is defined as $\mathcal{O}_{d_1 \times d_2} := \{\mathbf{O} \in \mathbb{R}^{d_1 \times d_2} : \mathbf{O}^\top \mathbf{O} = \mathbf{I}_{d_2}\}$. For two matrices $\mathbf{X}, \mathbf{Y} \in \mathbb{R}^{d_1 \times d_2}$, their Procrustes distance is defined as $\text{dist}(\mathbf{X}, \mathbf{Y}) = \min_{\mathbf{O} \in \mathcal{O}_{d_1 \times d_2}} \|\mathbf{X} - \mathbf{Y}\mathbf{O}\|_{\text{F}}$. For an arbitrary matrix \mathbf{X} , we denote $\text{col}(\mathbf{X})$ as its column space. Additionally, the projection matrix onto $\text{col}(\mathbf{X})$ is denoted as $\mathcal{P}_{\mathbf{X}} = \mathbf{X}\mathbf{X}^\dagger$, where \mathbf{X}^\dagger refers to the pseudo-inverse of \mathbf{X} .

The gradient of a scalar-valued function $f(\mathbf{X})$ with a matrix variable $\mathbf{X} \in \mathbb{R}^{d \times d}$ is an $d \times d$ matrix, whose (i, j) -th entry is $[\nabla f(\mathbf{X})]_{i,j} = \frac{\partial f(\mathbf{X})}{\partial X_{ij}}$ for $i, j \in [d]$. Alternatively, we can view the gradient as a linear operator satisfying $\nabla f(\mathbf{X})[\mathbf{Z}] = \langle \nabla f(\mathbf{X}), \mathbf{Z} \rangle = \sum_{i,j} \frac{\partial f(\mathbf{X})}{\partial X_{ij}} Z_{ij}$ for any $\mathbf{Z} \in \mathbb{R}^{d \times d}$. Similarly, the Hessian and the third-order derivative of $f(\mathbf{X})$ can be viewed as multi-linear operators defined by

$$\begin{aligned} \nabla^2 f(\mathbf{X})[\mathbf{Z}, \mathbf{W}] &= \sum_{i,j,k,l} \frac{\partial^2 f(\mathbf{X})}{\partial X_{ij} \partial X_{kl}} Z_{ij} W_{kl}, \text{ for any } \mathbf{Z}, \mathbf{W} \in \mathbb{R}^{d \times d}, \\ \nabla^3 f(\mathbf{X})[\mathbf{Z}, \mathbf{W}, \mathbf{U}] &= \sum_{i,j,k,l,m,n} \frac{\partial^3 f(\mathbf{X})}{\partial X_{ij} \partial X_{kl} \partial X_{mn}} Z_{ij} W_{kl} U_{mn}, \text{ for any } \mathbf{Z}, \mathbf{W}, \mathbf{U} \in \mathbb{R}^{d \times d}. \end{aligned} \tag{2}$$

Given $f(n)$ and $g(n)$, we write $f(n) = O(g(n))$ when there exists a universal constant $C > 0$ satisfying $f(n) \leq Cg(n)$ for all large enough n . Similarly, the notation $f(n) = \Omega(g(n))$ implies the existence of a universal constant $C > 0$ satisfying $f(n) \geq Cg(n)$ for all large enough n . Lastly, we use $f(n) = \Theta(g(n))$ if $f(n) = O(g(n))$ and $f(n) = \Omega(g(n))$. Finally, we use the symbols $\tilde{O}, \tilde{\Omega}, \tilde{\Theta}$ to hide poly-logarithmic factors.

2 Main Results

First, we present our assumptions on the gradient- and Hessian-Lipschitz continuity for the function f , which we require to hold only within a neighborhood of the implicit region \mathcal{M} .

Definition 1 ((L, \mathcal{M}, τ) -gradient-Lipschitz) The function f is **(L, \mathcal{M}, τ) -gradient-Lipschitz** if for all $\mathbf{x}, \mathbf{x}' \in \mathcal{N}_{\mathcal{M}}(\tau)$, we have $\|\nabla f(\mathbf{x}) - \nabla f(\mathbf{x}')\| \leq L \|\mathbf{x} - \mathbf{x}'\|$.

Definition 2 ($(\rho, \mathcal{M}, \tau)$ -Hessian-Lipschitz) The function f is **$(\rho, \mathcal{M}, \tau)$ -Hessian-Lipschitz** if for all $\mathbf{x}, \mathbf{x}' \in \mathcal{N}_{\mathcal{M}}(\tau)$, we have $\|\nabla^2 f(\mathbf{x}) - \nabla^2 f(\mathbf{x}')\| \leq \rho \|\mathbf{x} - \mathbf{x}'\|$.

Unlike the classical definitions of gradient- and Hessian-Lipschitz functions, which require smoothness conditions to hold globally, Definitions 1 and 2 impose these conditions only within a τ -neighborhood of the implicit region \mathcal{M} . These localized gradient- and Hessian-Lipschitz conditions are particularly advantageous when the smoothness

constants scale with the dimensionality of the problem. In such cases, the global smoothness constants scale with the ambient dimension d , while their localized counterparts depend only on $\dim(\mathcal{M}) = k$. Consequently, when the algorithm operates within the neighborhood of the implicit region, the convergence rate is determined by the local smoothness factors, resulting in a significantly faster rate compared to working over the entire space.

Recall that our goal is to identify conditions guaranteeing the efficient convergence to \mathcal{M} -SOSPs. Unfortunately, practical algorithms can only compute an *approximate* SOSP, where the stationarity conditions are satisfied within some small tolerance, as formally defined below.

Definition 3 (approximate (\mathcal{M} -)SOSP) Suppose that f is (L, \mathcal{M}, τ) -gradient-Lipschitz and $(\rho, \mathcal{M}, \tau)$ -Hessian-Lipschitz. Given a tolerance parameter $\epsilon > 0$, a point $\mathbf{x} \in \mathcal{N}_{\mathcal{M}}(\tau)$ is called **ϵ -SOSP** if $\|\nabla f(\mathbf{x})\| \leq \epsilon$ and $\nabla^2 f(\mathbf{x}) \succeq -\sqrt{\rho\epsilon} \mathbf{I}$. Additionally, \mathbf{x} is called **ϵ - \mathcal{M} -SOSP** if \mathbf{x} is ϵ -SOSP and $\mathbf{x} \in \mathcal{N}_{\mathcal{M}}(\epsilon/L)$ where $\epsilon/L \leq \tau$.

Closely related is the notion of *approximate* strict saddle points, defined as follows:

Definition 4 (Approximate strict saddle point) Given a tolerance parameter $\epsilon > 0$, a point \mathbf{x} is called **ϵ -strict saddle** if $\|\nabla f(\mathbf{x})\| \leq \epsilon$ and $\lambda_{\min}(\nabla^2 f(\mathbf{x})) < -\sqrt{\rho\epsilon}$, where $\lambda_{\min}(\cdot)$ denotes the minimum eigenvalue.

Intuitively, we say “ \mathbf{x} is an approximate SOSP” or “ \mathbf{x} is an approximate strict saddle” if \mathbf{x} is an ϵ -SOSP or ϵ -strict saddle with sufficiently a small parameter $\epsilon > 0$. An approximate \mathcal{M} -SOSP is defined analogously. Let $\mathcal{X}(\epsilon)$ and $\mathcal{X}_{\mathcal{M}}(\epsilon)$ respectively denote the set of all ϵ -SOSPs and ϵ - \mathcal{M} -SOSPs of f . Moreover, for simplicity and whenever it is clear from the context, we use \mathcal{X} and $\mathcal{X}_{\mathcal{M}}$ to denote $\mathcal{X}(0)$ and $\mathcal{X}_{\mathcal{M}}(0)$, respectively. Our goal is to recover a point from $\mathcal{X}_{\mathcal{M}}(\epsilon)$ for sufficiently small tolerance $\epsilon > 0$. By definition, these points are approximate SOSPs and lie within the proximity of the implicit region \mathcal{M} .

As previously highlighted, the concept of a *signal-residual decomposition* is central to our analysis. At each iteration t , the current point \mathbf{x}_t is decomposed as $\mathbf{x}_t = \mathbf{x}_t^{\sharp} + \mathbf{x}_t^{\perp}$, where \mathbf{x}_t^{\sharp} represents the signal, defined as $\mathbf{x}_t^{\sharp} = \mathcal{P}_{\mathcal{M}}(\mathbf{x}_t)$, and \mathbf{x}_t^{\perp} denotes the residual, defined as $\mathbf{x}_t^{\perp} = \mathcal{P}_{\mathcal{M}}^{\perp}(\mathbf{x}_t) := \mathbf{x}_t - \mathbf{x}_t^{\sharp}$. This decomposition immediately implies that \mathbf{x}_t is an ϵ - \mathcal{M} -SOSP if and only if \mathbf{x}_t is an ϵ -SOSP and that $\|\mathbf{x}_t^{\perp}\| \leq \epsilon/L$. Therefore, to ensure efficient convergence to an approximate \mathcal{M} -SOSP, it suffices to: (1) ensure that the iterates efficiently converge to an approximate SOSP; and (2) maintain a small residual norm for the iterates. The first property will be analyzed in Section 2.1, while the second will be addressed in Section 2.2.

2.1 Efficient Convergence to Approximate SOSPs

We first formalize the intuition behind the PGD algorithm discussed in Section 1.1 by stating its convergence guarantee from [20].

Theorem 1 (Theorem 3 of [20]; informal) *Suppose that f is $(L, \mathcal{M}, +\infty)$ -gradient-Lipschitz and $(\rho, \mathcal{M}, +\infty)$ -Hessian-Lipschitz with some parameters $L, \rho > 0$. Then, with an overwhelming probability, the PGD algorithm with perturbation radius $\gamma = \tilde{\Theta}(\epsilon/L)$ outputs an ϵ -SOSP within $T = \tilde{O}\left(\frac{\Delta_f}{\eta\epsilon^2}\right)$ iterations. Here, $\Delta_f = f(\mathbf{x}_0) - \min_{\mathbf{x} \in \mathbb{R}^d} f(\mathbf{x})$.*

Indeed, if PGD encounters N_T approximate strict saddle points along its trajectory, it must apply precisely N_T isotropic perturbations, each with radius γ . Intuitively, a single isotropic perturbation of an approximate strict saddle point \mathbf{x} with radius γ can increase its residual norm by $O(\gamma)$. Consequently, the final increase in the residual norm $\|\mathbf{x}_T\|$ caused by perturbations can be as large as $O(\gamma N_T)$. As shown in [20] and also demonstrated in our analysis, N_T can be as large as $O(\epsilon^{-3/2})$. Thus, if the perturbation radius is set to $\gamma = \tilde{\Theta}(\epsilon/L)$, as required by Theorem 1, the final residual norm of PGD scales as $\tilde{O}(\epsilon^{-3/2} \cdot \epsilon/L) = \tilde{O}(\epsilon^{-1/2}/L) \gg 1$. In other words, *ensuring the convergence of PGD to an approximate SOSP may inevitably lead to the divergence of the residual norm in the over-parameterized regime.*

To address this challenge, we prove that PGD can efficiently escape approximate strict saddle points using a significantly smaller perturbation radius. The detailed implementation of this variant of PGD, which we call *infinitesimally-perturbed gradient descent* (IPGD), can be found in Algorithm 1.

Algorithm 1 Infinitesimally-perturbed gradient descent (IPGD)

Input: Perturbation radius γ , tolerance parameter ϵ , stepsize η , initial point \mathbf{x}_0 , Hessian-Lipschitz parameter ρ , optimality gap Δ_f , and failure probability χ .

```

1:  $F \leftarrow \frac{1}{C} \cdot \frac{\epsilon^{3/2}}{\sqrt{\rho}(\log^3(\frac{1}{\gamma}) + \log^3(\frac{\rho d \Delta_f}{\chi \epsilon}))}$ ,  $G \leftarrow \frac{1}{C} \cdot \frac{\epsilon}{\log^2(1/\gamma)}$ ,  $T_{\text{escape}} \leftarrow$ 
    $\frac{C}{\eta\sqrt{\rho\epsilon}} \left( \log\left(\frac{1}{\gamma}\right) + \log\left(\frac{\rho d \Delta_f}{\chi \epsilon}\right) \right)$ , for a sufficiently large constant  $C > 0$ 
2:  $T_{\text{noise}} \leftarrow -T_{\text{escape}} - 1$ 
3: for  $t = 0, 1, \dots$  do
4:   if  $\|\nabla f(\mathbf{x}_t)\| \leq G$  and  $t - T_{\text{noise}} > T_{\text{escape}}$  then
5:      $\mathbf{z}_t \leftarrow \mathbf{x}_t$ 
6:      $\mathbf{x}_t \leftarrow \mathbf{x}_t + \boldsymbol{\xi}_t$  where  $\boldsymbol{\xi}_t \sim \text{Unif}(\mathbb{B}(\gamma))$ ,  $T_{\text{noise}} \leftarrow t$ 
7:   end if
8:   if  $t - T_{\text{noise}} = T_{\text{escape}}$  and  $f(\mathbf{x}_t) - f(\mathbf{z}_{T_{\text{noise}}}) \geq -F$  then
9:     Return  $\mathbf{z}_{T_{\text{noise}}}$ 
10:  end if
11:   $\mathbf{x}_{t+1} \leftarrow \mathbf{x}_t - \eta \nabla f(\mathbf{x}_t)$ 
12: end for
```

Our first theorem demonstrates that IPGD achieves nearly the same convergence guarantee as PGD (differing only by a logarithmic factor), while requiring an arbitrarily smaller perturbation radius.

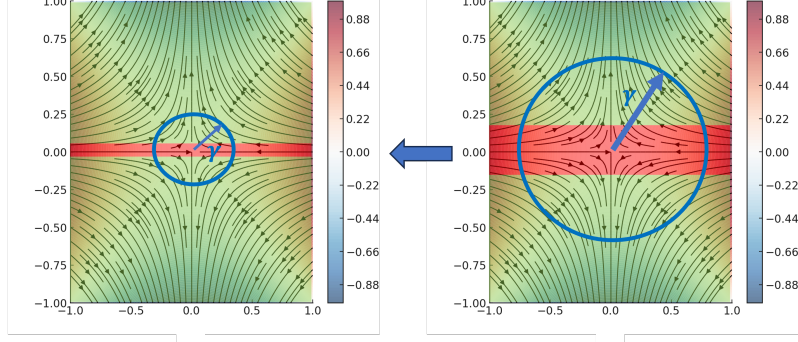


Fig. 3: (Right) The stuck and escape regions of PGD are depicted in green and red, respectively. A wide stuck region necessitates proportionally larger perturbations for escape. **(Left)** Our results demonstrate that the width of the stuck region can be reduced to an arbitrarily small value, at the cost of a poly-logarithmic increase in the number of iterations.

Theorem 2 (Convergence of IPGD to an approximate SOSP) *Suppose that f is $(L, \mathcal{M}, +\infty)$ -gradient-Lipschitz and $(\rho, \mathcal{M}, +\infty)$ -Hessian-Lipschitz. Then, with probability of at least $1 - \chi$, IPGD (Algorithm 1) with any perturbation radius satisfying $\gamma = O\left(\min\left\{\sqrt{\frac{\epsilon}{\rho}} \log^{-4}\left(\frac{\rho d \Delta_f}{\chi \epsilon}\right), \frac{\epsilon}{L}\right\}\right)$ and stepsize $\eta \leq 1/L$ outputs an ϵ -SOSP within $T = O\left(\frac{\Delta_f}{\eta \epsilon^2} \left(\log^4\left(\frac{1}{\gamma}\right) + \log^4\left(\frac{\rho d \Delta_f}{\chi \epsilon}\right)\right)\right)$ iterations. Here, $\Delta_f = f(\mathbf{x}_0) - \min_{\mathbf{x} \in \mathbb{R}^d} f(\mathbf{x})$.*

Unlike Theorem 1, our result demonstrates that IPGD can efficiently converge to an approximate SOSP using a positive perturbation radius that is significantly smaller than $\tilde{\Theta}(\epsilon/L)$, which is required in Theorem 1. This improvement comes at the cost of increasing the number of iterations only by a factor of $\log^4(1/\gamma)$. This implies that the total increase in the residual norm caused by perturbations can be kept small, without significantly impacting the convergence rate.

Analogous to [20], our approach to proving Theorem 2 is based on characterizing the volume of the “stuck region” surrounding an approximate strict saddle point. Specifically, let us assume that \mathbf{z} is a strict saddle point of f . [20] defines the *stuck region* $\mathcal{R}_{\text{stuck}}$ and the *escape region* $\mathcal{R}_{\text{escape}}$ as follows:

$$\mathcal{R}_{\text{escape}} := \{\mathbf{x}_0 \in \mathbb{B}_{\mathbf{z}}(\gamma) : f(\mathbf{x}_t) - f(\mathbf{x}_0) < -F_{\text{PGD}}, \text{ within } t \leq T_{\text{PGD}} \text{ GD updates}\}, \quad (3)$$

$$\mathcal{R}_{\text{stuck}} := \{\mathbf{x}_0 \in \mathbb{B}_{\mathbf{z}}(\gamma) : f(\mathbf{x}_t) - f(\mathbf{x}_0) \geq -F_{\text{PGD}}, \text{ within } t \leq T_{\text{PGD}} \text{ GD updates}\}, \quad (4)$$

for appropriately chosen values of F_{PGD} and T_{PGD} . Evidently, any point in $\mathcal{R}_{\text{escape}}$ successfully escapes the strict saddle point \mathbf{z} within the specified number of GD updates, whereas any point in $\mathcal{R}_{\text{stuck}}$ remains trapped and fails to do so. The key insight from [20] is that $\mathcal{R}_{\text{stuck}}$ forms a narrow band with a “width” proportional to ϵ/\sqrt{d} .

Consequently, even if \mathbf{z} lies within this region, a single perturbation with a radius scaling as ϵ is likely to move the perturbed point into $\mathcal{R}_{\text{escape}}$ (see the right panel of Figure 3). Our main contribution is to demonstrate that the width of $\mathcal{R}_{\text{stuck}}$ can be reduced to γ/\sqrt{d} , for an arbitrarily small value $\gamma > 0$ (potentially much smaller than ϵ), while only requiring F_{PGD} and T_{PGD} to scale poly-logarithmically in $1/\gamma$. Specifically, we show that this can be achieved by adjusting F_{IPGD} and T_{IPGD} as $F_{\text{IPGD}} \leftarrow F_{\text{PGD}}/\text{poly log}(1/\gamma)$ and $T_{\text{IPGD}} \leftarrow T_{\text{PGD}} \cdot \text{poly log}(1/\gamma)$. An immediate implication of this is that a perturbation radius of γ is sufficient to guarantee an efficient escape (see the left panel of Figure 3).

2.2 Implicit Regularization

Indeed, even if the infinitesimal perturbations of IPGD do not cause a significant deviation from the implicit region \mathcal{M} , there remains the possibility that the iterates may drift away from this region during the standard GD updates. To characterize this deviation, we provide a fine-grained control over the dynamics of the residual norm $\|\mathbf{x}_t^\perp\|$. At a high level, a single GD update can be reformulated as:

$$\begin{aligned}\mathbf{x}_{t+1} &= \mathbf{x}_t - \eta \nabla f(\mathbf{x}_t) \\ &= \mathbf{x}_t^\sharp - \eta \nabla f(\mathbf{x}_t^\sharp) + \mathbf{x}_t^\perp - \eta \left(\nabla f(\mathbf{x}_t) - \nabla f(\mathbf{x}_t^\sharp) \right) \\ &= \mathbf{x}_t^\sharp - \eta \nabla f(\mathbf{x}_t^\sharp) + \left(\mathbf{I} - \eta \nabla^2 f(\mathbf{x}_t^\sharp) \right) \mathbf{x}_t^\perp + \eta H(\mathbf{x}_t^\perp), \text{ where } \|H(\mathbf{x}_t^\perp)\| \leq \rho \|\mathbf{x}_t^\perp\|^2.\end{aligned}\tag{5}$$

The last equality follows from the Hessian-Lipschitzness of f . Based on the above equation, the one-step dynamic of the residual norm $\|\mathbf{x}_t^\perp\|$ can be controlled by applying the projection $\mathcal{P}_{\mathcal{M}}^\perp(\cdot)$ to both sides:

$$\|\mathbf{x}_{t+1}^\perp\| = \|\mathcal{P}_{\mathcal{M}}^\perp(\mathbf{x}_{t+1})\| \leq \underbrace{\left\| \mathcal{P}_{\mathcal{M}}^\perp(\mathbf{x}_t^\sharp - \eta \nabla f(\mathbf{x}_t^\sharp)) \right\|}_{\text{signal deviation}} + \underbrace{\left\| \left(\mathbf{I} - \eta \nabla^2 f(\mathbf{x}_t^\sharp) \right) \mathbf{x}_t^\perp \right\|}_{\text{residual deviation}} + \eta \rho \|\mathbf{x}_t^\perp\|^2.\tag{6}$$

In the above inequality, we used the simple property that, for any $\mathbf{x}, \mathbf{y} \in \mathbb{R}^d$, we have $\|\mathcal{P}_{\mathcal{M}}^\perp(\mathbf{x} + \mathbf{y})\| \leq \|\mathcal{P}_{\mathcal{M}}^\perp(\mathbf{x})\| + \|\mathbf{y}\|$ (see Lemma 16). According to the above decomposition, for sufficiently small residual norm $\|\mathbf{x}_t^\perp\|$, the dynamic of the residual norm is mainly governed by the *signal deviation* and *residual deviation*. The favorable landscape properties of f within the implicit domain \mathcal{M} can be leveraged to effectively control the signal deviation. In particular, the signal deviation is completely eliminated if the implicit region \mathcal{M} is *closed under GD updates*, as formally defined below.

Assumption 3 (Closure of \mathcal{M} under GD updates) *For any $\mathbf{x} \in \mathcal{M}$ and stepsize $\eta > 0$, we have $\mathbf{x} - \eta \nabla f(\mathbf{x}) \in \mathcal{M}$.*

This assumption ensures that the GD iterates remain within the implicit region, provided the initial point lies within that region. While this assumption may appear

restrictive at first and is certainly not universally valid for all implicit regions, we demonstrate in the following three examples that it holds for appropriately chosen implicit regions in sparse recovery, low-rank matrix recovery, and, more generally, models involving sparse basis function decomposition.

Example 1 (Sparse recovery) Consider the sparse recovery problem discussed in Section 1 and its aforementioned implicit region $\mathcal{M} = \{(\mathbf{u}, \mathbf{v}) : u_i = v_i = 0 \text{ if } \theta_i^* = 0\}$. For a general loss function $f(\mathbf{u}, \mathbf{v}) = L(\mathbf{u} \odot \mathbf{v})$, a single GD update can be written as:

$$\begin{bmatrix} \mathbf{u}_+ \\ \mathbf{v}_+ \end{bmatrix} = \begin{bmatrix} \mathbf{u} - \eta \nabla_{\mathbf{u}} f(\mathbf{u}, \mathbf{v}) \\ \mathbf{v} - \eta \nabla_{\mathbf{v}} f(\mathbf{u}, \mathbf{v}) \end{bmatrix} = \begin{bmatrix} \mathbf{u} - \eta \nabla L(\mathbf{u} \odot \mathbf{v}) \odot \mathbf{v} \\ \mathbf{v} - \eta \nabla L(\mathbf{u} \odot \mathbf{v}) \odot \mathbf{u} \end{bmatrix}. \quad (7)$$

Based on the above formula, it is easy to verify that if $(\mathbf{u}, \mathbf{v}) \in \mathcal{M}$, then $(\mathbf{u}_+, \mathbf{v}_+) \in \mathcal{M}$.

Example 2 (Low-rank matrix recovery) Consider the symmetric low-rank matrix recovery problem discussed in Section 1 and its associated implicit region $\mathcal{M} = \{\mathbf{X} \in \mathbb{R}^{n \times r'} : \text{rank}(\mathbf{X}) \leq r\}$. For a general loss function $f(\mathbf{X}) = L(\mathbf{X}\mathbf{X}^\top)$, a single GD update can be written as:

$$\mathbf{X}_+ = \mathbf{X} - \eta \nabla f(\mathbf{X}) = \left(1 - 2\eta \nabla L(\mathbf{X}\mathbf{X}^\top)\right) \mathbf{X}. \quad (8)$$

Indeed, it is easy to verify that if $\mathbf{X} \in \mathcal{M}$, then $\mathbf{X}_+ \in \mathcal{M}$. Moreover, a similar property can be established for other choices of implicit regions (see Section 6), as well as the asymmetric variant of low-rank matrix recovery and its extension to low-rank tensor decomposition.

Example 3 (Models with sparse basis function decomposition) The recent paper [17] demonstrates that, although the dynamics of GD can vary significantly across different deep neural network models, they tend to exhibit a sparse behavior when projected onto a suitable orthonormal function basis (see [17, Definition 1]). While the explicit characterization of this orthonormal function basis depends on the specific task, its mere existence is sufficient to define the corresponding implicit region as the set of parameters with a sparse representation—characterized by sparse basis coefficients—after projection onto this basis. It can be verified that this implicit region remains closed under GD updates, provided the GD trajectory satisfies a condition known as *gradient independence* (see [17, Theorem 1]). [17] illustrates that the gradient independence condition is approximately satisfied across a wide range of deep neural networks.

An arguably more challenging task is to control the residual deviation, which we discuss next. Consider the eigen-decomposition of the Hessian $\nabla^2 f(\mathbf{x}) = \mathbf{V}\mathbf{D}\mathbf{V}^\top$, where $\mathbf{V} \in \mathbb{R}^{d \times d}$ is an orthonormal matrix whose columns correspond to the eigenvectors of $\nabla^2 f(\mathbf{x})$, and $\mathbf{D} \in \mathbb{R}^{d \times d}$ is a diagonal matrix containing the eigenvalues of $\nabla^2 f(\mathbf{x})$. The decomposition of the Hessian into *positive semi-definite* (PSD) and *negative semi-definite* (NSD) components is defined as $\nabla^2 f(\mathbf{x}) = \nabla_+^2 f(\mathbf{x}) + \nabla_-^2 f(\mathbf{x})$, where $\nabla_+^2 f(\mathbf{x}) = \mathbf{V}\mathbf{D}_+\mathbf{V}^\top$ and $\nabla_-^2 f(\mathbf{x}) = \mathbf{V}\mathbf{D}_-\mathbf{V}^\top$. Here \mathbf{D}_+ is a diagonal matrix whose (i, i) -th entry is given by $\max\{0, \mathbf{D}_{ii}\}$. Similarly, \mathbf{D}_- is defined as a matrix whose (i, i) -th entry is given by $\min\{0, \mathbf{D}_{ii}\}$.

Definition 5 (Deviation rate) The **deviation rate** of f at a point \mathbf{x} from \mathcal{M} is defined as $r(\mathbf{x}) = r_-(\mathbf{x}) + 3r_+(\mathbf{x})$, where $r_-(\mathbf{x})$ and $r_+(\mathbf{x})$ are the **negative deviation rate** and **positive deviation rate** of f at point \mathbf{x} respectively, and are given as:

$$r_-(\mathbf{x}) = \begin{cases} \frac{-1}{\|\mathbf{x}^\perp\|^2} \langle \mathbf{x}^\perp, \nabla_+^2 f(\mathbf{x}^\sharp) \mathbf{x}^\perp \rangle & \text{if } \mathbf{x}^\perp \neq 0; \\ 0 & \text{if } \mathbf{x}^\perp = 0 \end{cases}, \quad (9)$$

$$r_+(\mathbf{x}) = \begin{cases} \frac{-1}{\|\mathbf{x}^\perp\|^2} \langle \mathbf{x}^\perp, \nabla_-^2 f(\mathbf{x}^\sharp) \mathbf{x}^\perp \rangle & \text{if } \mathbf{x}^\perp \neq 0, \\ 0 & \text{if } \mathbf{x}^\perp = 0. \end{cases} \quad (10)$$

Accordingly, the **τ -deviation rate** $R(\tau)$ of f is defined as:

$$R(\tau) = \sup_{\mathbf{x} \in \mathcal{N}_{\mathcal{M}}(\tau)} r(\mathbf{x}). \quad (11)$$

Clearly, we have $r_-(\mathbf{x}) \leq 0$ and $r_+(\mathbf{x}) \geq 0$ for every $\mathbf{x} \in \mathbb{R}^d$. Intuitively, the magnitudes of the negative and positive deviation rates at any point represent the effective negative and positive curvatures of the Hessian, respectively, evaluated at the signal \mathbf{x}^\sharp , along the direction of the residual \mathbf{x}^\perp . As we will show in the next proposition, the deviation rate $r(\mathbf{x})$, which is a weighted sum of these two quantities, governs the growth rate of the residual norm.

Proposition 4 (Residual norm dynamic) *Suppose that f is (L, \mathcal{M}, τ) -gradient-Lipschitz and $(\rho, \mathcal{M}, \tau)$ -Hessian-Lipschitz. Moreover, assume that the implicit region \mathcal{M} is closed under GD updates (Assumption 3) and $\|\mathbf{x}_t^\perp\| \leq \tau$. Then, a single GD update $\mathbf{x}_{t+1} = \mathbf{x}_t - \eta \nabla f(\mathbf{x}_t)$ with any fixed stepsize $\eta \leq 1/L$ satisfies:*

$$\|\mathbf{x}_{t+1}^\perp\| \leq \left(1 + \frac{\eta}{2} r(\mathbf{x}_t) + \frac{\eta \rho}{2} \|\mathbf{x}_t^\perp\|\right) \|\mathbf{x}_t^\perp\|. \quad (12)$$

Based on the above proposition, the dynamic of the residual norm under GD updates is controlled by the deviation rate, expressed as $r(\mathbf{x}_t) = r_-(\mathbf{x}_t) + 3r_+(\mathbf{x}_t)$. Proposition 4 indicates that a large deviation rate can lead to rapid growth of the residual norm, while a small or negative deviation rate results in slower growth or even shrinkage. In Section 6, we demonstrate that this relationship is also observed in practice across a wide range of problems.

To provide a better intuition on the role of Proposition 4 in our analysis, let us, for simplicity, assume that $\|\mathbf{x}_t^\perp\| \leq \tau \leq 2/(T\eta\rho)$ for all $0 \leq t \leq T-1$.³ Unfolding the dynamics of $\|\mathbf{x}_t^\perp\|$ for $t = 0, 1, \dots, T-1$ yields:

$$\|\mathbf{x}_T^\perp\| \leq \exp \left\{ \frac{\eta}{2} \left(\sum_{t=0}^{T-1} r(\mathbf{x}_t) \right) + \frac{\eta \rho}{2} \left(\sum_{t=0}^{T-1} \|\mathbf{x}_t^\perp\| \right) \right\} \|\mathbf{x}_0^\perp\| \leq 3 \exp\{\eta T R(\tau)\} \|\mathbf{x}_0^\perp\|. \quad (13)$$

The first inequality follows from $1 + x \leq \exp\{x\}$ and the second inequality follows from the imposed bound on $\{\|\mathbf{x}_t^\perp\|\}_{t=0}^{T-1}$ and the definition of the τ -deviation rate

³This assumption is not required in our formal analysis but is introduced here to provide a crisp intuition.

$R(\tau)$. Assuming that $\|\mathbf{x}_0^\perp\|$ is small, in order to ensure that $\|\mathbf{x}_T^\perp\| = O(\|\mathbf{x}_0^\perp\|)$, we require $R(\tau) \leq 1/(\eta T)$. As we will show later, the required number of iterations T is primarily dictated by the behavior of the projected iterates onto the implicit region \mathcal{M} , represented by the signal \mathbf{x}_t^\sharp . Consequently, a faster convergence of \mathbf{x}_t^\sharp to an \mathcal{M} -SOSP leads to a smaller value of T , which in turn results in a more relaxed bound on $R(\tau)$. Our next theorem formalizes this trade-off.

Theorem 5 (Convergence of IPGD to \mathcal{M} -SOSP) *Suppose that f is (L, \mathcal{M}, τ) -gradient-Lipschitz and $(\rho, \mathcal{M}, \tau)$ -Hessian-Lipschitz with $\tau \geq \epsilon/L$. Moreover, assume that the following conditions are satisfied:*

C1 The implicit region \mathcal{M} is closed under GD updates (Assumption 3).

C2 The initial point satisfies $\|\mathbf{x}_0^\perp\| \leq O\left(\min\left\{\frac{\epsilon}{L}, \frac{1}{\eta\rho T}\right\}\right)$.

C3 The τ -deviation rate $R(\tau)$ satisfies $R(\tau) = O\left(\frac{1}{\eta T}\right)$.

Then, with probability at least $1 - \chi$, IPGD (Algorithm 1) with any perturbation radius satisfying $\gamma = O\left(\min\left\{\frac{\epsilon^{5/2}}{\sqrt{\rho}L\Delta_f}, \frac{\epsilon^{7/2}}{\rho^{3/2}\Delta_f^2}\right\} \cdot \log^{-7}\left(\frac{\rho d\Delta_f}{\chi\epsilon}\right)\right)$ and stepsize $\eta \leq 1/L$ outputs an ϵ - \mathcal{M} -SOSP within $T = O\left(\frac{\Delta_f}{\eta\epsilon^2}\left(\log^4\left(\frac{1}{\gamma}\right) + \log^4\left(\frac{\rho d\Delta_f}{\chi\epsilon}\right)\right)\right)$ iterations.

Below, we discuss a few key insights from Theorem 5.

Lipschitz conditions

The convergence of IPGD to an approximate \mathcal{M} -SOSP only requires gradient- and Hessian-Lipschitz properties within an (ϵ/L) -neighborhood of the implicit region \mathcal{M} . This is a significant improvement over the global Lipschitz conditions required for PGD and for the convergence of IPGD to a general SOSP (Theorem 2). This relaxation is possible because, by controlling the residual norm via Proposition 4, the trajectory of IPGD can be confined to a small neighborhood around the implicit region.

Initialization

The convergence of IPGD to an approximate \mathcal{M} -SOSP depends on the initial point being close to the implicit region, which corresponds to a small initial residual norm. While it may not always be feasible to determine such an initialization for an arbitrary implicit region \mathcal{M} , it is often possible to ensure that $\mathbf{0} \in \mathcal{M}$. In this case, a small or zero initialization naturally satisfies this condition. Notably, it is straightforward to verify that $\mathbf{0} \in \mathcal{M}$ holds for the implicit regions discussed in Examples 1 to 3.

Deviation rate

The most restrictive condition in Theorem 5 is the upper bound imposed on the τ -deviation rate. Noting the dependency of T on ϵ , this condition requires that, to achieve an ϵ - \mathcal{M} -SOSP, the τ -deviation rate within an ϵ/L -neighborhood of the implicit region must scale quadratically with ϵ . While this condition is satisfied empirically in certain learning problems, rigorously proving it can be a daunting task, and in some cases, may even be impossible.

Nevertheless, we demonstrate that this requirement can be significantly relaxed if the objective function f exhibits additional structures within the implicit region \mathcal{M} .

2.3 Improved Convergence with Additional Structures

A desirable geometric structure that can facilitate the convergence of IPGD is the so-called strict saddle property on the implicit region \mathcal{M} , which we introduce next.

Definition 6 (\mathcal{M} -strict saddle property) We say the function f satisfies the $(\bar{\epsilon}_g, \bar{\epsilon}_H, \bar{\epsilon}_{\mathcal{M}})$ - \mathcal{M} -strict saddle property for some parameters $\bar{\epsilon}_g, \bar{\epsilon}_H, \bar{\epsilon}_{\mathcal{M}} > 0$ if, for any $\mathbf{x} \in \mathcal{M}$, at least one of following conditions holds:

- $\|\nabla f(\mathbf{x})\| \geq \bar{\epsilon}_g$;
- $\lambda_{\min}(\nabla^2 f(\mathbf{x})) \leq -\bar{\epsilon}_H$;
- $\text{dist}(\mathbf{x}, \mathcal{X}_{\mathcal{M}}) \leq \bar{\epsilon}_{\mathcal{M}}$, that is, there exists an exact \mathcal{M} -SOSP $\mathbf{z} \in \mathcal{M}$ satisfying $\nabla f(\mathbf{z}) = 0$ and $\nabla^2 f(\mathbf{z}) \succeq 0$ such that $\|\mathbf{x} - \mathbf{z}\| \leq \bar{\epsilon}_{\mathcal{M}}$.

Intuitively, the \mathcal{M} -strict saddle property partitions the implicit region \mathcal{M} into three distinct areas: (i) a region where the gradient norm is large; (ii) a region containing only approximate strict saddle points, i.e., points with sufficiently negative curvature; and (iii) a neighborhood surrounding the exact \mathcal{M} -SOSPs.

This property is akin to the global strict saddle property [42, Assumption A2], with the key distinction that it is only imposed on the implicit region \mathcal{M} , whereas the global variant must hold for every $\mathbf{x} \in \mathbb{R}^d$. While the global strict saddle property holds for generic functions [18, Theorem 2.9], the associated parameters $(\bar{\epsilon}_g, \bar{\epsilon}_H, \bar{\epsilon}_{\mathcal{M}})$ tend to degrade as the level of over-parameterization increases, leading to overly conservative convergence rate for the algorithm. Therefore, imposing this condition solely on the implicit region \mathcal{M} —rather than the entire \mathbb{R}^d —can lead to less conservative parameter choices. For example, several problems, including matrix sensing, matrix completion, and tensor decomposition, have been shown to exhibit strict saddle properties with desirable parameters within their implicit regions [19, 42].⁴ In contrast, in over-parameterized regimes, the global strict saddle property is conjectured to hold only with unfavorable parameters, resulting in poor convergence rates [50, Page 5].

In conjunction with Theorem 5, if the function f additionally satisfies the $(\bar{\epsilon}_g, \bar{\epsilon}_H, \bar{\epsilon}_{\mathcal{M}})$ - \mathcal{M} -strict saddle property, then IPGD converges to an $\bar{\epsilon}_{\mathcal{M}}$ -neighborhood of an exact \mathcal{M} -SOSP, while staying close to the implicit region \mathcal{M} .

Proposition 6 (Convergence of IPGD under strict saddle property) *Suppose that f is (L, \mathcal{M}, τ) -gradient-Lipschitz and $(\rho, \mathcal{M}, \tau)$ -Hessian-Lipschitz with $\tau \geq \epsilon/L$, and satisfies the $(\bar{\epsilon}_g, \bar{\epsilon}_H, \bar{\epsilon}_{\mathcal{M}})$ - \mathcal{M} -strict saddle property. Furthermore, suppose that Conditions C1-C3 from Theorem 5 hold. Let $\bar{\epsilon} = \frac{1}{4} \min \left\{ \bar{\epsilon}_g, \bar{\epsilon}_H^2 / \rho \right\}$ and suppose $\epsilon \leq \min \left\{ \frac{3}{4} \bar{\epsilon}_g, \frac{L}{2\rho} \bar{\epsilon}_H \right\}$. Then, with probability of at least $1 - \chi$, IPGD (Algorithm 1) with any perturbation radius satisfying*

⁴The original results consider a slightly different setting, assuming the problem is exactly-parameterized, whereas we address the over-parameterized setting, where $\mathbf{x} \in \mathcal{M} \subset \mathbb{R}^d$ with $\dim(\mathcal{M}) = k < d$. However, a simple lifting trick can establish the equivalence between these cases.

$\gamma = O\left(\min\left\{\frac{\bar{\epsilon}^{3/2}\epsilon}{\sqrt{\rho}L\Delta_f}, \frac{\bar{\epsilon}^{7/2}}{\rho^{3/2}\Delta_f^2}\right\} \cdot \log^{-7}\left(\frac{\rho d\Delta_f}{\chi\bar{\epsilon}}\right)\right)$ and stepsize $\eta \leq 1/L$ outputs a point \mathbf{x}_T satisfying:

$$\left\|\mathbf{x}_T^\perp\right\| \leq \frac{\epsilon}{L}, \quad \text{dist}\left(\mathbf{x}_T^\sharp, \mathcal{X}_\mathcal{M}\right) \leq \bar{\epsilon}_\mathcal{M}, \quad (14)$$

within $T = O\left(\frac{\Delta_f}{\eta\bar{\epsilon}^2}\left(\log^4\left(\frac{1}{\gamma}\right) + \log^4\left(\frac{\rho d\Delta_f}{\chi\bar{\epsilon}}\right)\right)\right)$ iterations.

Proposition 6 establishes that, under the \mathcal{M} -strict saddle property, setting the gradient threshold ϵ in IPGD to $\bar{\epsilon} = \frac{1}{4} \min\{\bar{\epsilon}_g, \bar{\epsilon}_H^2/\rho\}$ ensures that the output lies within an $\bar{\epsilon}_\mathcal{M}$ -neighborhood of an exact \mathcal{M} -SOSP. Notably, such a guarantee is unattainable without the strict saddle property and cannot be derived solely from Theorem 5. In particular, while Theorem 5 demonstrates that the output of IPGD is approximately an \mathcal{M} -SOSP, it does not establish a bound on the distance between the obtained point and an exact \mathcal{M} -SOSP.

Additionally, Proposition 6 offers another distinct advantage: under the assumption that $\bar{\epsilon} = \Theta(1)$, the required bound on the deviation rate simplifies to $R(\tau) = \tilde{O}(1/\Delta_f)$, which is a significant relaxation compared to the stricter requirement $R(\tau) = \tilde{O}(\epsilon^2/\Delta_f)$ in Theorem 5. As we will show later, both $\bar{\epsilon} = \Theta(1)$ and $R(\tau) = \tilde{O}(1/\Delta_f)$ can be established for the over-parameterized matrix sensing.

Finally, we note that while the \mathcal{M} -strict saddle property is a desirable property, it is not sufficient to guarantee convergence to a reasonably accurate \mathcal{M} -SOSP, particularly in settings where $\bar{\epsilon}_\mathcal{M} = \Omega(1)$. In such cases, IPGD may still require the same conditions as those in Theorem 5 to ensure the output is an ϵ - \mathcal{M} -SOSP with $\epsilon \ll \bar{\epsilon}_\mathcal{M}$, even under the strict saddle property. To truly accelerate the convergence of IPGD, an additional condition, akin to strong convexity within a local region of an \mathcal{M} -SOSP, is necessary. Unfortunately, however, strong convexity—even locally—is rarely satisfied in over-parameterized problems. A more relaxed notion is a regularity property, which we impose only on the implicit region \mathcal{M} .

Definition 7 (\mathcal{M} -regularity property) We say the function f satisfies the (α, β, ζ) - \mathcal{M} -regularity property for some parameters $\alpha, \beta, \zeta > 0$ if, for any $\mathbf{x} \in \mathcal{N}_{\mathcal{X}_\mathcal{M}}(\zeta) \cap \mathcal{M}$, we have:

$$\langle \nabla f(\mathbf{x}), \mathbf{x} - \mathcal{P}_{\mathcal{X}_\mathcal{M}}(\mathbf{x}) \rangle \geq \frac{\alpha}{2} \|\mathbf{x} - \mathcal{P}_{\mathcal{X}_\mathcal{M}}(\mathbf{x})\|^2 + \frac{1}{2\beta} \|\nabla f(\mathbf{x})\|^2. \quad (15)$$

The (α, β, ζ) - \mathcal{M} -regularity property is a weaker condition than local strong convexity. In fact, it can be shown that gradient Lipschitzness and one-point strong convexity together imply this property (see [49, Section II.B] for a proof). However, unlike local strong convexity—which typically fails to hold even in the exactly-parameterized regime⁵—the (α, β, ζ) - \mathcal{M} -regularity property is generally easier to establish. For example, it has been verified for several nonconvex optimization problems, such as matrix factorization [20], matrix sensing [41], and matrix completion [51] in the exactly-parameterized regime.

⁵Strong convexity provably fails within any neighborhood if the solution set forms a connected set. This occurs in various models, including s -sparse recovery and low-rank matrix recovery.

Intuitively, (α, β, ζ) - \mathcal{M} -regularity property entails that, within a small neighborhood of any \mathcal{M} -SOSP, the gradient $\nabla f(\mathbf{x})$ is positively correlated with the error vector $\mathbf{x} - \mathcal{P}_{\mathcal{X}_{\mathcal{M}}}(\mathbf{x})$. This implies that vanilla GD, initialized at a point exactly within \mathcal{M} , converges efficiently to an \mathcal{M} -SOSP. Our next result shows that even if the initial point is not exactly in \mathcal{M} , vanilla GD can still exploit the (α, β, ζ) - \mathcal{M} -regularity property and converge linearly to an approximate \mathcal{M} -SOSP.

Proposition 7 (Local linear convergence of GD under regularity property) *Suppose that f is (L, \mathcal{M}, τ) -gradient-Lipschitz and $(\rho, \mathcal{M}, \tau)$ -Hessian-Lipschitz with $\tau \geq \epsilon/L$, and satisfies the (α, β, ζ) - \mathcal{M} -regularity property. Suppose that the initial point \mathbf{x}_0 satisfies $\|\mathbf{x}_0^\perp\| = O(\frac{\eta\alpha\epsilon}{L})$ and $\text{dist}(\mathbf{x}_0^\sharp, \mathcal{X}_{\mathcal{M}}) \leq \zeta$. Furthermore, suppose that Conditions C1 and C3 from Theorem 5 hold. Then, GD with stepsize $\eta \leq \frac{1}{10 \max\{\alpha, \beta, L\}}$ outputs a solution \mathbf{x}_T satisfying*

$$\text{dist}(\mathbf{x}_T, \mathcal{X}_{\mathcal{M}}) \leq \frac{\epsilon}{L} \quad (16)$$

within $T = O\left(\frac{1}{\eta\alpha} \log\left(\frac{L\zeta}{\epsilon}\right)\right)$ iterations.

Note that the improvement in the iteration count—from $\text{poly}(1/\epsilon)$ to $\log(1/\epsilon)$ —enabled by the regularity condition naturally relaxes the dependence of the deviation rate $R(\tau)$ on ϵ to $\log^{-1}(1/\epsilon)$. This is significantly less restrictive than the requirement in Theorem 5, where $R(\tau)$ must scale as ϵ^2 .

Finally, by leveraging both the strict saddle property and the \mathcal{M} -regularity property, we can establish linear convergence to an \mathcal{M} -SOSP. Specifically, using the strict saddle property, we first run IPGD to obtain a point within a ζ -neighborhood of an \mathcal{M} -SOSP. Then, by exploiting the regularity condition, we apply vanilla GD to achieve linear convergence to an \mathcal{M} -SOSP. This combined approach, which we call *IPGD with local improvement* (IPGD+), is outlined in Algorithm 2.

Algorithm 2 IPGD with local improvement: IPGD+ $(\gamma, \epsilon, \eta, \mathbf{x}_0, \rho, \Delta_f, \chi, T')$

```

1:  $\mathbf{x}_0 \leftarrow \text{IPGD}(\gamma, \epsilon, \eta, \mathbf{x}_0, \rho, \Delta_f, \chi)$ 
2: for  $t = 0, 1, \dots, T'$  do
3:    $\mathbf{x}_{t+1} \leftarrow \mathbf{x}_t - \eta \nabla f(\mathbf{x}_t)$ 
4: end for

```

Theorem 8 (Global near-linear convergence of IPGD+ under strict saddle and regularity properties) *Suppose that f is (L, \mathcal{M}, τ) -gradient-Lipschitz and $(\rho, \mathcal{M}, \tau)$ -Hessian-Lipschitz with $\tau \geq \epsilon/L$. Moreover, suppose that f satisfies the (α, β, ζ) - \mathcal{M} -regularity property and $(\bar{\epsilon}_g, \bar{\epsilon}_H, \bar{\epsilon}_{\mathcal{M}})$ - \mathcal{M} -strict saddle property with $\bar{\epsilon}_{\mathcal{M}} \leq \zeta$. Suppose that the initial point satisfies $\|\mathbf{x}_0^\perp\| = O\left(\min\left\{\eta\alpha \cdot \frac{\epsilon}{L}, \frac{1}{\eta\rho T}\right\}\right)$. Furthermore, suppose that Conditions C1 and C3 from Theorem 5 hold. Let $\bar{\epsilon} = O\left(\min\left\{\bar{\epsilon}_g, \frac{\bar{\epsilon}_H^2}{\rho}\right\}\right)$ and $T' = O\left(\frac{1}{\eta\alpha} \log\left(\frac{L\zeta}{\epsilon}\right)\right)$. Then, with probability of at least $1 - \chi$, IPGD+ (Algorithm 2) with any perturbation radius satisfying*

$\gamma = O\left(\min\left\{\frac{\bar{\epsilon}^{3/2}\epsilon}{\sqrt{\rho}L\Delta_f}, \frac{\bar{\epsilon}^{7/2}}{\rho^{3/2}\Delta_f^2}\right\} \cdot \log^{-7}\left(\frac{\rho d\Delta_f}{\chi\bar{\epsilon}}\right)\right)$ and stepsize $\eta \leq \frac{1}{10 \max\{\alpha, \beta, L\}}$ outputs a solution satisfying

$$\text{dist}(\mathbf{x}_T, \mathcal{X}_{\mathcal{M}}) \leq \frac{\epsilon}{L} \quad (17)$$

within a total of $T = O\left(\frac{\Delta_f}{\eta\bar{\epsilon}^2} \left(\log^4\left(\frac{1}{\gamma}\right) + \log^4\left(\frac{\rho d\Delta_f}{\chi\bar{\epsilon}}\right)\right) + \frac{1}{\eta\alpha} \log\left(\frac{L\zeta}{\epsilon}\right)\right)$ iterations.

To better interpret the above result, let us focus solely on its dependency on the final desired error ϵ . Theorem 8 implies that, under the \mathcal{M} -strict saddle and \mathcal{M} -regularity properties, IPGD+ reaches an ϵ -neighborhood of an \mathcal{M} -SOSP in at most $T = O(\log^4(1/\epsilon))$ iterations, provided that the initial point satisfies $\|\mathbf{x}_0^\perp\| = O(\epsilon)$ and the deviation rate satisfies $R(\tau) = O(\log^{-4}(1/\epsilon))$. As we will show in Section 6, the conditions of Theorem 8 are provably satisfied for the over-parameterized matrix sensing problem.

We note that IPGD+ is similar to the PGD with local improvement (referred to as PGDli) introduced in [20]. However, IPGD+ has a slower convergence rate by a factor of $\log^3(1/\epsilon)$. This slowdown stems from the use of a smaller perturbation radius, which is necessary to enable implicit regularization and ensure that the iterates remain close to the implicit region \mathcal{M} .

Next, we provide the proofs for our main results. To this end, in Section 3, we first prove the convergence of IPGD to an approximate SOSP, thereby establishing Theorem 2. Next, in Section 4, we establish the implicit regularization of IPGD and use this property to show the convergence of IPGD to an approximate \mathcal{M} -SOSP, ultimately proving Theorem 5. Finally, in Section 5, we refine our results by proving the improved convergence guarantees of Theorem 8 under additional local structural assumptions.

3 Establishing Convergence of IPGD to an Approximate SOSP

To establish the convergence of IPGD, our analysis carefully refines the convergence analysis of PGD from [20, 23], extending it to accommodate infinitesimal perturbations.

To establish the convergence of IPGD to an approximate SOSP, we divide our analysis into two parts:

- **Bounding the iteration count:** We derive an upper bound on the maximum number of iterations that IPGD can take before meeting its termination criterion, thereby characterizing its convergence rate.
- **Establishing the error guarantee:** We demonstrate that, upon termination, the returned solution satisfies the conditions for an approximate SOSP.

To provide a bound on the iteration count, let us define N_{large} as the number of iterations where the gradient norm satisfies $\|\nabla f(\mathbf{x}_t)\| > G$. Moreover, let N_{perturb} be the number of iterations in which a perturbation is applied to \mathbf{x}_t (Line 6 of Algorithm 1).

Formally, these are given by:

$$N_{\text{large}} = |\{t : \|\nabla f(\mathbf{x}_t)\| > G\}|, \quad N_{\text{perturb}} = |\{t : \text{perturbation is added to } \mathbf{x}_t\}|.$$

The following lemma provides an upper bound on the total number of iterations of the algorithm in terms of N_{large} and N_{perturb} .

Lemma 9 *Let $t = T$ denote the last iteration of IPGD (Algorithm 1). We have*

$$T \leq N_{\text{large}} + N_{\text{perturb}} \cdot T_{\text{escape}}. \quad (18)$$

Proof At every iteration t , IPGD takes one of the following steps:

- If $\|\nabla f(\mathbf{x}_t)\| > G$ and no perturbation has been applied in the past T_{escape} iterations, IPGD performs a single GD update.
- If $\|\nabla f(\mathbf{x}_t)\| \leq G$ and no perturbation has been applied in the past T_{escape} iterations, IPGD applies a perturbation to \mathbf{x}_t , followed by T_{escape} GD updates.

By combining these observations with the definitions of N_{large} and N_{perturb} , we obtain $T \leq N_{\text{large}} + N_{\text{perturb}} \cdot T_{\text{escape}}$, thereby completing the proof. \square

Based on the above lemma, in order to bound the iteration count, it suffices to provide separate bounds on N_{large} and N_{perturb} . Towards this goal, we utilize a classic descent lemma for GD updates.

Lemma 10 (Descent lemma for GD updates; [52, Section 1.2.3]) *Suppose that the conditions of Theorem 2 are satisfied. For the GD update $\mathbf{x}_{t+1} = \mathbf{x}_t - \eta \nabla f(\mathbf{x}_t)$ with $\eta \leq \frac{1}{L}$, we have:*

$$f(\mathbf{x}_{t+1}) - f(\mathbf{x}_t) \leq -\frac{1}{2}\eta \|\nabla f(\mathbf{x}_t)\|^2. \quad (19)$$

Equipped with Lemma 9 and Lemma 10, we are now ready to establish an upper bound on the maximum number of iterations of IPGD:

Proposition 11 (Bounding the iteration count of IPGD) *Suppose that the conditions of Theorem 2 are satisfied. Then, IPGD terminates within $T \leq \frac{4C^2\Delta_f}{\eta\epsilon^2} \left(\log^4\left(\frac{1}{\gamma}\right) + \log^4\left(\frac{\rho d\Delta_f}{\chi\epsilon}\right) \right)$ iterations.*

Proof Indeed, if $\|\nabla f(\mathbf{x}_t)\| > G$, Lemma 10 implies that a single GD update $\mathbf{x}_{t+1} = \mathbf{x}_t - \eta \nabla f(\mathbf{x}_t)$ reduces the objective by at least

$$f(\mathbf{x}_{t+1}) - f(\mathbf{x}_t) \leq -\frac{1}{2}\eta \|\nabla f(\mathbf{x}_t)\|^2 \leq -\frac{1}{2}\eta G = -\frac{1}{2}\eta \left(\frac{1}{C} \cdot \frac{\epsilon}{\log^2(1/\gamma)} \right) = -\frac{\eta\epsilon}{2C \log^2(1/\gamma)} \quad (20)$$

where the first equality is due to the definition of G in Algorithm 1. This implies that:

$$N_{\text{large}} \leq \frac{\Delta_f}{\frac{\eta\epsilon}{2C\log^2(1/\gamma)}} = \frac{2C\Delta_f \log^2(1/\gamma)}{\eta\epsilon}. \quad (21)$$

Next, we provide an upper bound on N_{perturb} . Let t_k denote the iteration in which the k -th perturbation is applied to \mathbf{x}_{t_k} . For every $1 \leq k \leq N_{\text{perturb}} - 1$, we must have

$$f(\mathbf{x}_{t_k+T_{\text{escape}}}) - f(\mathbf{z}_{t_k}) < -F = -\frac{1}{C} \cdot \frac{\epsilon^{3/2}}{\sqrt{\rho} \left(\log^3\left(\frac{1}{\gamma}\right) + \log^3\left(\frac{\rho d \Delta_f}{\chi \epsilon}\right) \right)}, \quad (22)$$

as otherwise, the algorithm would have terminated within the first $N_{\text{perturb}} - 1$ perturbations, contradicting the definition of N_{perturb} . The equality follows from the definition of F in Algorithm 1. This implies that

$$N_{\text{perturb}} \leq \frac{\Delta_f}{\frac{1}{C} \cdot \frac{\epsilon^{3/2}}{\sqrt{\rho} \log^3(1/\gamma)}} = \frac{C\sqrt{\rho}\Delta_f \left(\log^3\left(\frac{1}{\gamma}\right) + \log^3\left(\frac{\rho d \Delta_f}{\chi \epsilon}\right) \right)}{\epsilon^{3/2}}. \quad (23)$$

Invoking Lemma 9, we obtain

$$\begin{aligned} T &\leq N_{\text{large}} + N_{\text{perturb}} \cdot T_{\text{escape}} \\ &\leq \frac{2C\Delta_f \log^2(1/\gamma)}{\eta\epsilon} + \frac{C\sqrt{\rho}\Delta_f \left(\log^3\left(\frac{1}{\gamma}\right) + \log^3\left(\frac{\rho d \Delta_f}{\chi \epsilon}\right) \right)}{\epsilon^{3/2}} \cdot \frac{C \left(\log\left(\frac{1}{\gamma}\right) + \log\left(\frac{\rho d \Delta_f}{\chi \epsilon}\right) \right)}{\eta\sqrt{\rho\epsilon}} \\ &\leq \frac{4C^2\Delta_f \left(\log^4\left(\frac{1}{\gamma}\right) + \log^4\left(\frac{\rho d \Delta_f}{\chi \epsilon}\right) \right)}{\eta\epsilon^2}. \end{aligned} \quad (24)$$

This completes the proof. \square

Next, we establish that, upon termination, the returned solution is indeed an approximate SOSP. To this goal, we rely on the following key proposition, which encapsulates the main novelty of our proof.

Proposition 12 (Escaping strict saddle points with infinitesimal perturbation) *Suppose that the conditions of Theorem 2 are satisfied. Moreover, suppose the input \mathbf{z}_t satisfies $\|\nabla f(\mathbf{z}_t)\| \leq G$ and $\lambda_{\min}(\nabla^2 f(\mathbf{z}_t)) < -\sqrt{\rho\epsilon}$. Then, with probability at least $1 - \frac{\chi}{N_{\text{perturb}}}$, a single perturbation $\mathbf{x}_t = \mathbf{z}_t + \xi_t$, where $\xi_t \sim \text{Unif}(\mathbb{B}(\gamma))$, with perturbation radius satisfying $\gamma = O\left(\min\left\{\sqrt{\frac{\epsilon}{\rho}} \log^{-3}\left(\frac{\rho d \Delta_f}{\chi \epsilon}\right), \frac{\epsilon}{L}\right\}\right)$ followed by T_{escape} iterations of GD updates $\mathbf{x}_{t+1} = \mathbf{x}_t - \eta \nabla f(\mathbf{x}_t)$ with $\eta \leq \frac{1}{L}$ satisfies*

$$f(\mathbf{x}_{t+T_{\text{escape}}}) - f(\mathbf{z}_t) < -F, \quad (25)$$

$$\text{where } F := \frac{\epsilon^{3/2}}{4608\sqrt{\rho} \left(\log^3\left(\frac{1}{\gamma}\right) + \log^3\left(\frac{\rho d \Delta_f}{\chi \epsilon}\right) \right)}.$$

Before presenting the proof of the above proposition, we first show how it can be used to complete the proof of Theorem 2.

Proof of Theorem 2 Proposition 11 readily establishes the presented upper bound on the iteration count. Moreover, the termination criterion ensures that $\|\nabla f(\mathbf{z}_{T_{\text{noise}}})\| \leq G$ and $f(\mathbf{x}_{T_{\text{noise}}+T_{\text{escape}}}) - f(\mathbf{z}_{T_{\text{noise}}}) \geq -F$. By Proposition 12, it follows that $\lambda_{\min}(\nabla^2 f(\mathbf{z}_{T_{\text{noise}}})) \geq -\sqrt{\rho\epsilon}$ with probability at least $1 - \frac{\chi}{N_{\text{perturb}}}$. Since the algorithm can visit at most N_{perturb} , a simple union bound implies that $\mathbf{z}_{T_{\text{noise}}}$ is an ϵ -SOSP with probability at least $1 - N_{\text{perturb}} \cdot \frac{\chi}{N_{\text{perturb}}} = 1 - \chi$, thereby completing the proof. \square

Now, we proceed with the proof of Proposition 12. We first introduce the following lemma from [23].

Lemma 13 (Improve or localize, adapted from Lemma 5.4 in [23]) *Let \mathbf{x}_0 be any initial point. Suppose the GD updates $\mathbf{x}_{t+1} = \mathbf{x}_t - \eta \nabla f(\mathbf{x}_t)$ are generated with step size $\eta \leq \frac{1}{L}$. Then, for all $t \geq 0$, we have*

$$\|\mathbf{x}_t - \mathbf{x}_0\| \leq \sqrt{2\eta t (f(\mathbf{x}_0) - f(\mathbf{x}_t))}. \quad (26)$$

Our next result is at the core of the guaranteed escape of IPGD from an approximate strict saddle point. To explain the intuition behind this result, let \mathbf{z} be an approximate strict saddle point, satisfying $\|\nabla f(\mathbf{z})\| \leq \epsilon$ and $\lambda_{\min}(\nabla^2 f(\mathbf{z})) < -\sqrt{\rho\epsilon}$. Let \mathbf{v} be the eigenvector corresponding to the most negative eigenvalue of $\nabla^2 f(\mathbf{z})$. Consider any two initial points $\mathbf{x}_0, \mathbf{x}'_0$ such that $\mathbf{x}_0, \mathbf{x}'_0 \in \mathbb{B}_{\mathbf{z}}(\gamma)$ and $\mathbf{x}_0 - \mathbf{x}'_0 = \omega \cdot \mathbf{v}$ for some $\omega > 0$. Our next result demonstrates that GD, when initialized at one of these points, must decrease the objective function rapidly, enabling an escape from \mathbf{z} .

Lemma 14 *Let \mathbf{z} be an approximate strict saddle point satisfying $\|\nabla f(\mathbf{z})\| \leq \epsilon$ and $\lambda_{\min}(\nabla^2 f(\mathbf{z})) < -\sqrt{\rho\epsilon}$. Let \mathbf{v} be the eigenvector corresponding to the most negative eigenvalue of $\nabla^2 f(\mathbf{z})$. Consider two points $\mathbf{x}_0, \mathbf{x}'_0$ satisfying $\mathbf{x}_0, \mathbf{x}'_0 \in \mathbb{B}_{\mathbf{z}}(\gamma)$ and $\mathbf{x}_0 - \mathbf{x}'_0 = \omega \cdot \mathbf{v}$ for some $0 < \omega \leq 2\gamma$. Then, the two sequences $\{\mathbf{x}_t\}_{t=0}^T$ and $\{\mathbf{x}'_t\}_{t=0}^T$ generated by GD updates with constant stepsize $\eta \leq \frac{1}{L}$ satisfy the following property within $T \leq \frac{2}{\eta\sqrt{\rho\epsilon}} \log(\frac{1}{\omega})$ iterations:*

$$\min\{f(\mathbf{x}_T), f(\mathbf{x}'_T)\} - f(\mathbf{z}) \leq -\frac{\epsilon^{3/2}}{576\sqrt{\rho}} \log^{-3}\left(\frac{1}{\omega}\right) + \epsilon\gamma + \frac{L}{2}\gamma^2. \quad (27)$$

Proof To streamline the presentation, let us define the following quantity:

$$\phi := \frac{\sqrt{\epsilon}}{6\sqrt{\rho} \log(\frac{1}{\omega})}. \quad (28)$$

Let T be the first iteration satisfying $\max\{\|\mathbf{x}_T - \mathbf{z}\|, \|\mathbf{x}'_T - \mathbf{z}\|\} \geq \phi$. First, we show that $T \leq \frac{2}{\eta\sqrt{\rho\epsilon}} \log(\frac{1}{\omega})$. Evidently, we have $\max\{\|\mathbf{x}_t - \mathbf{z}\|, \|\mathbf{x}'_t - \mathbf{z}\|\} < \phi$ for all $0 \leq t \leq T-1$. We denote $\delta_t = \mathbf{x}_t - \mathbf{x}'_t$, $\mathbf{H} = \nabla^2 f(\mathbf{z})$, and $\Delta_t = \int_0^1 (\nabla^2 f(\mathbf{x}'_t + s\delta_t) - \mathbf{H}) ds$. Then, for every $0 \leq t \leq T-1$, we have

$$\|\Delta_t\| \leq \int_0^1 \rho \|\mathbf{x}'_t + s\delta_t - \mathbf{z}\| ds \leq \rho \max\{\|\mathbf{x}_t - \mathbf{z}\|, \|\mathbf{x}'_t - \mathbf{z}\|\} < \rho\phi, \quad (29)$$

where we use the Hessian Lipschitzness in the first inequality. By the Fundamental Theorem of Calculus, we have $\nabla f(\mathbf{x}_{t-1}) - \nabla f(\mathbf{x}'_{t-1}) = \mathbf{H}\delta_{t-1} + \mathbf{\Delta}_{t-1}\delta_{t-1}$, which in turn implies

$$\begin{aligned}\delta_t &= \delta_{t-1} - \eta(\nabla f(\mathbf{x}_{t-1}) - \nabla f(\mathbf{x}'_{t-1})) \\ &= (\mathbf{I} - \eta\mathbf{H})\delta_{t-1} - \eta\mathbf{\Delta}_{t-1}\delta_{t-1} \\ &= (\mathbf{I} - \eta\mathbf{H})^t\delta_0 - \eta\sum_{s=0}^{t-1}(\mathbf{I} - \eta\mathbf{H})^{t-s-1}\mathbf{\Delta}_s\delta_s.\end{aligned}\tag{30}$$

Upon defining $p_t := \|(\mathbf{I} - \eta\mathbf{H})^t\delta_0\|$ and $q_t := \left\|\eta\sum_{s=0}^{t-1}(\mathbf{I} - \eta\mathbf{H})^{t-s-1}\mathbf{\Delta}_s\delta_s\right\|$, the above equality implies that

$$p_t - q_t \leq \|\delta_t\| \leq p_t + q_t.\tag{31}$$

Therefore, to control $\|\delta_t\|$, it suffices to control p_t and q_t separately. Since $\mathbf{x}_0 - \mathbf{x}'_0 = \omega \cdot \mathbf{v}$ where \mathbf{v} is the eigenvector corresponding to the most negative eigenvalue of $\nabla^2 f(\mathbf{z})$, we have

$$p_t = (1 - \eta\lambda_{\min})^t\omega \geq (1 + \eta\sqrt{\rho\epsilon})^t\omega,\tag{32}$$

where we denote $\lambda_{\min} := \lambda_{\min}(\nabla^2 f(\mathbf{z})) \leq -\sqrt{\rho\epsilon}$. Next, we use induction to show that $q_t \leq \frac{1}{2}p_t$ for all $0 \leq t \leq T$. Indeed, the base case for $t = 0$ holds since $q_0 = 0$. Now, suppose that $q_s \leq \frac{1}{2}p_s$ for all $0 \leq s \leq t-1$. Then, an upper bound on q_t can be derived as follows

$$\begin{aligned}q_t &\leq \eta\sum_{s=0}^{t-1}\left\|(\mathbf{I} - \eta\mathbf{H})^{t-s-1}\right\|\|\mathbf{\Delta}_s\|\|\delta_s\| \\ &\leq \eta\sum_{s=0}^{t-1}(1 - \eta\lambda_{\min})^{t-s-1}\|\mathbf{\Delta}_s\|\|\delta_s\| \\ &\stackrel{(a)}{\leq} \rho\phi \cdot \eta\sum_{s=0}^{t-1}(1 - \eta\lambda_{\min})^{t-s-1} \cdot \frac{3}{2}p_s \\ &\leq \frac{3}{2}\eta\rho\phi \cdot \sum_{s=0}^{t-1}(1 - \eta\lambda_{\min})^{t-s-1} \cdot (1 - \eta\lambda_{\min})^s p_0 \\ &= \frac{3}{2}\eta t\rho\phi \cdot p_{t-1} \\ &\stackrel{(b)}{\leq} \frac{1}{2}p_t.\end{aligned}\tag{33}$$

Here in (a), we use $\|\mathbf{\Delta}_t\| \leq \rho\phi$ and the assumption $\|\delta_s\| \leq p_s + q_s \leq \frac{3}{2}p_s$ for all $0 \leq s \leq t-1$.

In (b), we use the fact that $t \leq \frac{2}{\eta\sqrt{\rho\epsilon}}\log\left(\frac{1}{\omega}\right)$ and $\phi = \frac{\sqrt{\epsilon}}{6\sqrt{\rho}}\log^{-1}\left(\frac{1}{\omega}\right) \leq \frac{1}{4}$, which implies

$$\eta t\rho\phi \leq \eta \cdot \frac{2}{\eta\sqrt{\rho\epsilon}}\log\left(\frac{4\phi}{\omega}\right) \cdot \rho \cdot \frac{\sqrt{\epsilon}}{6\sqrt{\rho}}\log^{-1}\left(\frac{1}{\omega}\right) \leq \frac{1}{3}.\tag{34}$$

Provided with this result, we further have

$$\|\delta_t\| \geq p_t - q_t \geq \frac{1}{2}p_t \geq \frac{1}{2}(1 + \eta\sqrt{\rho\epsilon})^t\omega.\tag{35}$$

Therefore, within $T = \log\left(\frac{4\phi}{\omega}\right) / \log(1 + \eta\sqrt{\rho\epsilon})$ iterations, we must have $\|\delta_T\| \geq 2\phi$. Note that $\phi \leq \frac{1}{4}$ and $\log(1 + \eta\sqrt{\rho\epsilon}) \geq \frac{\eta\sqrt{\rho\epsilon}}{1 + \eta\sqrt{\rho\epsilon}} \geq \frac{1}{2}\eta\sqrt{\rho\epsilon}$. Hence, we have $T \leq \frac{2}{\eta\sqrt{\rho\epsilon}}\log\left(\frac{1}{\omega}\right)$. This further implies

$$\max\{\|\mathbf{x}_T - \mathbf{z}\|, \|\mathbf{x}'_T - \mathbf{z}\|\} \geq \frac{\|\mathbf{x}_T - \mathbf{x}'_T\|}{2} = \frac{1}{2}\|\delta_T\| \geq \phi.\tag{36}$$

Now, without loss of generality, assume $\|\mathbf{x}_T - \mathbf{z}\| \geq \phi$. Then, we have $\|\mathbf{x}_T - \mathbf{x}_0\| \geq \phi - \gamma \geq \frac{1}{2}\phi$, and Lemma 13 implies that

$$f(\mathbf{x}_T) - f(\mathbf{x}_0) \leq -\frac{1}{8\eta T} \cdot \phi^2 \leq -\frac{\epsilon^{3/2}}{576\sqrt{\rho}} \log^{-3}\left(\frac{1}{\omega}\right), \quad (37)$$

where the last inequality follows from the provided upper bound on T and the definition of ϕ . On the other hand, we have

$$f(\mathbf{x}_0) - f(\mathbf{z}) \leq \langle \nabla f(\mathbf{z}), \mathbf{x}_0 - \mathbf{z} \rangle + \frac{L}{2} \|\mathbf{x}_0 - \mathbf{z}\|^2 \leq \epsilon\gamma + \frac{L}{2}\gamma^2. \quad (38)$$

Combining the above two inequalities leads to

$$f(\mathbf{x}_T) - f(\mathbf{z}) \leq -\frac{\epsilon^{3/2}}{576\sqrt{\rho}} \log^{-3}\left(\frac{1}{\omega}\right) + \epsilon\gamma + \frac{L}{2}\gamma^2, \quad (39)$$

which is the desired result. \square

To proceed, we define the “stuck region” as follows

$$\begin{aligned} \mathcal{X}_{\text{stuck}} &:= \{\mathbf{x}_0 \in \mathbb{B}_{\mathbf{z}}(\gamma) : f(\mathbf{x}_T) - f(\mathbf{z}) \geq -F \\ &\quad \text{where } \mathbf{x}_{t+1} = \mathbf{x}_t - \eta \nabla f(\mathbf{x}_t), \forall 0 \leq t \leq T-1\}. \end{aligned} \quad (40)$$

Here $F = \frac{\epsilon^{3/2}}{4608\sqrt{\rho}(\log^3(\frac{1}{\gamma}) + \log^3(\frac{\rho d \Delta_f}{\chi \epsilon}))}$ and $T = \frac{2}{\eta\sqrt{\rho}\epsilon} \log(\frac{1}{\omega})$. Our next lemma shows that the probability of $\mathbf{x}_0 \sim \text{Unif}(\mathbb{B}_{\mathbf{z}}(\gamma))$ falling within the stuck region is small.

Lemma 15 *Consider the setting of Lemma 14. Suppose that $\omega = \sqrt{\frac{2\pi}{d+1}} \frac{\chi}{N_{\text{perturb}}} \gamma$ and $\gamma = O\left(\min\left\{\sqrt{\frac{\epsilon}{\rho}} \log^{-4}\left(\frac{\rho d \Delta_f}{\chi \epsilon}\right), \frac{\epsilon}{L}\right\}\right)$. Then, for $\mathbf{x}_0 \sim \text{Unif}(\mathbb{B}_{\mathbf{z}}(\gamma))$, we have*

$$\mathbb{P}(\mathbf{x}_0 \in \mathcal{X}_{\text{stuck}}) \leq \frac{\chi}{N_{\text{perturb}}}. \quad (41)$$

Proof Using Lemma 14, we show that for any two GD sequences with initial points $\mathbf{x}_0, \mathbf{x}'_0 \in \mathbb{B}_{\mathbf{z}}(\gamma)$ satisfying $\mathbf{x}_0 - \mathbf{x}'_0 = \omega \mathbf{v}$, at least one of them lies outside the stuck region. To this goal, we write

$$\begin{aligned} \min\{f(\mathbf{x}_T), f(\mathbf{x}'_T)\} - f(\mathbf{z}) &\leq -\frac{\epsilon^{3/2}}{576\sqrt{\rho}} \log^{-3}\left(\frac{1}{\omega}\right) + \epsilon\gamma + \frac{L}{2}\gamma^2 \\ &\stackrel{(a)}{\leq} -\frac{\epsilon^{3/2}}{2304\sqrt{\rho}(\log^3(\frac{1}{\gamma}) + \log^3(\frac{\rho d \Delta_f}{\chi \epsilon}))} + \epsilon\gamma + \frac{L}{2}\gamma^2 \\ &\stackrel{(b)}{\leq} -\frac{\epsilon^{3/2}}{4608\sqrt{\rho}(\log^3(\frac{1}{\gamma}) + \log^3(\frac{\rho d \Delta_f}{\chi \epsilon}))} = -F. \end{aligned} \quad (42)$$

Here in (a), we use the fact that $\omega = \sqrt{\frac{2\pi}{d+1}} \frac{\chi}{N_{\text{perturb}}} \gamma$ and Equation (23). Moreover, (b) follows from the facts that $L\gamma^2 = O(\epsilon\gamma)$ since $\gamma = O(\frac{\epsilon}{L})$ and $\epsilon\gamma = O\left(\frac{\epsilon^{3/2}}{\sqrt{\rho}(\log^3(\frac{1}{\gamma}) + \log^3(\frac{\rho d \Delta_f}{\chi \epsilon}))}\right)$

since $\gamma = O\left(\sqrt{\frac{\epsilon}{\rho}} \log^{-3}\left(\frac{\rho d \Delta_f}{\chi \epsilon}\right)\right)$. This implies that the width of the stuck region in the direction \mathbf{v} is at most ω . Hence, we can control $\mathbb{P}(\mathbf{x}_0 \in \mathcal{X}_{\text{stuck}})$ as follows

$$\begin{aligned} \mathbb{P}(\mathbf{x}_0 \in \mathcal{X}_{\text{stuck}}) &= \frac{\text{vol}(\mathcal{X}_{\text{stuck}})}{\text{vol}(\mathbb{B}^d(\gamma))} \leq \frac{\omega \cdot \text{vol}(\mathbb{B}^{d-1}(\gamma))}{\text{vol}(\mathbb{B}^d(\gamma))} = \frac{\omega \Gamma(d/2 + 1)}{\sqrt{\pi} \gamma \Gamma(d/2 + 1/2)} \leq \frac{\omega}{\gamma} \sqrt{\frac{d+1}{2\pi}} \\ &\leq \frac{\chi}{N_{\text{perturb}}}. \end{aligned} \quad (43)$$

Here, $\text{vol}(\mathcal{X})$ denotes the volume of the set \mathcal{X} . For the d -dimensional unit ball, we have $\text{vol}(\mathbb{B}^d(1)) = \frac{\pi^{d/2}}{\Gamma(\frac{d}{2}+1)}$, where $\Gamma(\cdot)$ is the Gamma function defined as $\Gamma\left(\frac{d}{2} + 1\right) = \sqrt{\pi} \left(d - \frac{1}{2}\right) \cdot \left(d - \frac{3}{2}\right) \cdots \frac{1}{2}$ for $d = 1, 2, \dots$. Moreover, in the second inequality, we use $\frac{\Gamma(x+1)}{\Gamma(x+1/2)} < \sqrt{x + \frac{1}{2}}$ for all $x \geq 0$. \square

We are now ready to provide the proof of Proposition 12.

Proof of Proposition 12 The proof is immediately implied by Lemma 15, after noting that $T = \frac{2}{\eta\sqrt{\rho\epsilon}} \log(\frac{1}{\omega}) \leq \frac{4}{\eta\sqrt{\rho\epsilon}} \left(\log\left(\frac{1}{\gamma}\right) + \log\left(\frac{\rho d \Delta_f}{\chi \epsilon}\right)\right) \leq T_{\text{escape}}$. \square

4 Establishing Implicit Regularization of IPGD

To establish the implicit regularization of IPGD, we first show how the deviation rate (Definition 5) governs the residual norm dynamic, as outlined in Proposition 4. First, we present a basic property of projection operator $\mathcal{P}_{\mathcal{M}}^\perp(\cdot)$:

Lemma 16 *For any $\mathbf{x}, \mathbf{y} \in \mathbb{R}^d$, we have $\|\mathcal{P}_{\mathcal{M}}^\perp(\mathbf{x} + \mathbf{y})\| \leq \|\mathcal{P}_{\mathcal{M}}^\perp(\mathbf{x})\| + \|\mathbf{y}\|$.*

Proof Upon defining $\mathbf{u}^* = \arg \min_{\mathbf{u} \in \mathcal{M}} \|\mathbf{u} - (\mathbf{x} + \mathbf{y})\|$ and $\mathbf{v}^* = \arg \min_{\mathbf{v} \in \mathcal{M}} \|\mathbf{v} - \mathbf{x}\|$, we have:

$$\|\mathcal{P}_{\mathcal{M}}^\perp(\mathbf{x} + \mathbf{y})\| = \|\mathbf{u}^* - (\mathbf{x} + \mathbf{y})\| \leq \|\mathbf{v}^* - (\mathbf{x} + \mathbf{y})\| \leq \|\mathbf{v}^* - \mathbf{x}\| + \|\mathbf{y}\| = \|\mathcal{P}_{\mathcal{M}}^\perp(\mathbf{x})\| + \|\mathbf{y}\|, \quad (44)$$

which completes the proof. \square

Our next lemma provides a useful control over the dynamic of $\|\mathbf{x}_{t+1}^\perp\|$:

Lemma 17 (Upper bound on the residual norm) *Suppose that conditions of Proposition 4 are satisfied. Then, we have:*

$$\|\mathbf{x}_{t+1}^\perp\| \leq \left\| \left(\mathbf{I} - \eta \nabla^2 f(\mathbf{x}_t^\sharp) \right) \mathbf{x}_t^\perp \right\| + \frac{\eta \rho}{2} \|\mathbf{x}_t^\perp\|^2. \quad (45)$$

Proof We first decompose \mathbf{x}_{t+1} as follows:

$$\mathbf{x}_{t+1} = \mathbf{x}_t^\sharp - \eta \nabla f(\mathbf{x}_t^\sharp) + \mathbf{x}_t^\perp - \eta \left(\nabla f(\mathbf{x}_t) - \nabla f(\mathbf{x}_t^\sharp) \right). \quad (46)$$

Applying the projection $\mathcal{P}_{\mathcal{M}}^\perp(\cdot)$ to both sides, we obtain

$$\begin{aligned} \|\mathbf{x}_{t+1}^\perp\| &= \|\mathcal{P}_{\mathcal{M}}^\perp(\mathbf{x}_{t+1})\| \\ &= \left\| \mathcal{P}_{\mathcal{M}}^\perp \left(\mathbf{x}_t^\sharp - \eta \nabla f(\mathbf{x}_t^\sharp) + \mathbf{x}_t^\perp - \eta \left(\nabla f(\mathbf{x}_t) - \nabla f(\mathbf{x}_t^\sharp) \right) \right) \right\| \\ &\leq \left\| \mathcal{P}_{\mathcal{M}}^\perp \left(\mathbf{x}_t^\sharp - \eta \nabla f(\mathbf{x}_t^\sharp) \right) \right\| + \left\| \mathbf{x}_t^\perp - \eta \left(\nabla f(\mathbf{x}_t) - \nabla f(\mathbf{x}_t^\sharp) \right) \right\|, \end{aligned} \quad (47)$$

where the inequality follows from Lemma 16. Since $\mathbf{x}_t^\sharp \in \mathcal{M}$ and \mathcal{M} is assumed to be closed under GD updates, we have $\left\| \mathcal{P}_{\mathcal{M}}^\perp \left(\mathbf{x}_t^\sharp - \eta \nabla f(\mathbf{x}_t^\sharp) \right) \right\| = 0$, which implies:

$$\|\mathbf{x}_{t+1}^\perp\| \leq \left\| \mathbf{x}_t^\perp + \eta \left(\nabla f(\mathbf{x}_t^\sharp) - \nabla f(\mathbf{x}_t) \right) \right\|. \quad (48)$$

Applying the Fundamental Theorem of Calculus to the above inequality leads to:

$$\begin{aligned} \|\mathbf{x}_{t+1}^\perp\| &\leq \left\| \left(\mathbf{I} - \eta \int_0^1 \nabla^2 f \left(\mathbf{x}_t^\sharp + \tau \mathbf{x}_t^\perp \right) d\tau \right) \mathbf{x}_t^\perp \right\| \\ &\leq \left\| \left(\mathbf{I} - \eta \nabla^2 f(\mathbf{x}_t^\sharp) \right) \mathbf{x}_t^\perp \right\| + \eta \left(\int_0^1 \left\| \nabla^2 f \left(\mathbf{x}_t^\sharp + \tau \mathbf{x}_t^\perp \right) - \nabla^2 f(\mathbf{x}_t^\sharp) \right\| d\tau \right) \|\mathbf{x}_t^\perp\| \\ &\leq \left\| \left(\mathbf{I} - \eta \nabla^2 f(\mathbf{x}_t^\sharp) \right) \mathbf{x}_t^\perp \right\| + \frac{\eta \rho}{2} \|\mathbf{x}_t^\perp\|^2. \end{aligned} \quad (49)$$

where in the last inequality, we use the local Hessian-Lipschitzness of f . \square

Equipped with Lemma 17, we are now ready to present the proof of Proposition 4.

Proof of Proposition 4 Due to Lemma 17, the result trivially holds if $\|\mathbf{x}_t^\perp\| = 0$. Therefore, we assume $\|\mathbf{x}_t^\perp\| > 0$. Let $\lambda_1 \geq \lambda_2 \geq \dots \geq \lambda_d$ denote the eigenvalues of $\nabla^2 f(\mathbf{x}^\sharp)$ with the corresponding eigenvectors $\mathbf{v}_1, \mathbf{v}_2, \dots, \mathbf{v}_d$. One can write:

$$\begin{aligned} \left\| \left(\mathbf{I} - \eta \nabla^2 f(\mathbf{x}_t^\sharp) \right) \mathbf{x}_t^\perp \right\|^2 &= \left\| \sum_{i=1}^d (1 - \eta \lambda_i) \langle \mathbf{v}_i, \mathbf{x}_t^\perp \rangle \mathbf{v}_i \right\|^2 \\ &= \sum_{i=1}^d (1 - \eta \lambda_i)^2 \langle \mathbf{v}_i, \mathbf{x}_t^\perp \rangle^2 \\ &= \sum_{i=1}^d \left(1 - 2\eta \lambda_i + \eta^2 \lambda_i^2 \right) \langle \mathbf{v}_i, \mathbf{x}_t^\perp \rangle^2. \end{aligned} \quad (50)$$

On the other hand, since $\eta \leq \frac{1}{L}$, we have $\eta^2 \lambda_i^2 \leq \eta |\lambda_i|$, which implies:

$$\begin{cases} 1 - 2\eta \lambda_i + \eta^2 \lambda_i^2 \leq 1 - \eta \lambda_i, & \text{if } \lambda_i > 0, \\ 1 - 2\eta \lambda_i + \eta^2 \lambda_i^2 \leq 1 - 3\eta \lambda_i, & \text{if } \lambda_i < 0. \end{cases} \quad (51)$$

Therefore, we have

$$\begin{aligned}
& \left\| \left(\mathbf{I} - \eta \nabla^2 f(\mathbf{x}_t^\sharp) \right) \mathbf{x}_t^\perp \right\|^2 \\
& \leq \sum_{i:\lambda_i > 0} (1 - \eta \lambda_i) \left\langle \mathbf{v}_i, \mathbf{x}_t^\perp \right\rangle^2 + \sum_{i:\lambda_i < 0} (1 - 3\eta \lambda_i) \left\langle \mathbf{v}_i, \mathbf{x}_t^\perp \right\rangle^2 \\
& = \left\| \mathbf{x}_t^\perp \right\|^2 + \eta \left(- \sum_{i:\lambda_i > 0} \lambda_i \left\langle \mathbf{v}_i, \mathbf{x}_t^\perp \right\rangle^2 - \sum_{i:\lambda_i < 0} 3\lambda_i \left\langle \mathbf{v}_i, \mathbf{x}_t^\perp \right\rangle^2 \right) \\
& \stackrel{(a)}{=} \left\| \mathbf{x}_t^\perp \right\|^2 + \eta \left(- \left\langle \mathbf{x}_t^\perp, \nabla_+^2 f(\mathbf{x}_t^\sharp) \mathbf{x}_t^\perp \right\rangle - 3 \left\langle \mathbf{x}_t^\perp, \nabla_-^2 f(\mathbf{x}_t^\sharp) \mathbf{x}_t^\perp \right\rangle \right) \\
& = \left\| \mathbf{x}_t^\perp \right\|^2 + \eta \left(\frac{-1}{\left\| \mathbf{x}_t^\perp \right\|^2} \left\langle \mathbf{x}_t^\perp, \nabla_+^2 f(\mathbf{x}_t^\sharp) \mathbf{x}_t^\perp \right\rangle + \frac{-3}{\left\| \mathbf{x}_t^\perp \right\|^2} \left\langle \mathbf{x}_t^\perp, \nabla_-^2 f(\mathbf{x}_t^\sharp) \mathbf{x}_t^\perp \right\rangle \right) \left\| \mathbf{x}_t^\perp \right\|^2 \\
& \stackrel{(b)}{=} \left\| \mathbf{x}_t^\perp \right\|^2 + \eta (r_-(\mathbf{x}_t) + 3r_+(\mathbf{x}_t)) \left\| \mathbf{x}_t^\perp \right\|^2 \\
& \stackrel{(c)}{=} (1 + \eta r(\mathbf{x}_t)) \left\| \mathbf{x}_t^\perp \right\|^2.
\end{aligned} \tag{52}$$

Here, (a) follows from the definitions of the PSD and NSD components of the Hessian. Additionally, (b) and (c) follow from the definition of the deviation rate. This implies that:

$$\left\| \left(\mathbf{I} - \eta \nabla^2 f(\mathbf{x}_t^\sharp) \right) \mathbf{x}_t^\perp \right\| \leq \sqrt{1 + \eta r(\mathbf{x}_t)} \left\| \mathbf{x}_t^\perp \right\| \leq \left(1 + \frac{\eta}{2} r(\mathbf{x}_t) \right) \left\| \mathbf{x}_t^\perp \right\|. \tag{53}$$

This inequality combined with Lemma 17 completes the proof. \square

We now proceed with the proof of Theorem 5. To this end, we first revisit the steps of IPGD. At each iteration, IPGD performs one of the following two operations: 1) GD update, or 2) addition of a small perturbation. For the GD update, we can directly apply Proposition 4 to control the residual norm. For the small perturbation step, we can only invoke a conservative bound $\left\| \mathbf{x}_{t+1}^\perp \right\| \leq \left\| \mathbf{x}_t^\perp \right\| + \gamma$. The next lemma combines these two cases and establishes a uniform upper bound on the residual norm across all iterations via an auxiliary sequence.

Lemma 18 *Suppose that the conditions of Proposition 4 are satisfied for all $0 \leq t \leq T$. Define the sequence:*

$$a_{t+1} = \left(1 + \frac{\eta}{2} R(\tau) + \frac{\eta \rho}{2} a_t \right) a_t, \quad \text{with } a_0 = \left\| \mathbf{x}_0^\perp \right\| + N_{\text{perturb}} \cdot \gamma. \tag{54}$$

Then, the residual norm satisfies $\left\| \mathbf{x}_t^\perp \right\| \leq a_t$ for every $t = 0, 1, \dots, T$.

Proof Let $t_1 \leq \dots \leq t_{N_{\text{perturb}}}$ be the iteration indices at which the perturbations are added. Define the series $\{b_t\}_{t=0}^T$ with $b_0 = \left\| \mathbf{x}_0^\perp \right\|$ and

$$b_{t+1} = \begin{cases} \left(1 + \frac{\eta}{2} R(\tau) + \frac{\eta \rho}{2} b_t \right) b_t & t \notin \{t_1, \dots, t_{N_{\text{perturb}}}\}, \\ \left(1 + \frac{\eta}{2} R(\tau) + \frac{\eta \rho}{2} (b_t + \gamma) \right) (b_t + \gamma) & t \in \{t_1, \dots, t_{N_{\text{perturb}}}\}. \end{cases} \tag{55}$$

According to Proposition 4, we have $\left\| \mathbf{x}_t^\perp \right\| \leq b_t$ for every t . Therefore, it suffices to show that $b_t \leq a_t$ for every t . To this end, we argue that shifting the perturbations to earlier iterations

can only increase the elements of the sequence. Without loss of generality, assume that $t_{N_{\text{perturb}}} > 0$; otherwise, the claim follows immediately. Now, consider a modified sequence $\{b'_t\}_{t=0}^T$, where the index of the last perturbation is shifted one step earlier. Specifically, we define $b'_t = b_t$ for all $t \leq t_{N_{\text{perturb}}} - 1$, and apply the last perturbation at iteration $t_{N_{\text{perturb}}} - 1$. By doing so, we have

$$\begin{aligned} b'_{t_{N_{\text{perturb}}}} &= \left(1 + \frac{\eta}{2}R(\tau) + \frac{\eta\rho}{2}(b_{t_{N_{\text{perturb}}} - 1} + \gamma)\right)(b_{t_{N_{\text{perturb}}} - 1} + \gamma) \\ &\geq \left(1 + \frac{\eta}{2}R(\tau) + \frac{\eta\rho}{2}b_{t_{N_{\text{perturb}}} - 1}\right)b_{t_{N_{\text{perturb}}} - 1} + \gamma \\ &= b_{t_{N_{\text{perturb}}}} + \gamma. \end{aligned} \quad (56)$$

This implies that

$$\begin{aligned} b'_{t_{N_{\text{perturb}}} + 1} &= \left(1 + \frac{\eta}{2}R(\tau) + \frac{\eta\rho}{2}b'_{t_{N_{\text{perturb}}}}\right)b'_{t_{N_{\text{perturb}}}} \\ &\geq \left(1 + \frac{\eta}{2}R(\tau) + \frac{\eta\rho}{2}(b_{t_{N_{\text{perturb}}} - 1} + \gamma)\right)(b_{t_{N_{\text{perturb}}} - 1} + \gamma) \\ &\geq b_{t_{N_{\text{perturb}}} + 1}. \end{aligned} \quad (57)$$

Note that both sequences $\{b_t\}_{t=0}^T$ and $\{b'_t\}_{t=0}^T$ follow the GD updates for $t \geq t_{N_{\text{perturb}}} + 1$ (i.e., no perturbations are added after iteration $t_{N_{\text{perturb}}}$). Therefore, we must have $b'_t \geq b_t$ for $t \geq t_{N_{\text{perturb}}} + 1$. Combined with the fact that $b'_t = b_t$ for all $t \leq t_{N_{\text{perturb}}} - 1$, it follows that $b'_t \geq b_t$ for $0 \leq t \leq T$. By repeating this procedure and shifting all the perturbations to iteration $t = 0$, we establish that $a_t \geq b_t$ for $0 \leq t \leq T$, thereby completing the proof. \square

Our next lemma provides an upper bound for the sequence $\{a_t\}_{t=0}^T$.

Lemma 19 Suppose that $T = O\left(\frac{\Delta_f}{\eta\epsilon^2}\left(\log^4\left(\frac{1}{\gamma}\right) + \log^4\left(\frac{\rho d \Delta_f}{\chi\epsilon}\right)\right)\right)$ and $R(\tau) = O\left(\frac{1}{\eta T}\right)$. Then, for the sequence defined in Lemma 18, we have

$$a_t \leq a_0 \left(1 + \eta R(\tau) + \frac{1}{T}\right)^t, \quad t = 0, 1, \dots, T. \quad (58)$$

Proof of Lemma 19 Note that $a_{t+1} = a_0 \prod_{s=0}^t (1 + \eta R(\tau) + \eta \rho a_s)$. Hence, it suffices to prove $a_t \leq \frac{1}{\eta \rho T}$ for all $0 \leq t \leq T - 1$. We prove this by induction on t . It is easy to verify the base case $t = 0$. Now, assume that $a_s \leq \frac{1}{\eta \rho T}$ for all $0 \leq s \leq t$. Then, we have

$$\begin{aligned} a_{t+1} &= a_0 \prod_{s=0}^t (1 + \eta R(\tau) + \eta \rho a_s) \\ &\leq a_0 \left(1 + \eta R(\tau) + \frac{1}{T}\right)^t \\ &\stackrel{(a)}{\leq} a_0 \exp\left\{\eta R(\tau)t + \frac{t}{T}\right\} \\ &\stackrel{(b)}{\leq} 10a_0 \\ &\stackrel{(c)}{\leq} \frac{1}{\eta \rho T}, \end{aligned} \quad (59)$$

where (a) is due to $1 + x \leq \exp\{x\}$ for all $x \in \mathbb{R}$. Moreover, (b) is due to the condition that $R(\tau) = O\left(\frac{1}{\eta T}\right)$. Lastly, (c) follows from

$$a_0 = \|\mathbf{x}_0^\perp\| + N_{\text{perturb}} \cdot \gamma \leq \frac{1}{20\eta\rho T} + \frac{C\sqrt{\rho}\Delta_f \left(\log^3\left(\frac{1}{\gamma}\right) + \log^3\left(\frac{\rho d\Delta_f}{\chi\epsilon}\right)\right)}{\epsilon^{3/2}} \cdot \gamma \leq \frac{1}{10\eta\rho T} \quad (60)$$

where we use the facts that $T = O\left(\frac{\Delta_f}{\eta\epsilon^2} \left(\log^4\left(\frac{1}{\gamma}\right) + \log^4\left(\frac{\rho d\Delta_f}{\chi\epsilon}\right)\right)\right)$, and $\gamma = O\left(\frac{\epsilon^{7/2}}{\rho^{3/2}\Delta_f^2} \log^{-7}\left(\frac{\rho d\Delta_f}{\chi\epsilon}\right)\right)$. This completes the proof. \square

Now we are ready to provide the proof of Theorem 5.

Proof of Theorem 5 First, according to Lemmas 18 and 19, we have that for all $0 \leq t \leq T$,

$$\|\mathbf{x}_t^\perp\| \leq a_t \leq \left(\|\mathbf{x}_0^\perp\| + N_{\text{perturb}} \cdot \gamma\right) \left(1 + \eta R(\tau) + \frac{1}{T}\right)^t \leq \frac{\epsilon}{L}, \quad (61)$$

where the final inequality uses the facts that $\|\mathbf{x}_0^\perp\| \leq \frac{\epsilon}{10L}$, $N_{\text{perturb}} = \frac{C\sqrt{\rho}\Delta_f \left(\log^3\left(\frac{1}{\gamma}\right) + \log^3\left(\frac{\rho d\Delta_f}{\chi\epsilon}\right)\right)}{\epsilon^{3/2}}$, $\gamma = O\left(\frac{\epsilon^{5/2}}{\sqrt{\rho}L\Delta_f} \log^{-3}\left(\frac{\rho d\Delta_f}{\chi\epsilon}\right)\right)$, and $R(\tau) = O\left(\frac{1}{\eta T}\right)$. Given the fact $\|\mathbf{x}_t^\perp\| \leq \frac{\epsilon}{L}$ for all $0 \leq t \leq T$, the gradient and Hessian of the objective function remain Lipschitz continuous along the entire trajectory $\{\mathbf{x}_t\}_{t=0}^T$. Thus, we can apply Theorem 2, which guarantees that, under the stated conditions, with probability at least $1 - \chi$, IPGD outputs a point \mathbf{x}_T that is an ϵ -SOSP after $T = O\left(\frac{\Delta_f}{\eta\epsilon^2} \left(\log^4\left(\frac{1}{\gamma}\right) + \log^4\left(\frac{\rho d\Delta_f}{\chi\epsilon}\right)\right)\right)$ iterations. Combining the above two results ensures that \mathbf{x}_T is an ϵ - \mathcal{M} -SOSP. \square

5 Establishing Improved Convergence of IPGD with Additional Structures

In this section, we present the proofs of the improved convergence results for IPGD stated in Section 2.3. We start with the proof of Proposition 6.

Proof of Proposition 6 The proof of Theorem 5 can be easily modified to show that, with probability at least $1 - \chi$, after $T = O\left(\frac{\Delta_f}{\eta\epsilon^2} \left(\log^4(1/\gamma) + \log^4\left(\frac{\rho d\Delta_f}{\chi\epsilon}\right)\right)\right)$ iterations, IPGD returns a solution \mathbf{x}_T that satisfies

$$\|\mathbf{x}_T^\perp\| \leq \frac{\epsilon}{L}, \quad \mathbf{x}_T \text{ is an } \bar{\epsilon}\text{-}\mathcal{M}\text{-SOSP.} \quad (62)$$

The details of this modification are omitted for brevity. Hence, we have

$$\|\nabla f(\mathbf{x}_T^\sharp)\| \leq \|\nabla f(\mathbf{x}_T)\| + \|\nabla f(\mathbf{x}_T) - \nabla f(\mathbf{x}_T^\sharp)\| \leq \bar{\epsilon} + L \|\mathbf{x}_T^\perp\| \leq \bar{\epsilon} + \epsilon \leq \bar{\epsilon}_g, \quad (63)$$

and

$$\lambda_{\min}(\nabla^2 f(\mathbf{x}_T^\sharp)) \geq \lambda_{\min}(\nabla^2 f(\mathbf{x}_T)) - \|\nabla^2 f(\mathbf{x}_T) - \nabla^2 f(\mathbf{x}_T^\sharp)\| \geq -\sqrt{\rho\epsilon} - \rho \cdot \frac{\epsilon}{L} \geq -\bar{\epsilon}_H. \quad (64)$$

Here we use the local gradient and Hessian Lipschitzness, which can be used since $\|\mathbf{x}_T^\perp\| \leq \frac{\epsilon}{L}$, $\bar{\epsilon} = \frac{1}{4} \min\{\bar{\epsilon}_g, \bar{\epsilon}_H^2/\rho\}$, and $\epsilon \leq \min\left\{\frac{3}{4}\bar{\epsilon}_g, \frac{L}{2\rho}\bar{\epsilon}_H\right\}$. Finally, since the objective function satisfies the \mathcal{M} -strict saddle property, we have

$$\text{dist}(\mathbf{x}_T^\sharp, \mathcal{X}_\mathcal{M}) \leq \bar{\epsilon}_\mathcal{M}. \quad (65)$$

This completes the proof. \square

Next, we turn to prove Proposition 7. To this goal, we first present the following lemma, which shows that the \mathcal{M} -regularity can be utilized to control the deviation of the iterates from the implicit region.

Lemma 20 *Suppose that the conditions of Proposition 7 are satisfied. Consider the GD updates $\mathbf{x}_{t+1} = \mathbf{x}_t - \eta \nabla f(\mathbf{x}_t)$ for $0 \leq t \leq T$. If $\mathbf{x}_t^\sharp \in \mathcal{N}_{\mathcal{X}_\mathcal{M}}(\zeta)$, then, we have*

$$\text{dist}(\mathbf{x}_{t+1}, \mathcal{X}_\mathcal{M}) \leq \left(1 - \frac{\eta\alpha}{4}\right) \text{dist}(\mathbf{x}_t, \mathcal{X}_\mathcal{M}) + (2 + \eta L) \|\mathbf{x}_t^\perp\|. \quad (66)$$

Proof of Lemma 20 We have

$$\text{dist}(\mathbf{x}_{t+1}, \mathcal{X}_\mathcal{M}) \leq \underbrace{\text{dist}(\mathbf{x}_t^\sharp - \eta \nabla f(\mathbf{x}_t^\sharp), \mathcal{X}_\mathcal{M})}_{(I)} + \underbrace{\|\mathbf{x}_t^\sharp - \eta \nabla f(\mathbf{x}_t^\sharp) - \mathbf{x}_{t+1}\|}_{(II)}. \quad (67)$$

To control (I), we write

$$\begin{aligned} (I)^2 &= \min_{\mathbf{x}^* \in \mathcal{X}_\mathcal{M}} \|\mathbf{x}_t^\sharp - \eta \nabla f(\mathbf{x}_t^\sharp) - \mathbf{x}^*\|^2 \\ &\leq \|\mathbf{x}_t^\sharp - \eta \nabla f(\mathbf{x}_t^\sharp) - \mathcal{P}_{\mathcal{X}_\mathcal{M}}(\mathbf{x}_t^\sharp)\|^2 \\ &= \|\mathbf{x}_t^\sharp - \mathcal{P}_{\mathcal{X}_\mathcal{M}}(\mathbf{x}_t^\sharp)\|^2 + \eta \langle \mathcal{P}_{\mathcal{X}_\mathcal{M}}(\mathbf{x}_t^\sharp) - \mathbf{x}_t^\sharp, \nabla f(\mathbf{x}_t^\sharp) \rangle + \eta^2 \|\nabla f(\mathbf{x}_t^\sharp)\|^2 \\ &\stackrel{(a)}{\leq} \left(1 - \frac{\eta\alpha}{2}\right) \|\mathbf{x}_t^\sharp - \mathcal{P}_{\mathcal{X}_\mathcal{M}}(\mathbf{x}_t^\sharp)\|^2 + \left(\eta^2 - \frac{\eta}{2\beta}\right) \|\nabla f(\mathbf{x}_t^\sharp)\|^2 \\ &\stackrel{(b)}{\leq} \left(1 - \frac{\eta\alpha}{2}\right) \|\mathbf{x}_t^\sharp - \mathcal{P}_{\mathcal{X}_\mathcal{M}}(\mathbf{x}_t^\sharp)\|^2, \end{aligned} \quad (68)$$

where in (a), we use the \mathcal{M} -regularity since $\mathbf{x}_t^\sharp \in \mathcal{N}_{\mathcal{X}_\mathcal{M}}(\zeta) \cap \mathcal{M}$, and in (b), we use $\eta \leq \frac{1}{2\beta}$. Therefore, we derive

$$(I) \leq \sqrt{1 - \frac{\eta\alpha}{2}} \text{dist}(\mathbf{x}_t^\sharp, \mathcal{X}_\mathcal{M}) \leq \left(1 - \frac{\eta\alpha}{4}\right) \left(\text{dist}(\mathbf{x}_t, \mathcal{X}_\mathcal{M}) + \|\mathbf{x}_t^\perp\|\right). \quad (69)$$

In the last inequality, we use the triangle inequality and the basic inequality $\sqrt{1-x} \leq 1 - \frac{1}{2}x$ for all $x \leq 1$. Next, we control (II) as follows

$$(II) \leq \|\mathbf{x}_t^\perp\| + \eta \|\nabla f(\mathbf{x}_t^\sharp) - \nabla f(\mathbf{x}_t)\| \leq (1 + \eta L) \|\mathbf{x}_t^\perp\|. \quad (70)$$

Combining these two inequalities, we obtain

$$\begin{aligned} \text{dist}(\mathbf{x}_{t+1}, \mathcal{X}_\mathcal{M}) &\leq \left(1 - \frac{\eta\alpha}{4}\right) \left(\text{dist}(\mathbf{x}_t, \mathcal{X}_\mathcal{M}) + \|\mathbf{x}_t^\perp\|\right) + (1 + \eta L) \|\mathbf{x}_t^\perp\| \\ &\leq \left(1 - \frac{\eta\alpha}{4}\right) \text{dist}(\mathbf{x}_t, \mathcal{X}_\mathcal{M}) + (2 + \eta L) \|\mathbf{x}_t^\perp\|. \end{aligned} \quad (71)$$

This completes the proof. \square

The lemma introduces a useful inequality that will be used in the proof of Proposition 7.

Lemma 21 (Adapted from Lemma 47 in [53]) *Suppose that the series $\{a_t\}_{t=0}^\infty$ satisfies $a_{t+1} \leq Ax_t + B, \forall t \geq 0$ where $A > 0, A \neq 1$ and $a_0 + \frac{B}{A-1} \geq 0$. Then, we have*

$$a_t \leq A^t \left(a_0 + \frac{B}{A-1} \right) - \frac{B}{A-1}. \quad (72)$$

We are now ready to present the proof of Proposition 7.

Proof of Proposition 7 First, notice that, for every $0 \leq t \leq T$,

$$\|\mathbf{x}_t^\perp\| \stackrel{(a)}{\leq} \left(1 + \eta R(\tau) + \frac{1}{T} \right)^T \|\mathbf{x}_0^\perp\| \stackrel{(b)}{=} O(\|\mathbf{x}_0^\perp\|) \stackrel{(c)}{=} O\left(\frac{\eta\alpha\epsilon}{L}\right). \quad (73)$$

Here, (a) follows exactly the same steps as the proof of Theorem 5; in (b), we use the assumption $R(\tau) = O\left(\frac{1}{\eta T}\right)$ and the inequality $(1 + x/T)^T \leq \exp(x)$; and (c) is due to our assumption $\|\mathbf{x}_0^\perp\| = O\left(\frac{\eta\alpha\epsilon}{L}\right)$. Now, without loss of generality, assume $\zeta \geq \frac{\epsilon}{2L}$. Otherwise, we immediately obtain $\text{dist}(\mathbf{x}_0, \mathcal{X}_M) \leq \text{dist}(\mathbf{x}_0^\sharp, \mathcal{X}_M) + \|\mathbf{x}_0^\perp\| \leq \frac{\epsilon}{2L} + \frac{\eta\alpha\epsilon}{L} \leq \frac{\epsilon}{L}$ as desired. Next, we prove by induction that $\mathbf{x}_t^\sharp \in \mathcal{N}_{\mathcal{X}_M}(\zeta)$ for all $0 \leq t \leq T$. The induction holds at initialization by construction. Suppose that $\mathbf{x}_t^\sharp \in \mathcal{N}_{\mathcal{X}_M}(\zeta)$. For iteration $t+1$, according to Lemma 20, we have

$$\begin{aligned} \text{dist}(\mathbf{x}_{t+1}, \mathcal{X}_M) &\leq \left(1 - \frac{\eta\alpha}{4} \right) \text{dist}(\mathbf{x}_t, \mathcal{X}_M) + (2 + \eta L) \|\mathbf{x}_t^\perp\| \\ &\leq \left(1 - \frac{\eta\alpha}{4} \right) \text{dist}(\mathbf{x}_t^\sharp, \mathcal{X}_M) + \|\mathbf{x}_t^\perp\| + (2 + \eta L) \|\mathbf{x}_t^\perp\| \\ &\leq \left(1 - \frac{\eta\alpha}{4} \right) \zeta + 4 \max_{0 \leq t \leq T} \|\mathbf{x}_t^\perp\| \\ &\stackrel{(a)}{\leq} \left(1 - \frac{\eta\alpha}{4} \right) \zeta + O\left(\frac{\eta\alpha}{L}\epsilon\right) \\ &\stackrel{(b)}{\leq} \zeta. \end{aligned} \quad (74)$$

In (a), we use Equation (73). Step (b) follows from the assumption that $\zeta \geq \frac{\epsilon}{2L}$. This completes the inductive step. Given that we established $\mathbf{x}_t^\sharp \in \mathcal{N}_{\mathcal{X}_M}(\zeta), 0 \leq t \leq T$, we can invoke Lemma 20 for any $0 \leq t \leq T-1$, which yields

$$\text{dist}(\mathbf{x}_{t+1}, \mathcal{X}_M) \leq \left(1 - \frac{\eta\alpha}{4} \right) \text{dist}(\mathbf{x}_t, \mathcal{X}_M) + (2 + \eta L) \|\mathbf{x}_t^\perp\|. \quad (75)$$

Upon setting $A = 1 - \frac{\eta\alpha}{4}$ and $B = (2 + \eta L) \max_{0 \leq t \leq T} \|\mathbf{x}_t^\perp\|$ in Lemma 21, we have

$$\begin{aligned} \text{dist}(\mathbf{x}_T, \mathcal{X}_M) &\leq \left(1 - \frac{\eta\alpha}{4} \right)^T \text{dist}(\mathbf{x}_0, \mathcal{X}_M) + \frac{8 + 4\eta L}{\eta\alpha} \max_{0 \leq t \leq T} \{\|\mathbf{x}_t^\perp\|\} \\ &\stackrel{(a)}{\leq} \left(1 - \frac{\eta\alpha}{4} \right)^T \cdot 2\zeta + \frac{8 + 4\eta L}{\eta\alpha} \max_{0 \leq t \leq T} \{\|\mathbf{x}_t^\perp\|\} \\ &\stackrel{(b)}{\leq} \left(1 - \frac{\eta\alpha}{4} \right)^T \cdot 2\zeta + \frac{\epsilon}{2L}. \end{aligned} \quad (76)$$

In (a), we use the fact that $\text{dist}(\mathbf{x}_0, \mathcal{X}_{\mathcal{M}}) \leq \text{dist}(\mathbf{x}_0^\sharp, \mathcal{X}_{\mathcal{M}}) + \|\mathbf{x}_0^\perp\| \leq 2\zeta$; and in (b), we use Equation (73) and $\eta \leq \frac{1}{L}$. Thus, within $T = O\left(\frac{1}{\eta\alpha} \log(L\zeta/\epsilon)\right)$ iterations, we have

$$\text{dist}(\mathbf{x}_T, \mathcal{X}_{\mathcal{M}}) \leq \frac{\epsilon}{L}. \quad (77)$$

This completes the proof. \square

Proof of Theorem 8 The proof readily follows by combining Proposition 6 and Proposition 7. \square

6 Application: Over-parameterized Matrix Sensing

In this section, we apply our general framework to the over-parameterized matrix sensing. In this problem, the aim is to recover an $n \times n$ and rank- r PSD matrix \mathbf{M}^* from a set of linear measurements $\{(y_i, \mathbf{A}_i)\}_{i=1}^N$, where $y_i = \langle \mathbf{A}_i, \mathbf{M}^* \rangle$ for $i = 1, \dots, N$. To this end, a common approach is to employ a factorized model $\mathbf{M} = \mathbf{X}\mathbf{X}^\top$, where $\mathbf{X} \in \mathbb{R}^{n \times r'}$ and $r' \geq r$, and minimize the following mean-squared error

$$\min_{\mathbf{X} \in \mathbb{R}^{n \times r'}} f(\mathbf{X}) = \frac{1}{4N} \sum_{i=1}^N (\langle \mathbf{A}_i, \mathbf{X}\mathbf{X}^\top \rangle - y_i)^2. \quad (\text{MS})$$

When the search rank r' exceeds the true rank r , the problem is over-parameterized. For simplicity, we define the linear operator $\mathcal{A} : \mathbb{R}^{n \times n} \rightarrow \mathbb{R}^N$ and its adjoint $\mathcal{A}^* : \mathbb{R}^N \rightarrow \mathbb{R}^{n \times n}$ as $\mathcal{A}(\mathbf{M}) = \frac{1}{\sqrt{N}} [\langle \mathbf{A}_1, \mathbf{M} \rangle \cdots \langle \mathbf{A}_N, \mathbf{M} \rangle]^\top$ and $\mathcal{A}^*(\mathbf{y}) = \frac{1}{\sqrt{N}} \sum_{i=1}^N y_i \mathbf{A}_i$, respectively. A typical assumption on \mathcal{A} is that it satisfies the so-called *restricted isometry property* (RIP), defined below.

Definition 8 (RIP) We say that a linear operator \mathcal{A} satisfies the (δ, r) -RIP if

$$(1 - \delta) \|\mathbf{X}\|_{\text{F}}^2 \leq \|\mathcal{A}(\mathbf{X})\|^2 \leq (1 + \delta) \|\mathbf{X}\|_{\text{F}}^2, \quad \text{for all } \mathbf{X} \in \mathbb{R}^{n \times n} \text{ with } \text{rank}(\mathbf{X}) \leq r.$$

Intuitively, the RIP condition requires the operator \mathcal{A} to be nearly isotropic over all low-rank matrices, a property that holds when \mathcal{A} exhibits a certain type of randomness. For instance, it is well-known that for a Gaussian operator \mathcal{A} , where all the elements of the matrices \mathbf{A}_i are independently drawn from a standard Normal distribution, (δ, r) -RIP holds with a high probability, provided that the number of measurements satisfies $N = \Omega(dr/\delta^2)$ [54].

To apply our proposed framework, we first need to define the implicit region \mathcal{M} . To this end, we denote the nonzero singular values of \mathbf{M}^* in descending order as $\sigma_1^* \geq \cdots \geq \sigma_r^* > 0$, with $\kappa = \sigma_1^*/\sigma_r^*$ representing the condition number. The singular value decomposition (SVD) of \mathbf{M}^* is given by $\mathbf{M}^* = \mathbf{V}^* \mathbf{\Sigma}^* \mathbf{V}^{*\top}$, where $\mathbf{\Sigma}^* \in \mathbb{R}^{r \times r}$ is a diagonal matrix containing the nonzero eigenvalues of \mathbf{M}^* , and $\mathbf{V}^* \in \mathcal{O}_{n \times r}$ is

the matrix of corresponding eigenvectors. Moreover, let $\mathbf{V}^{\perp} \in \mathcal{O}_{n \times (n-r)}$ denote the orthogonal complement of \mathbf{V}^* . We define the implicit region as follows:

$$\mathcal{M} = \left\{ \mathbf{X} \in \mathbb{R}^{n \times r'} : \text{rank}(\mathbf{X}) \leq r, \|\mathcal{P}_{\mathbf{V}^{\perp}} \mathcal{P}_{\mathbf{X}}\| \leq 4\sqrt{r}\kappa\delta, \|\mathbf{X}\| \leq 2\sqrt{\sigma_1^*} \right\}. \quad (78)$$

Intuitively, the implicit region above corresponds to the set of rank- r matrices whose column spaces do not deviate significantly from that of the true solution, and whose norms are bounded from above. We also note that every true solution of the form $\mathbf{X}^* \mathbf{X}^{*\top} = \mathbf{M}^*$ can be equivalently characterized as $\mathcal{X}^* = \{\mathbf{X} : \mathbf{X} = \mathbf{V}^* \mathbf{\Sigma}^{*1/2} \mathbf{O}^\top, \mathbf{O} \in \mathcal{O}_{r' \times r}\}$ [55, Lemma 20]. This implies that $\mathcal{X}^* \subset \mathcal{M}$. Moreover, \mathbf{X} is \mathcal{M} -SOSP if and only if $\mathbf{X} \in \mathcal{X}^*$ —that is, $\mathcal{X}_{\mathcal{M}} = \mathcal{X}^*$ —provided that the linear operator \mathcal{A} satisfies $(\delta, 5r)$ -RIP with $\delta \leq \frac{1}{10}$ [49, Theorem 37]. Therefore, to approximately recover the true rank- r solution from \mathcal{X}^* , it suffices to recover an approximate \mathcal{M} -SOSP.

Toward this goal, we show that the conditions of Theorem 8 are guaranteed to hold, leading to a nearly linear convergence of IPGD to an \mathcal{M} -SOSP. To this goal, first, we introduce an important implication of the RIP condition, which will be used extensively throughout this section.

Lemma 22 (Lemma 2.3. and Lemma C.2. in [5]) *Suppose that \mathcal{A} satisfies (δ, r) -RIP. Then for any matrix $\mathbf{M} \in \mathbb{R}^{n \times n}$, we have $\|(\mathcal{A}^* \mathcal{A} - I)(\mathbf{M})\| \leq \delta \|\mathbf{M}\|_*$, where $\|\mathbf{M}\|_*$ is the nuclear norm of \mathbf{M} . Moreover, if $\text{rank}(\mathbf{M}) \leq r$, we further have $\|(\mathcal{A}^* \mathcal{A} - I)(\mathbf{M})\| \leq \sqrt{r}\delta \|\mathbf{M}\|$.*

For simplicity, we denote $\mathbf{\Delta} = \mathbf{M}^* - \mathbf{X}\mathbf{X}^\top$.

Local gradient- and Hessian-Lipschitzness

We first show that $f(\mathbf{X})$ defined in (MS) satisfies the local gradient- and Hessian-Lipschitzness properties.

Proposition 23 *Suppose that \mathcal{A} satisfies $(\delta, 2r)$ -RIP with $\delta \leq \frac{1}{10\sqrt{r}}$. With the implicit region defined as (78), the function $f(\mathbf{X})$ is (L, \mathcal{M}, τ) -gradient-Lipschitz and $(\rho, \mathcal{M}, \tau)$ -Hessian-Lipschitz, with parameters $L = 15\sigma_1^*$, $\rho = 15\sqrt{\sigma_1^*}$, and $\tau = \frac{1}{10}\sqrt{\frac{\sigma_1^*}{d}}$.*

Proof First, we provide the second and third-order derivatives of the objective function $f(\mathbf{X})$

$$\nabla^2 f(\mathbf{X})[\mathbf{Z}, \mathbf{Z}] = \left\langle \mathcal{A}^* \mathcal{A} \left(\mathbf{X}\mathbf{Z}^\top + \mathbf{Z}\mathbf{X}^\top \right) \mathbf{X} - \mathcal{A}^* \mathcal{A}(\mathbf{\Delta})\mathbf{Z}, \mathbf{Z} \right\rangle, \quad (79)$$

$$\nabla^3 f(\mathbf{X})[\mathbf{Z}, \mathbf{Z}, \mathbf{Z}] = 6 \left\langle \mathbf{Z}\mathbf{Z}^\top, \mathcal{A}^* \mathcal{A} \left(\mathbf{X}\mathbf{Z}^\top \right) \right\rangle. \quad (80)$$

The first formula follows from [42, Lemma 7]. We omit the derivation of the second formula, as it can be obtained in a similar manner. To derive the gradient and Hessian Lipschitz constants, we use the following equivalent definitions for smooth functions [56, Theorem 9.19]:

$$L := \sup_{\mathbf{X}, \mathbf{Y}} \frac{\|\nabla f(\mathbf{X}) - \nabla f(\mathbf{Y})\|_{\text{F}}}{\|\mathbf{X} - \mathbf{Y}\|_{\text{F}}} = \sup_{\mathbf{X}} \left\| \nabla^2 f(\mathbf{X}) \right\| = \sup_{\mathbf{X}, \|\mathbf{Z}\|_{\text{F}} \leq 1} \left| \nabla^2 f(\mathbf{X})[\mathbf{Z}, \mathbf{Z}] \right|, \quad (81)$$

$$\rho := \sup_{\mathbf{X}, \mathbf{Y}} \frac{\|\nabla^2 f(\mathbf{X}) - \nabla^2 f(\mathbf{Y})\|_{\text{F}}}{\|\mathbf{X} - \mathbf{Y}\|_{\text{F}}} = \sup_{\mathbf{X}} \|\nabla^3 f(\mathbf{X})\| = \sup_{\mathbf{X}, \|\mathbf{Z}\|_{\text{F}} \leq 1} \left| \nabla^3 f(\mathbf{X})[\mathbf{Z}, \mathbf{Z}, \mathbf{Z}] \right|. \quad (82)$$

We first provide an upper bound for L . For any $\mathbf{X} \in \mathcal{N}_{\mathcal{M}}(\tau)$ and $\|\mathbf{Z}\|_{\text{F}} \leq 1$, Equation (79) implies

$$\begin{aligned} \left| \nabla^2 f(\mathbf{X})[\mathbf{Z}, \mathbf{Z}] \right| &\leq \left| \left\langle (\mathbf{X}\mathbf{Z}^{\top} + \mathbf{Z}\mathbf{X}^{\top}) \mathbf{X} - \Delta \mathbf{Z}, \mathbf{Z} \right\rangle \right| \\ &\quad + \left\| (\mathcal{A}^* \mathcal{A} - I) (\mathbf{X}\mathbf{Z}^{\top} + \mathbf{Z}\mathbf{X}^{\top}) \right\| \|\mathbf{X}\|_{\text{F}} \|\mathbf{Z}\|_{\text{F}} + \|(\mathcal{A}^* \mathcal{A} - I)(\Delta)\| \|\mathbf{Z}\|_{\text{F}}^2 \\ &\leq 2\|\mathbf{X}\|^2 + \|\Delta\| + \left\| (\mathcal{A}^* \mathcal{A} - I) (\mathbf{X}\mathbf{Z}^{\top} + \mathbf{Z}\mathbf{X}^{\top}) \right\| \|\mathbf{X}\|_{\text{F}} + \|(\mathcal{A}^* \mathcal{A} - I)(\Delta)\|, \end{aligned} \quad (83)$$

where in the last inequality, we use triangle inequality and the fact that $\|\mathbf{Z}\|_{\text{F}} \leq 1$ repeatedly. Note that $\mathbf{X} \in \mathcal{N}_{\mathcal{M}}(\tau)$ implies that $\text{rank}(\mathbf{X}^{\sharp}) \leq r$, $\|\mathbf{X}^{\sharp}\| \leq 2\sqrt{\sigma_1^*}$, and $\|\mathbf{X}^{\perp}\|_{\text{F}} \leq \tau$. Consider the following decomposition:

$$\Delta = \Delta^{\sharp} + \Delta^{\perp}, \quad \text{where} \quad \Delta^{\sharp} = \mathbf{M}^* - \mathbf{X}^{\sharp} \mathbf{X}^{\sharp\top}, \quad \Delta^{\perp} = -\mathbf{X}^{\perp} \mathbf{X}^{\sharp\top} - \mathbf{X}^{\sharp} \mathbf{X}^{\perp\top} - \mathbf{X}^{\perp} \mathbf{X}^{\perp\top}. \quad (84)$$

We have $\text{rank}(\Delta^{\sharp}) \leq 2r$, $\|\Delta^{\sharp}\| \leq 4\sigma_1^*$, and $\|\Delta^{\perp}\|_{\text{F}} \leq 2\|\mathbf{X}^{\sharp}\| \|\mathbf{X}^{\perp}\|_{\text{F}} + \|\mathbf{X}^{\perp}\|_{\text{F}}^2 \leq 6\sqrt{\sigma_1^*}\tau$.

Consequently, we obtain $\|\Delta\| \leq 4\sigma_1^* + 6\sqrt{\sigma_1^*}\tau \leq 5\sigma_1^*$ since $\tau \leq \frac{1}{10}\sqrt{\frac{\sigma_1^*}{d}}$. Moreover, one can write

$$\begin{aligned} \|(\mathcal{A}^* \mathcal{A} - I)(\Delta)\| &\leq \|(\mathcal{A}^* \mathcal{A} - I)(\Delta^{\sharp})\| + \|(\mathcal{A}^* \mathcal{A} - I)(\Delta^{\perp})\| \\ &\stackrel{(a)}{\leq} \sqrt{2r}\delta \|\Delta^{\sharp}\| + \delta \|\Delta^{\perp}\|_* \\ &\stackrel{(b)}{\leq} 4\sqrt{2r}\sigma_1^*\delta + \delta \cdot 6\sqrt{d\sigma_1^*}\tau \\ &\stackrel{(c)}{\leq} 10\sqrt{r}\sigma_1^*\delta, \end{aligned} \quad (85)$$

where, in (a), we apply Lemma 22. Moreover, in (b), we use the facts that $\|\Delta^{\sharp}\| \leq 4\sigma_1^*$ and $\|\Delta^{\perp}\|_* \leq \sqrt{d} \|\Delta^{\perp}\|_{\text{F}} \leq 6\sqrt{d\sigma_1^*}\tau$. Finally, in (c), we use the fact that $\tau = \frac{1}{10}\sqrt{\frac{\sigma_1^*}{d}}$. Similarly, we obtain $\|(\mathcal{A}^* \mathcal{A} - I)(\mathbf{X}\mathbf{Z}^{\top} + \mathbf{Z}\mathbf{X}^{\top})\| \leq 5\sqrt{r}\sigma_1^*\delta$. Combining the derived bounds, we obtain

$$\left| \nabla^2 f(\mathbf{X})[\mathbf{Z}, \mathbf{Z}] \right| \leq 13\sigma_1^* + 15\sqrt{r}\sigma_1^*\delta \leq 15\sigma_1^*, \quad (86)$$

where we use the fact that $\delta \leq \frac{1}{10\sqrt{r}}$. This implies that the objective function is gradient Lipschitz with Lipschitz constant $L = 15\sigma_1^*$ within $\mathcal{N}_{\mathcal{M}}(\tau)$. In a similar fashion, we can show that the objective function is Hessian Lipschitz with Lipschitz constant $\rho = 15\sqrt{\sigma_1^*}$ within $\mathcal{N}_{\mathcal{M}}(\tau)$. We omit the details for brevity. \square

Closure of \mathcal{M} under GD updates

Next, we establish the closure of \mathcal{M} under GD updates.

Proposition 24 Suppose that \mathcal{A} satisfies $(\delta, 2r)$ -RIP with $\delta \leq \frac{1}{10\sqrt{r}}$. For any $\mathbf{X} \in \mathcal{M}$, we have $\mathbf{X}^+ := \mathbf{X} - \eta \nabla f(\mathbf{X}) \in \mathcal{M}$, provided that the step-size satisfies $\eta \leq \frac{1}{10\sigma_1^*}$.

Before proving the above proposition, we first present a few helper lemmas.

Lemma 25 (Adapted from [57, Lemma 2.1.2 and Lemma 2.1.3]) *For any $\mathbf{U}, \mathbf{U}^* \in \mathcal{O}_{n \times r}$, we have*

$$\|\mathcal{P}_{\mathbf{U}^\perp} \mathcal{P}_{\mathbf{U}^*}\| = \|\mathcal{P}_{\mathbf{U}} - \mathcal{P}_{\mathbf{U}^*}\| \leq \min_{\mathbf{R} \in \mathcal{O}^{r \times r}} \|\mathbf{U}\mathbf{R} - \mathbf{U}^*\| \leq \sqrt{2} \|\mathcal{P}_{\mathbf{U}} - \mathcal{P}_{\mathbf{U}^*}\| = \sqrt{2} \|\mathcal{P}_{\mathbf{U}^\perp} \mathcal{P}_{\mathbf{U}^*}\|. \quad (87)$$

Lemma 26 (Adapted from [58, Theorem 2.4]) *For any $\mathbf{X}, \mathbf{Y} \in \mathbb{R}^{n_1 \times n_2}$, we have*

$$\|\mathcal{P}_{\mathbf{X}} - \mathcal{P}_{\mathbf{Y}}\| \leq \min \left\{ \left\| (\mathbf{X} - \mathbf{Y})\mathbf{X}^\dagger \right\|, \left\| (\mathbf{X} - \mathbf{Y})\mathbf{Y}^\dagger \right\| \right\}. \quad (88)$$

Lemma 27 *For any two invertible matrices \mathbf{A} and \mathbf{B} , we have*

$$\left\| \mathbf{A}^{-1} - \mathbf{B}^{-1} \right\| \leq \left\| \mathbf{A}^{-1} \right\| \left\| \mathbf{B}^{-1} \right\| \left\| \mathbf{A} - \mathbf{B} \right\|. \quad (89)$$

Proof The result follows by observing that $\mathbf{A}^{-1} - \mathbf{B}^{-1} = \mathbf{A}^{-1}(\mathbf{B} - \mathbf{A})\mathbf{B}^{-1}$ and applying the submultiplicativity of the operator norm $\left\| \mathbf{A}^{-1} - \mathbf{B}^{-1} \right\| \leq \left\| \mathbf{A}^{-1} \right\| \left\| \mathbf{B}^{-1} \right\| \left\| \mathbf{A} - \mathbf{B} \right\|$. \square

Proof of Proposition 24 Note that

$$\mathbf{X}^+ := \mathbf{X} - \eta \nabla f(\mathbf{X}) = \left(\mathbf{I} - \eta \mathcal{A}^* \mathcal{A}(\mathbf{X}\mathbf{X}^\top - \mathbf{M}^*) \right) \mathbf{X} = (\mathbf{I} + \eta \mathcal{A}^* \mathcal{A}(\Delta)) \mathbf{X}. \quad (90)$$

Based on the definition \mathcal{M} in Equation (78), to show that $\mathbf{X}^+ = (\mathbf{I} + \eta \mathcal{A}^* \mathcal{A}(\Delta)) \mathbf{X} \in \mathcal{M}$, we need to verify the following three conditions

- (A) $\text{rank}(\mathbf{X}^+) \leq r$;
- (B) $\|\mathbf{X}^+\| \leq 2\sqrt{\sigma_1^*}$;
- (C) $\|\mathcal{P}_{\mathbf{V}^{\star\perp}} \mathcal{P}_{\mathbf{X}^+}\| \leq 4\sqrt{r}\kappa\delta$.

Verification of (A)

This is already shown in Example 2.

Verification of (B)

This can be established as follows:

$$\begin{aligned} \left\| \mathbf{X}^+ \right\| &\leq \left\| (\mathbf{I} + \eta \Delta) \mathbf{X} \right\| + \left\| (\mathcal{A}^* \mathcal{A} - \mathbf{I})(\Delta) \right\| \left\| \mathbf{X} \right\| \\ &\stackrel{(a)}{\leq} \left\| \left(\mathbf{I} - \eta \mathbf{X}\mathbf{X}^\top \right) \mathbf{X} \right\| + \eta \sigma_1^* \left\| \mathbf{X} \right\| + 4\sqrt{2r}\sigma_1^* \delta \left\| \mathbf{X} \right\| \\ &\stackrel{(b)}{=} \left(1 + \eta \left(\sigma_1^* + 4\sqrt{2r}\sigma_1^* \delta - \left\| \mathbf{X} \right\|^2 \right) \right) \left\| \mathbf{X} \right\| \\ &\stackrel{(c)}{\leq} \left(1 + \eta \left(\sigma_1^* + 4\sqrt{2r}\sigma_1^* \delta - 4\sigma_1^* \right) \right) \cdot 2\sqrt{\sigma_1^*} \\ &\leq 2\sqrt{\sigma_1^*}. \end{aligned} \quad (91)$$

In (a), we use triangle inequality and Lemma 22 along with the facts that $\text{rank}(\Delta) \leq 2r$ and $\|\Delta\| \leq 4\sigma_1^*$. In (b), we use the fact that the function $f(x) = x - \eta x^3$ is increasing in the interval $[0, \frac{1}{\sqrt{3\eta}}]$, which implies $\|(\mathbf{I} - \eta \mathbf{X} \mathbf{X}^\top) \mathbf{X}\| = \|\mathbf{X}\| - \eta \|\mathbf{X}\|^3$ since $\|\mathbf{X}\| \leq 2\sqrt{\sigma_1^*} \leq \frac{1}{\sqrt{3\eta}}$. Lastly, in (c), we use the fact that the function $g(x) = (1 + \eta(\sigma_1^* + 4\sqrt{2r}\sigma_1^*\delta - x^2))x$ is also increasing in the range $[0, \frac{1}{3\sqrt{\eta}}]$.

Verification of (C)

We first define $\tilde{\mathbf{X}}^+ = (\mathbf{I} + \eta\Delta)\mathbf{X}$. Then, we have the following decomposition

$$\|\mathcal{P}_{\mathbf{V}^* \perp} \mathcal{P}_{\mathbf{X}^+}\| \leq \underbrace{\|\mathcal{P}_{\mathbf{V}^* \perp} \mathcal{P}_{\tilde{\mathbf{X}}^+}\|}_{\text{(I)}} + \underbrace{\|\mathcal{P}_{\tilde{\mathbf{X}}^+} - \mathcal{P}_{\mathbf{X}^+}\|}_{\text{(II)}}. \quad (92)$$

We control these two terms separately. Note that $\mathcal{P}_{\mathbf{X}} = \mathbf{X} \mathbf{X}^\dagger$ where \mathbf{X}^\dagger is the pseudo-inverse of \mathbf{X} . Hence, we have

$$\begin{aligned} \mathcal{P}_{\mathbf{V}^* \perp} \mathcal{P}_{\tilde{\mathbf{X}}^+} &= \mathcal{P}_{\mathbf{V}^* \perp} \tilde{\mathbf{X}}^+ (\tilde{\mathbf{X}}^+)^{\dagger} \\ &= \mathcal{P}_{\mathbf{V}^* \perp} (\mathbf{I} + \eta\Delta) \mathbf{X} (\tilde{\mathbf{X}}^+)^{\dagger} \\ &\stackrel{(a)}{=} \mathcal{P}_{\mathbf{V}^* \perp} (\mathbf{I} - \eta \mathbf{X} \mathbf{X}^\top) \mathbf{X} (\tilde{\mathbf{X}}^+)^{\dagger} \\ &\stackrel{(b)}{=} \mathcal{P}_{\mathbf{V}^* \perp} \mathcal{P}_{\mathbf{X}} (\mathbf{I} - \eta \mathbf{X} \mathbf{X}^\top) (\mathbf{I} + \eta\Delta)^{-1} \mathcal{P}_{\tilde{\mathbf{X}}^+}, \end{aligned} \quad (93)$$

where, in (a), we use the fact that $\mathcal{P}_{\mathbf{V}^* \perp} \mathbf{M}^* = \mathbf{0}$. Moreover, in (b), we use the fact that $\mathbf{X} (\tilde{\mathbf{X}}^+)^{\dagger} = (\mathbf{I} + \eta\Delta)^{-1} \tilde{\mathbf{X}}^+ (\tilde{\mathbf{X}}^+)^{\dagger} = (\mathbf{I} + \eta\Delta)^{-1} \mathcal{P}_{\tilde{\mathbf{X}}^+}$. Therefore, we obtain

$$\text{(I)} \leq \|\mathcal{P}_{\mathbf{V}^* \perp} \mathcal{P}_{\mathbf{X}}\| \underbrace{\left\| \mathcal{P}_{\mathbf{X}} (\mathbf{I} - \eta \mathbf{X} \mathbf{X}^\top) (\mathbf{I} + \eta\Delta)^{-1} \right\|}_{\text{(III)}}. \quad (94)$$

To proceed, we decompose $\mathbf{M}^* = \mathbf{V}^* \Sigma^* \mathbf{V}^{*\top}$ as

$$\mathbf{M}^* = \underbrace{\mathbf{V}_{\mathbf{X}} \Sigma^* \mathbf{V}_{\mathbf{X}}^\top}_{:= \mathbf{M}_{\mathbf{X}}^*} + \underbrace{(\mathbf{V}^* - \mathbf{V}_{\mathbf{X}}) \Sigma^* \mathbf{V}^{*\top} + \mathbf{V}_{\mathbf{X}} \Sigma^* (\mathbf{V}^* - \mathbf{V}_{\mathbf{X}})^\top}_{:= \Delta_{\mathbf{M}}}, \quad (95)$$

where $\mathbf{V}_{\mathbf{X}}$ is defined as $\mathbf{V}_{\mathbf{X}} = \arg \min_{\mathbf{V} \in \mathcal{O}_{n \times r}, \mathcal{P}_{\mathbf{X}} \mathbf{V} = \mathbf{V}} \|\mathbf{V}^* - \mathbf{V}\|$. Therefore, we can decompose (III) as

$$\begin{aligned} \text{(III)} &\leq \underbrace{\left\| \mathcal{P}_{\mathbf{X}} (\mathbf{I} - \eta \mathbf{X} \mathbf{X}^\top) (\mathbf{I} + \eta (\mathbf{M}_{\mathbf{X}}^* - \mathbf{X} \mathbf{X}^\top))^{-1} \right\|}_{\text{(III}_1)} \\ &\quad + \underbrace{\left\| \mathcal{P}_{\mathbf{X}} (\mathbf{I} - \eta \mathbf{X} \mathbf{X}^\top) \left((\mathbf{I} + \eta (\mathbf{M}_{\mathbf{X}}^* - \mathbf{X} \mathbf{X}^\top))^{-1} - (\mathbf{I} + \eta (\mathbf{M}^* - \mathbf{X} \mathbf{X}^\top))^{-1} \right) \right\|}_{\text{(III}_2)}. \end{aligned} \quad (96)$$

To control (III₁), we note that all the matrices involved share the same singular space. Therefore, we have

$$\begin{aligned}
(\text{III}_1) &= \left\| \left(\mathbf{I} - \eta \Sigma_{\mathbf{X}}^2 \right) \left(\mathbf{I} + \eta \left(\Sigma^* - \Sigma_{\mathbf{X}}^2 \right) \right)^{-1} \right\| \\
&\stackrel{(a)}{\leq} \left\| \left(\mathbf{I} + \eta \Sigma^* \right)^{-1} \right\| \\
&= \frac{1}{1 + \eta \sigma_r^*} \\
&\stackrel{(b)}{\leq} 1 - \frac{1}{2} \eta \sigma_r^*.
\end{aligned} \tag{97}$$

Here in (a), we use the inequality $\frac{x}{y} \leq \frac{x+a}{y+a}$ for every $x, y, a > 0$ and $y \geq x$. In (b), we use the inequality $\frac{1}{1+x} \leq 1 - \frac{1}{2}x$ for any $0 \leq x \leq 1$.

To control (III₂), we rely on Lemma 27. Upon setting $\mathbf{A} = \mathbf{I} + \eta (\mathbf{M}_{\mathbf{X}}^* - \mathbf{X}\mathbf{X}^\top)$ and $\mathbf{B} = \mathbf{I} + \eta (\mathbf{M}^* - \mathbf{X}\mathbf{X}^\top)$ in Lemma 27, we have

$$(\text{III}_2) \leq \left\| \mathbf{A}^{-1} - \mathbf{B}^{-1} \right\| \leq \left\| \mathbf{A}^{-1} \right\| \left\| \mathbf{B}^{-1} \right\| \left\| \mathbf{A} - \mathbf{B} \right\|. \tag{98}$$

To proceed, notice that

$$\max \left\{ \left\| \mathbf{A}^{-1} \right\|, \left\| \mathbf{B}^{-1} \right\| \right\} \leq \left\| \left(\mathbf{I} - \eta (\mathbf{X}\mathbf{X}^\top) \right)^{-1} \right\| = \frac{1}{1 - \eta \|\mathbf{X}\|^2} \leq 2. \tag{99}$$

In the last inequality, we use the fact that $\eta \leq \frac{1}{8\sigma_1^*}$ and $\|\mathbf{X}\| \leq 2\sqrt{\sigma_1^*}$. On the other hand, we have

$$\|\mathbf{A} - \mathbf{B}\| = \eta \|\Delta_{\mathbf{M}}\| \leq 2\sigma_1^* \|\mathbf{V}^* - \mathbf{V}_{\mathbf{X}}\| \leq 2\sqrt{2}\sigma_1^* \|\mathcal{P}_{\mathbf{V}^* \perp} \mathcal{P}_{\mathbf{X}}\|. \tag{100}$$

where, in the last inequality, we use Lemma 25. Therefore, we obtain $(\text{III}_2) \leq 8\sqrt{2}\sigma_1^* \|\mathcal{P}_{\mathbf{V}^* \perp} \mathcal{P}_{\mathbf{X}}\|$. Combining the derived bounds for (III₁) and (III₂), we have

$$(\text{I}) \leq \|\mathcal{P}_{\mathbf{V}^* \perp} \mathcal{P}_{\mathbf{X}}\| ((\text{III}_1) + (\text{III}_2)) \leq \left(1 - \frac{1}{2} \eta \sigma_r^* + 8\sqrt{2} \eta \sigma_1^* \|\mathcal{P}_{\mathbf{V}^* \perp} \mathcal{P}_{\mathbf{X}}\| \right) \|\mathcal{P}_{\mathbf{V}^* \perp} \mathcal{P}_{\mathbf{X}}\|. \tag{101}$$

Finally, we control (II). To this goal, we write

$$\begin{aligned}
(\text{II}) &\stackrel{(a)}{\leq} \left\| (\tilde{\mathbf{X}}^+ - \mathbf{X}^+) (\tilde{\mathbf{X}}^+)^{\dagger} \right\| \\
&= \eta \left\| (\mathcal{A}^* \mathcal{A} - I) (\Delta) (\mathbf{I} + \eta \Delta)^{-1} \tilde{\mathbf{X}}^+ (\tilde{\mathbf{X}}^+)^{\dagger} \right\| \\
&\leq \eta \left\| (\mathcal{A}^* \mathcal{A} - I) (\Delta) \right\| \left\| (\mathbf{I} + \eta \Delta)^{-1} \right\| \\
&\stackrel{(b)}{\leq} \eta \sqrt{2r} \delta \|\Delta\| \left\| (\mathbf{I} + \eta \Delta)^{-1} \right\| \\
&\stackrel{(c)}{\leq} 4\eta \sqrt{r} \sigma_1^* \delta,
\end{aligned} \tag{102}$$

where in (a), we use Lemma 26. Moreover, in (b), we use Lemma 22. Finally, in (c), we use $\|\Delta\| \leq 4\sigma_1^*$ and $\eta \leq \frac{1}{4\sqrt{2}\sigma_1^*}$. Combining the derived bounds for (I) and (II), we have

$$\|\mathcal{P}_{\mathbf{V}^* \perp} \mathcal{P}_{\mathbf{X}^+}\| \leq \left(1 - \frac{1}{4} \eta \sigma_r^* + \eta \sigma_1^* \|\mathcal{P}_{\mathbf{V}^* \perp} \mathcal{P}_{\mathbf{X}}\| \right) \|\mathcal{P}_{\mathbf{V}^* \perp} \mathcal{P}_{\mathbf{X}}\| + 2\eta \sqrt{r} \sigma_1^* \delta \leq 4\sqrt{r} \kappa \delta, \tag{103}$$

where the last inequality follows from $\|\mathcal{P}_{\mathbf{V}^* \perp} \mathcal{P}_{\mathbf{X}}\| \leq 4\sqrt{r} \kappa \delta$ by our assumption. This completes the proof. \square

\mathcal{M} -strict saddle property and \mathcal{M} -regularity property

Next, we establish the \mathcal{M} -strict saddle property and the \mathcal{M} -regularity property, both of which are essential for ensuring the efficient convergence of our algorithm.

Proposition 28 Suppose that \mathcal{A} satisfies $(\delta, 6r)$ -RIP with $\delta \leq \frac{1}{10}$. The following statements hold for $f(\mathbf{X})$ defined in (MS):

- It satisfies $\left(\frac{1}{160}\sigma_r^{*3/2}, \frac{1}{5}\sigma_r^*, \frac{1}{8}\sigma_r^{*1/2}\right)$ - \mathcal{M} -strict saddle property (Definition 6).
- It satisfies $\left(\frac{1}{2}\sigma_r^*, \frac{425}{64}\sigma_1^*, \frac{1}{4}\sigma_r^{*1/2}\right)$ - \mathcal{M} -regularity property (Definition 7).

To prove the above proposition, we establish a connection between the local geometry of $f(\mathbf{X})$ within the implicit region \mathcal{M} to that of the exactly-parameterized matrix sensing problem, defined as

$$\min_{\bar{\mathbf{X}} \in \mathbb{R}^{n \times r}} \bar{f}(\bar{\mathbf{X}}) = \frac{1}{4N} \sum_{i=1}^N (\langle \mathbf{A}_i, \bar{\mathbf{X}} \bar{\mathbf{X}}^\top \rangle - y_i)^2. \quad (\text{MS-exact})$$

We note that, unlike the over-parameterized setting in (MS), where the rank of the matrix variable can be as large as $r' \geq r$, the rank in (MS-exact) is fixed to the true value r . For the exactly-parameterized matrix sensing, all SOSPs coincide with the set of true solutions, defined as

$$\mathcal{X}_{\leq r}^* = \left\{ \mathbf{V}^* \Sigma^{*1/2} \mathbf{O} \in \mathbb{R}^{n \times r} : \mathbf{O} \in \mathcal{O}_{r \times r} \right\}, \quad (104)$$

provided that the linear operator \mathcal{A} satisfies $(\delta, 6r)$ -RIP with $\delta \leq \frac{1}{10}$ [42, Theorem 8].⁶ Moreover, this objective function satisfies the strict saddle property and exhibits strong local structure globally (i.e., over the exactly-parameterized space $\mathbb{R}^{n \times r}$), as detailed below.

Lemma 29 Assume the linear operator \mathcal{A} satisfies $(\delta, 6r)$ -RIP with $\delta \leq \frac{1}{10}$. The following statements hold for $\bar{f}(\bar{\mathbf{X}})$ defined in (MS-exact):

- It satisfies $\left(\epsilon, \frac{1}{5}\sigma_r^*, \frac{20\epsilon}{\sigma_r^*}\right)$ -strict saddle property, for any $\epsilon > 0$ [42, Theorem 8].
- It satisfies $\left(\frac{1}{2}\sigma_r^*, \frac{425}{64}\sigma_1^*, \frac{1}{4}\sigma_r^{*1/2}\right)$ -regularity property [59, Eq. 5.7].

To prove Proposition 28, we leverage the above lemma to show that, when restricted to the implicit region \mathcal{M} (as defined in Equation (78)), the function $f(\mathbf{X})$ satisfies the same properties with exactly the same parameters.

⁶Note that the definition of $\mathcal{X}_{\leq r}^*$ should not be confused with the previously introduced set $\mathcal{X}^* = \{\mathbf{X} : \mathbf{X} = \mathbf{V}^* \Sigma^{*1/2} \mathbf{O}^\top, \mathbf{O} \in \mathcal{O}_{r' \times r}\}$, which characterizes the true solutions in the over-parameterized space.

Proof of Proposition 28 We first establish a one-to-one mapping $h : \mathcal{M} \rightarrow \mathbb{R}^{n \times r}$, which maps an arbitrary $\mathbf{X} \in \mathcal{M}$ to a point $\bar{\mathbf{X}} = h(\mathbf{X}) \in \mathbb{R}^{n \times r}$. Specifically, for an arbitrary $\mathbf{X} \in \mathcal{M}$ with the SVD of the form $\mathbf{X} = \mathbf{L}_\mathbf{X} \mathbf{\Sigma}_\mathbf{X} \mathbf{R}_\mathbf{X}^\top$, where $\mathbf{L}_\mathbf{X} \in \mathcal{O}_{n \times r}$, $\mathbf{R}_\mathbf{X} \in \mathcal{O}_{r' \times r}$, and $\mathbf{\Sigma}_\mathbf{X} \in \mathbb{R}^{r \times r}$ is a diagonal matrix⁷, we define the mapping as $\bar{\mathbf{X}} = h(\mathbf{X}) = \mathbf{L}_\mathbf{X} \mathbf{\Sigma}_\mathbf{X} \in \mathbb{R}^{n \times r}$.

Proof of the first statement

Suppose that $\mathbf{X} \in \mathcal{M}$ satisfies $\|\nabla f(\mathbf{X})\|_F < \epsilon$ and $\text{dist}(\mathbf{X}, \mathcal{X}_\mathcal{M}) > \frac{20\epsilon}{\sigma_r^*}$. To establish the \mathcal{M} -strict saddle property with the specified parameters, it suffices to show that $\lambda_{\min}(\nabla^2 f(\mathbf{X})) \leq -\frac{1}{5}\sigma_r^*$. To this end, we first show that for $\bar{\mathbf{X}} = h(\mathbf{X})$, we also have $\|\nabla \bar{f}(\bar{\mathbf{X}})\|_F < \epsilon$ and $\text{dist}(\bar{\mathbf{X}}, \mathcal{X}_{\leq r}^*) > \frac{20\epsilon}{\sigma_r^*}$. One can write

$$\begin{aligned} \|\nabla f(\mathbf{X})\|_F &= \left\| \mathcal{A}^* \mathcal{A}(\mathbf{X}\mathbf{X}^\top - \mathbf{M}^*) \mathbf{X} \right\|_F \\ &= \left\| \mathcal{A}^* \mathcal{A}(\bar{\mathbf{X}}\bar{\mathbf{X}}^\top - \mathbf{M}^*) \bar{\mathbf{X}} \mathbf{R}_\mathbf{X}^\top \right\|_F \\ &= \left\| \mathcal{A}^* \mathcal{A}(\bar{\mathbf{X}}\bar{\mathbf{X}}^\top - \mathbf{M}^*) \bar{\mathbf{X}} \right\|_F \\ &= \|\nabla \bar{f}(\bar{\mathbf{X}})\|_F, \end{aligned} \tag{105}$$

where, in the second equality, we use the fact that $\mathbf{X}\mathbf{X}^\top = \bar{\mathbf{X}}\bar{\mathbf{X}}^\top$. This implies that $\|\nabla f(\mathbf{X})\|_F = \|\nabla \bar{f}(\bar{\mathbf{X}})\|_F \leq \epsilon$. To establish the second inequality, we write

$$\begin{aligned} \text{dist}(\mathbf{X}, \mathcal{X}_\mathcal{M}) &= \min_{\mathbf{O} \in \mathcal{O}_{r' \times r'}} \left\| \mathbf{X}\mathbf{O} - \left[\mathbf{V}^* \mathbf{\Sigma}^{*1/2} \mathbf{0}_{n \times (r'-r)} \right] \right\|_F \\ &\stackrel{(a)}{\leq} \min_{\bar{\mathbf{O}} \in \mathcal{O}_{r \times r}} \left\| \bar{\mathbf{X}} \mathbf{R}_\mathbf{X}^\top [\mathbf{R}_\mathbf{X} \bar{\mathbf{O}} \mathbf{R}_\mathbf{X}^\perp] - \left[\mathbf{V}^* \mathbf{\Sigma}^{*1/2} \mathbf{0}_{n \times (r'-r)} \right] \right\|_F \\ &= \min_{\bar{\mathbf{O}} \in \mathcal{O}_{r \times r}} \left\| \bar{\mathbf{X}} \bar{\mathbf{O}} - \mathbf{V}^* \mathbf{\Sigma}^{*1/2} \right\|_F \\ &= \text{dist}(\bar{\mathbf{X}}, \mathcal{X}_{\leq r}^*), \end{aligned} \tag{106}$$

where (a) follows after setting $\mathbf{O} = [\mathbf{R}_\mathbf{X} \bar{\mathbf{O}} \mathbf{R}_\mathbf{X}^\perp] \in \mathcal{O}_{r' \times r'}$ and choosing $\mathbf{R}_\mathbf{X}^\perp \in \mathcal{O}_{n \times (r'-r)}$ that satisfies $\mathbf{R}_\mathbf{X}^\top \mathbf{R}_\mathbf{X}^\perp = \mathbf{0}$. This implies that $\text{dist}(\bar{\mathbf{X}}, \mathcal{X}_{\leq r}^*) = \text{dist}(\mathbf{X}, \mathcal{X}_\mathcal{M}) > \frac{20\epsilon}{\sigma_r^*}$. Therefore, we have established that $\|\nabla f(\mathbf{X})\|_F \leq \epsilon$ and $\text{dist}(\bar{\mathbf{X}}, \mathcal{X}_{\leq r}^*) > \frac{20\epsilon}{\sigma_r^*}$. Based on these inequalities, the first statement of Lemma 29 implies that $\lambda_{\min}(\nabla^2 \bar{f}(\bar{\mathbf{X}})) \leq -\frac{1}{5}\sigma_r^*$. Next, we use this inequality to establish a similar bound for $\lambda_{\min}(\nabla^2 f(\mathbf{X}))$. This is achieved as follows:

⁷If $\text{rank}(\mathbf{X}) < r$, we construct $\mathbf{\Sigma}_\mathbf{X}$ by padding its diagonal with additional zero entries.

$$\begin{aligned}
\lambda_{\min}(\nabla^2 f(\mathbf{X})) &= \min_{\|\mathbf{Z}\|_{\text{F}} \leq 1} \nabla^2 f(\mathbf{X})[\mathbf{Z}, \mathbf{Z}] \\
&= \min_{\|\mathbf{Z}\|_{\text{F}} \leq 1} \left\langle \mathcal{A}^* \mathcal{A} \left(\mathbf{X} \mathbf{Z}^\top + \mathbf{Z} \mathbf{X}^\top \right) \mathbf{X} + \mathcal{A}^* \mathcal{A} (\mathbf{X} \mathbf{X}^\top - \mathbf{M}^*) \mathbf{Z}, \mathbf{Z} \right\rangle \\
&\stackrel{(a)}{\leq} \min_{\|\bar{\mathbf{Z}}\|_{\text{F}} \leq 1} \left\langle \mathcal{A}^* \mathcal{A} \left(\bar{\mathbf{X}} \bar{\mathbf{Z}}^\top + \bar{\mathbf{Z}} \bar{\mathbf{X}}^\top \right) \bar{\mathbf{X}} \mathbf{R}_{\mathbf{X}}^\top + \mathcal{A}^* \mathcal{A} \left(\bar{\mathbf{X}} \bar{\mathbf{X}}^\top - \mathbf{M}^* \right) \bar{\mathbf{Z}} \mathbf{R}_{\mathbf{X}}^\top, \bar{\mathbf{Z}} \mathbf{R}_{\mathbf{X}}^\top \right\rangle \\
&= \lambda_{\min}(\nabla^2 \bar{f}(\bar{\mathbf{X}})) \\
&\leq -\frac{1}{5} \sigma_r^*,
\end{aligned} \tag{107}$$

where (a) follows after setting $\mathbf{Z} = \bar{\mathbf{Z}} \mathbf{R}_{\mathbf{X}}^\top$. Therefore, $f(\mathbf{X})$ satisfies $(\epsilon, \frac{1}{5} \sigma_r^*, \frac{20\epsilon}{\sigma_r^*})$ - \mathcal{M} -strict saddle property. Setting $\epsilon = \frac{1}{160} \sigma_r^{*3/2}$ completes the proof of the first statement of Proposition 28.

Proof of the second statement

According to the second statement of Lemma 29, for any $\bar{\mathbf{X}} \in \mathbb{R}^{n \times r}$ satisfying $\text{dist}(\bar{\mathbf{X}}, \mathcal{X}_{\leq r}^*) \leq \frac{1}{4} \sigma_r^{*1/2}$, we have

$$\left\langle \nabla \bar{f}(\bar{\mathbf{X}}), \bar{\mathbf{X}} - \mathcal{P}_{\mathcal{X}_{\leq r}^*}(\bar{\mathbf{X}}) \right\rangle \geq \frac{\alpha}{2} \text{dist}^2(\bar{\mathbf{X}}, \mathcal{X}_{\leq r}^*) + \frac{1}{2\beta} \|\nabla \bar{f}(\bar{\mathbf{X}})\|_{\text{F}}^2 \tag{108}$$

with $\alpha = \frac{1}{2} \sigma_r^*$ and $\beta = \frac{425}{64} \sigma_1^*$. To proceed, we first show that $\mathcal{P}_{\mathcal{X}_{\mathcal{M}}}(\mathbf{X}) \mathbf{R}_{\mathbf{X}} = \mathcal{P}_{\mathcal{X}_{\leq r}^*}(\bar{\mathbf{X}})$. Note that $\mathcal{P}_{\mathcal{X}_{\mathcal{M}}}(\mathbf{X}) = \mathbf{V}^* \Sigma^{*1/2} \mathbf{O}_{\mathbf{X}}$ where $\mathbf{O}_{\mathbf{X}}$ is given by

$$\begin{aligned}
\mathbf{O}_{\mathbf{X}} &= \arg \min_{\mathbf{O} \in \mathcal{O}_{r \times r'}} \left\| \mathbf{X} - \mathbf{V}^* \Sigma^{*1/2} \mathbf{O} \right\|_{\text{F}} \\
&= \arg \min_{\mathbf{O} \in \mathcal{O}_{r \times r'}} \left\| \bar{\mathbf{X}} \mathbf{R}_{\mathbf{X}}^\top - \mathbf{V}^* \Sigma^{*1/2} \mathbf{O} \right\|_{\text{F}} \\
&= \arg \min_{\mathbf{O} \in \mathcal{O}_{r \times r'}} \left\| \bar{\mathbf{X}} - \mathbf{V}^* \Sigma^{*1/2} \mathbf{O} \mathbf{R}_{\mathbf{X}} \right\|_{\text{F}}.
\end{aligned} \tag{109}$$

Therefore, we conclude that $\mathbf{O}_{\mathbf{X}} \mathbf{R}_{\mathbf{X}} = \mathbf{O}_{\bar{\mathbf{X}}}$ where $\mathbf{O}_{\bar{\mathbf{X}}} = \arg \min_{\mathbf{O} \in \mathcal{O}_{r \times r}} \left\| \bar{\mathbf{X}} - \mathbf{V}^* \Sigma^{*1/2} \mathbf{O} \right\|_{\text{F}}$. This implies that

$$\mathcal{P}_{\mathcal{X}_{\mathcal{M}}}(\mathbf{X}) \mathbf{R}_{\mathbf{X}} = \mathbf{V}^* \Sigma^{*1/2} \mathbf{O}_{\mathbf{X}} \mathbf{R}_{\mathbf{X}} = \mathbf{V}^* \Sigma^{*1/2} \mathbf{O}_{\bar{\mathbf{X}}} = \mathcal{P}_{\mathcal{X}_{\leq r}^*}(\bar{\mathbf{X}}).$$

Based on the above equality, we have

$$\begin{aligned}
\langle \nabla f(\mathbf{X}), \mathbf{X} - \mathcal{P}_{\mathcal{X}_{\mathcal{M}}}(\mathbf{X}) \rangle &= \left\langle \nabla \bar{f}(\bar{\mathbf{X}}) \mathbf{R}_{\mathbf{X}}^\top, \mathbf{X} - \mathcal{P}_{\mathcal{X}_{\mathcal{M}}}(\mathbf{X}) \right\rangle \\
&= \left\langle \nabla \bar{f}(\bar{\mathbf{X}}), \bar{\mathbf{X}} - \mathcal{P}_{\mathcal{X}_{\leq r}^*}(\bar{\mathbf{X}}) \right\rangle \\
&\geq \frac{\alpha}{2} \text{dist}^2(\bar{\mathbf{X}}, \mathcal{X}_{\leq r}^*) + \frac{1}{2\beta} \|\nabla \bar{f}(\bar{\mathbf{X}})\|_{\text{F}}^2 \\
&= \frac{\alpha}{2} \text{dist}^2(\mathbf{X}, \mathcal{X}_{\mathcal{M}}) + \frac{1}{2\beta} \|\nabla f(\mathbf{X})\|_{\text{F}}^2,
\end{aligned} \tag{110}$$

where, in the last equality, we use $\text{dist}(\bar{\mathbf{X}}, \mathcal{X}_{\leq r}^*) = \text{dist}(\mathbf{X}, \mathcal{X}_{\mathcal{M}})$ and $\|\nabla \bar{f}(\bar{\mathbf{X}})\|_{\text{F}} = \|\nabla f(\mathbf{X})\|_{\text{F}}$, established in Equation (105) and Equation (106), respectively. This completes the proof. \square

Bounding the deviation rate

Lastly, we establish an upper bound on the deviation rate.

Proposition 30 *Suppose that \mathcal{A} satisfies $(\delta, 2r)$ -RIP with $\delta \leq \frac{1}{10r}$. Then, for any $\tau \leq \frac{1}{10} \sqrt{\frac{\sigma_1^*}{d}}$, the τ -deviation rate satisfies $R(\tau) \leq 45\sigma_1^* r \kappa \delta$.*

Proof of Proposition 30 According to the definition of τ -deviation rate (Definition 5), we have

$$R(\tau) = \sup_{\mathbf{X} \in \mathcal{N}_{\mathcal{M}}(\tau)} r(\mathbf{X}) \leq \sup_{\mathbf{X} \in \mathcal{N}_{\mathcal{M}}(\tau)} 3r_+(\mathbf{X}) = \sup_{\mathbf{X} \in \mathcal{N}_{\mathcal{M}}(\tau) - \mathcal{M}} \left\{ -\frac{3\nabla_-^2 f(\mathbf{X}^\sharp) [\mathbf{X}^\perp, \mathbf{X}^\perp]}{\|\mathbf{X}^\perp\|_F^2} \right\}, \quad (111)$$

where the first inequality is due to the fact that $r_-(\mathbf{X}) \leq 0$ by definition. Therefore, to control $R(\tau)$, it suffices to provide a uniform upper bound on $-\nabla_-^2 f(\mathbf{X}^\sharp) [\mathbf{X}^\perp, \mathbf{X}^\perp]$ for every $\mathbf{X} \in \mathcal{N}_{\mathcal{M}}(\tau) - \mathcal{M}$. Recall that

$$\nabla^2 f(\mathbf{X})[\mathbf{Z}, \mathbf{Z}] = \left\langle \mathcal{A}^* \mathcal{A} (\mathbf{X} \mathbf{Z}^\top + \mathbf{Z} \mathbf{X}^\top) \mathbf{X} - \mathcal{A}^* \mathcal{A} (\Delta) \mathbf{Z}, \mathbf{Z} \right\rangle. \quad (112)$$

Upon setting $\mathbf{X} = \mathbf{X}^\sharp$ and $\mathbf{Z} = \mathbf{X}^\perp$, we obtain

$$\nabla^2 f(\mathbf{X}^\sharp) [\mathbf{X}^\perp, \mathbf{X}^\perp] = \left\langle -\mathcal{A}^* \mathcal{A} (\Delta^\sharp) \mathbf{X}^\perp + \mathcal{A}^* \mathcal{A} (\mathbf{X}^\sharp \mathbf{X}^{\perp\top} + \mathbf{X}^\perp \mathbf{X}^{\sharp\top}) \mathbf{X}^\sharp, \mathbf{X}^\perp \right\rangle, \quad (113)$$

where $\Delta^\sharp = \mathbf{M}^* - \mathbf{X}^\sharp \mathbf{X}^{\sharp\top}$. To calculate the NSD component of the Hessian, $\nabla_-^2 f(\mathbf{X}^\sharp) [\mathbf{X}^\perp, \mathbf{X}^\perp]$, we construct two auxiliary ‘‘Hessians’’ $\nabla^2 F(\mathbf{X}^\sharp), \nabla^2 H(\mathbf{X}^\sharp)$ defined as

$$\begin{aligned} \nabla^2 F(\mathbf{X}^\sharp) [\mathbf{Z}, \mathbf{Z}] &= \left\langle (\mathbf{X}^\sharp \mathbf{Z}^\top + \mathbf{Z} \mathbf{X}^{\sharp\top}) \mathbf{X}^\sharp - \Delta^\sharp \mathbf{Z}, \mathbf{Z} \right\rangle \\ &= \frac{1}{2} \left\| \mathbf{X}^\sharp \mathbf{Z}^\top + \mathbf{Z} \mathbf{X}^{\sharp\top} \right\|_F^2 + \left\langle (\mathbf{X}^\sharp \mathbf{X}^{\sharp\top} - \mathbf{M}^*) \mathbf{Z}, \mathbf{Z} \right\rangle, \\ \nabla^2 H(\mathbf{X}^\sharp) [\mathbf{Z}, \mathbf{Z}] &= \frac{1}{2} \left\| \mathbf{X}^\sharp \mathbf{Z}^\top + \mathbf{Z} \mathbf{X}^{\sharp\top} \right\|_F^2 + \left\langle \mathbf{X}^\sharp \mathbf{X}^{\sharp\top} \mathbf{Z}, \mathbf{Z} \right\rangle. \end{aligned} \quad (114)$$

Here $\nabla^2 F(\mathbf{X}^\sharp)$ is the expected version of $\nabla^2 f(\mathbf{X}^\sharp)$ (after setting $\delta = 0$ in (δ, r) -RIP) and $\nabla^2 H(\mathbf{X}^\sharp)$ is the positive semi-definite part of $\nabla^2 F(\mathbf{X}^\sharp)$. Now, we are ready to control $-\nabla_-^2 f(\mathbf{X}^\sharp) [\mathbf{X}^\perp, \mathbf{X}^\perp]$. First, we have

$$\begin{aligned} -\nabla_-^2 f(\mathbf{X}^\sharp) [\mathbf{X}^\perp, \mathbf{X}^\perp] &\leq -\nabla_-^2 F(\mathbf{X}^\sharp) [\mathbf{X}^\perp, \mathbf{X}^\perp] + \left| \left(\nabla^2 f(\mathbf{X}^\sharp) - \nabla^2 F(\mathbf{X}^\sharp) \right) [\mathbf{X}^\perp, \mathbf{X}^\perp] \right| \\ &\leq -\nabla_-^2 F(\mathbf{X}^\sharp) [\mathbf{X}^\perp, \mathbf{X}^\perp] + \left\| \nabla^2 f(\mathbf{X}^\sharp) - \nabla^2 F(\mathbf{X}^\sharp) \right\| \left\| \mathbf{X}^\perp \right\|_F^2. \end{aligned} \quad (115)$$

To proceed, we control $\|\nabla^2 f(\mathbf{X}^\sharp) - \nabla^2 F(\mathbf{X}^\sharp)\|$. For any arbitrary \mathbf{Z} satisfying $\|\mathbf{Z}\|_F \leq 1$, we have

$$\begin{aligned}
& \left| \left(\nabla^2 f(\mathbf{X}^\sharp) - \nabla^2 F(\mathbf{X}^\sharp) \right) [\mathbf{Z}, \mathbf{Z}] \right| \\
&= \left| \left\langle (I - \mathcal{A}^* \mathcal{A}) (\Delta^\sharp) \mathbf{Z} + (\mathcal{A}^* \mathcal{A} - I) (\mathbf{X}^\sharp \mathbf{Z}^\top + \mathbf{Z} \mathbf{X}^{\sharp\top}) \mathbf{X}^\sharp, \mathbf{Z} \right\rangle \right| \\
&\leq \left\| (\mathcal{A}^* \mathcal{A} - I) (\Delta^\sharp) \right\| \|\mathbf{Z}\|_F^2 + \left\| (\mathcal{A}^* \mathcal{A} - I) (\mathbf{X}^\sharp \mathbf{Z}^\top + \mathbf{Z} \mathbf{X}^{\sharp\top}) \right\| \|\mathbf{X}^\sharp\|_F \|\mathbf{Z}\|_F \\
&\stackrel{(a)}{\leq} \sqrt{r} \delta \|\Delta^\sharp\| + \sqrt{r} \delta \|\mathbf{X}^\sharp \mathbf{Z}^\top + \mathbf{Z} \mathbf{X}^{\sharp\top}\| \cdot \sqrt{r} \|\mathbf{X}^\sharp\| \\
&\leq \sqrt{r} \delta \max \left\{ \sigma_1^*, \|\mathbf{X}^\sharp\|^2 \right\} + 2r \delta \|\mathbf{X}^\sharp\|^2 \\
&\stackrel{(b)}{\leq} 12r \sigma_1^* \delta,
\end{aligned} \tag{116}$$

where, in (a), we use $(\delta, 2r)$ -RIP, and in (b) we use the fact that $\|\mathbf{X}^\sharp\| \leq 2\sqrt{\sigma_1^*}$. Next, we control $-\nabla_-^2 F(\mathbf{X}^\sharp) [\mathbf{X}^\perp, \mathbf{X}^\perp]$. Evidently, we have $\nabla^2 H(\mathbf{X}^\sharp) \succeq \mathbf{0}$. This implies that

$$-\nabla_-^2 F(\mathbf{X}^\sharp) [\mathbf{X}^\perp, \mathbf{X}^\perp] \leq -\nabla_-^2 (F - H)(\mathbf{X}^\sharp) [\mathbf{X}^\perp, \mathbf{X}^\perp] = \langle \mathbf{M}^* \mathbf{X}^\perp, \mathbf{X}^\perp \rangle, \tag{117}$$

where the equality holds since $\nabla^2 (F - H)(\mathbf{X}^\sharp) [\mathbf{X}^\perp, \mathbf{X}^\perp] = -\langle \mathbf{M}^* \mathbf{X}^\perp, \mathbf{X}^\perp \rangle \leq 0$, which in turn implies that $\nabla^2 (F - H)(\mathbf{X}^\sharp) = \nabla_-^2 (F - H)(\mathbf{X}^\sharp)$. Furthermore, we have

$$\langle \mathbf{M}^* \mathbf{X}^\perp, \mathbf{X}^\perp \rangle \leq \|\mathbf{M}^* \mathbf{X}^\perp\|_F \|\mathbf{X}^\perp\|_F \leq \sigma_1^* \|\mathcal{P}_{\mathbf{V}^*} \mathcal{P}_{\mathbf{X}^\perp}\| \|\mathbf{X}^\perp\|_F^2 \leq 3\sigma_1^* \sqrt{r} \kappa \delta \|\mathbf{X}^\perp\|_F^2. \tag{118}$$

In the last inequality, we use the fact that $\|\mathcal{P}_{\mathbf{V}^*} \mathcal{P}_{\mathbf{X}^\perp}\| = \|\mathcal{P}_{\mathbf{V}^* \perp} \mathcal{P}_{\mathbf{X}^\sharp}\| \leq 4\sqrt{r} \kappa \delta$ since $\mathbf{X}^\sharp \in \mathcal{M}$. Combining the obtained bounds in Equation (118) and Equation (116) with Equation (115), we obtain

$$-\nabla_-^2 f(\mathbf{X}^\sharp) [\mathbf{X}^\perp, \mathbf{X}^\perp] \leq (3\sigma_1^* \sqrt{r} \kappa \delta + 12\sigma_1^* r \delta) \|\mathbf{X}^\perp\|_F^2 \leq 15\sigma_1^* r \kappa \delta \|\mathbf{X}^\perp\|_F^2. \tag{119}$$

Combining this inequality with Equation (111) yields $R(\tau) \leq 45\sigma_1^* \kappa r \delta$ with $\tau = \frac{1}{10} \sqrt{\frac{\sigma_1^*}{d}}$. \square

Establishing near-linear convergence of IPGD+

With all the conditions in place, we are now ready to establish the near-linear convergence of IPGD+ for the over-parameterized matrix sensing.

Theorem 31 *Suppose that \mathcal{A} satisfies $(\delta, 6r)$ -RIP with $\delta = O\left(\frac{1}{r^2 \kappa^5 (\log^4(1/\gamma) + \log^4(\sigma_1^* d/\chi))}\right)$.*

*Assume that the initial point is chosen as $\mathbf{X}_0 = \mathbf{0}_{n \times r'}$. Let $\bar{\epsilon} = O\left(\frac{\sigma_r^{*2}}{\sqrt{\sigma_1^*}}\right)$ and $T' = O\left(\kappa \log\left(\frac{\sigma_1^*}{\epsilon}\right)\right)$. Then, with probability at least $1 - \chi$, IPGD+ with any perturbation radius satisfying $\gamma = O\left(\min\left\{\frac{\epsilon}{r \kappa^3 \sigma_1^*}, \frac{\sqrt{\sigma_r^*}}{r^2 \kappa^{6.5}}\right\} \cdot \log^{-7}\left(\frac{\sigma_1^* d}{\chi \epsilon}\right)\right)$ and step-size $\eta = O\left(\frac{1}{\sigma_1^*}\right)$ outputs a solution \mathbf{X}_T satisfying*

$$\text{dist}(\mathbf{X}_T, \mathcal{X}^*) \leq \frac{\epsilon}{15\sigma_1^*}, \tag{120}$$

within $T = O\left(\frac{r \kappa^3}{\eta \sigma_r^} \left(\log^4\left(\frac{1}{\gamma}\right) + \log^4\left(\frac{\sigma_1^* d}{\chi}\right)\right) + \kappa \log\left(\frac{\sigma_1^*}{\epsilon}\right)\right)$ iterations.*

As an immediate consequence of the above theorem, for sufficiently small ϵ , upon setting the perturbation radius $\gamma = \tilde{O}\left(\frac{\epsilon}{r\kappa^3\sigma_1^*}\right)$ and stepsize $\eta = \Theta\left(\frac{1}{\sigma_1^*}\right)$, with probability at least $1 - \chi$, we have $\text{dist}(\mathbf{X}_T, \mathcal{X}^*) = O(\epsilon/\sigma_1^*)$ after $T = \tilde{O}(r\kappa^4 \log^4(1/\epsilon))$ iterations.

Proof of Theorem 31 The proof is an application of Theorem 8. Indeed, Propositions 23, 24, 28 and 30 hold under the conditions of Theorem 31. Specifically, we have

- $f(\mathbf{X})$ in (MS) is (L, \mathcal{M}, τ) -gradient-Lipschitz and $(\rho, \mathcal{M}, \tau)$ -Hessian-Lipschitz with parameters $L = 15\sigma_1^*$, $\rho = 15\sqrt{\sigma_1^*}$, and $\tau \leq \frac{1}{10}\sqrt{\frac{\sigma_1^*}{d}}$.
- $f(\mathbf{X})$ satisfies the gradient closure property (Assumption 3).
- \mathcal{M} satisfies $(\bar{\epsilon}_g, \bar{\epsilon}_H, \bar{\epsilon}_M)$ - \mathcal{M} -strict saddle property with parameters $\bar{\epsilon}_g = \frac{1}{160}\sigma_r^{*3/2}$, $\bar{\epsilon}_H = \frac{1}{5}\sigma_r^*$, $\bar{\epsilon}_M = \frac{1}{8}\sigma_r^{*1/2}$. Moreover, it satisfies (α, β, ζ) - \mathcal{M} -regularity property with parameters $\alpha = \frac{1}{2}\sigma_r^*$, $\beta = \frac{425}{64}\sigma_1^*$, $\zeta = \frac{1}{4}\sigma_r^{*1/2}$.
- The deviation rate satisfies $R(\tau) \leq 45\sigma_1^* r\kappa\delta$ for any $\tau \leq \frac{1}{10}\sqrt{\frac{\sigma_1^*}{d}}$.

We now specify the input parameters required for the IPGD+ algorithm.

- Due to our choice of the initial point and the definition of the implicit region in Equation (78), we have $\|\mathbf{X}_0^\perp\| = 0$. Moreover, due to RIP, we have $\Delta_f = f(\mathbf{X}_0) - f^* = \frac{1}{4}\|\mathcal{A}(\mathbf{M}^*)\|^2 \leq \frac{1+\delta}{4}\|\mathbf{M}^*\|_F^2 \leq \frac{r}{2}\sigma_1^{*2}$.
- The stepsize satisfies $\eta \leq \frac{1}{10 \max\{\alpha, \beta, L\}} = \frac{1}{150\sigma_1^*}$.
- the gradient threshold satisfies $\bar{\epsilon} = O\left(\min\left\{\bar{\epsilon}_g, \frac{\bar{\epsilon}_H^2}{\rho}\right\}\right) = O\left(\frac{\sigma_r^{*2}}{\sqrt{\sigma_1^*}}\right)$.
- The perturbation radius γ satisfies

$$\begin{aligned} \gamma &= O\left(\min\left\{\frac{\bar{\epsilon}^{3/2} \cdot \epsilon}{\sqrt{\rho}L\Delta_f} \cdot \log^{-7}\left(\frac{\rho d\Delta_f}{\chi\epsilon}\right), \frac{\bar{\epsilon}^{7/2}}{\rho^{3/2}\Delta_f^2} \cdot \log^{-7}\left(\frac{\rho d\Delta_f}{\chi\epsilon}\right)\right\}\right) \\ &= O\left(\min\left\{\frac{\epsilon}{r\kappa^3\sigma_1^*} \cdot \log^{-7}\left(\frac{\sigma_1^* d}{\chi\epsilon}\right), \frac{\sqrt{\sigma_r^*}}{r^2\kappa^{6.5}} \cdot \log^{-7}\left(\frac{\sigma_1^* d}{\chi\epsilon}\right)\right\}\right). \end{aligned} \quad (121)$$

- The iteration count T' satisfies

$$T' = O\left(\frac{1}{\eta\alpha} \log\left(\frac{L\zeta}{\epsilon}\right)\right) = O\left(\kappa \log\left(\frac{\sigma_1^* \sqrt{\sigma_r^*}}{\epsilon}\right)\right) = O\left(\kappa \log\left(\frac{\sigma_1^*}{\epsilon}\right)\right) \quad (122)$$

Under these settings, Theorem 8 guarantees that after

$$\begin{aligned} T &= O\left(\frac{\Delta_f}{\eta\bar{\epsilon}^2} \left(\log^4\left(\frac{1}{\gamma}\right) + \log^4\left(\frac{\rho d\Delta_f}{\chi\bar{\epsilon}}\right)\right) + \frac{1}{\eta\alpha} \log\left(\frac{L\zeta}{\epsilon}\right)\right) \\ &= O\left(\frac{r\kappa^3}{\eta\sigma_r^*} \left(\log^4\left(\frac{1}{\gamma}\right) + \log^4\left(\frac{\sigma_1^* d}{\chi}\right)\right) + \kappa \log\left(\frac{\sigma_1^*}{\epsilon}\right)\right) \end{aligned}$$

iterations, IPGD+ outputs a solution \mathbf{X}_T satisfying $\text{dist}(\mathbf{X}_T, \mathcal{X}_M) \leq \frac{\epsilon}{15\sigma_1^*}$. Here, we set $\delta = O\left(\frac{1}{r^2\kappa^5(\log^4(1/\gamma) + \log^4(\sigma_1^* d/\chi))}\right)$ to ensure that $R(\tau) = O(1/(\eta T))$, as required by Theorem 8. Moreover, since $\mathcal{X}_M = \mathcal{X}^*$ when $\delta \leq \frac{1}{10}$, it follows that $\text{dist}(\mathbf{X}_T, \mathcal{X}^*) \leq \frac{\epsilon}{15\sigma_1^*}$, which completes the proof. \square

Next, we present a few key observations based on Theorem 31.

Initialization

To apply IPGD+ to the over-parameterized matrix sensing problem, we initialize the algorithm at the origin. It is straightforward to verify that the origin is a strict saddle point of (MS). As a result, IPGD+ automatically applies a small random perturbation to the initial point, allowing the algorithm to escape this saddle point. This strategy is akin to the small random initialization used for GD in [6].

Iteration complexity

The convergence rate of IPGD+ toward the true rank- r solution scales as $O(\log^4(1/\epsilon))$. While this convergence rate is significantly better than that of general saddle-escaping methods such as PGD—which fail to converge to the true solution in the over-parameterized setting where $r' > r$ —it remains worse than the linear convergence rate of $O(\log(1/\epsilon))$ achieved by GD with small random initialization [6]. This suboptimality primarily arises because our algorithm is designed to handle the worst-case landscape, where it may encounter up to $O(\log^3(1/\epsilon))$ saddle points. In contrast, [60] shows that for over-parameterized matrix sensing, GD encounters at most r saddle points before reaching the true rank- r solution. We believe this insight can also be incorporated into the analysis of IPGD+ to further improve its convergence rate.

Sample complexity

Theorem 31 requires the linear operator \mathcal{A} to satisfy the $(\delta, 6r)$ -RIP with $\delta = \tilde{O}\left(\frac{1}{r^2\kappa^5}\right)$. When the entries of the measurement matrices are drawn independently from a standard Normal distribution, the sample complexity needed to ensure $\delta = \tilde{O}\left(\frac{1}{r^2\kappa^5}\right)$ is $\tilde{\Omega}(\kappa^{10}dr^5)$. This bound achieves optimal dependence on the ambient dimension d and, notably, is independent of the over-parameterized rank r' , which can be as large as d .

7 Numerical Verification Beyond Over-parameterized Matrix Sensing

In this section, we empirically examine the performance of our algorithm in over-parameterized models beyond the symmetric matrix sensing setting. Specifically, we focus on two problem classes: *low-rank matrix recovery* (in both symmetric and asymmetric forms) and *sparse recovery*. Our analysis centers on IPGD+, as we conjecture that all considered instances satisfy the \mathcal{M} -strict saddle property and \mathcal{M} -regularity conditions necessary for the improved convergence guarantees of IPGD+.

Low-rank matrix recovery

The objective in low-rank matrix recovery is to recover a ground-truth rank- r matrix \mathbf{M}^* under various observation models. One such example is the symmetric matrix sensing model (discussed in Section 6), where the observation operator satisfies the RIP. However, other examples of low-rank matrix recovery, such as matrix completion, may not satisfy RIP.

In our experiments, we consider both *symmetric* and *asymmetric* variants of this problem. In the symmetric low-rank matrix recovery, the ground truth $\mathbf{M}^* \in \mathbb{R}^{n \times n}$ is assumed to be symmetric and PSD. As mentioned in Section 1, it is common to model \mathbf{M}^* as $\mathbf{M}^* = \mathbf{X}\mathbf{X}^\top$ with $\mathbf{X} \in \mathbb{R}^{n \times r'}$ and $r' \geq r$, and directly optimize the lifted loss $f(\mathbf{X}) = L(\mathbf{X}\mathbf{X}^\top)$. For this family of problems, we take the implicit region as $\mathcal{M} = \{\mathbf{X} \in \mathbb{R}^{n \times r'} \mid \text{rank}(\mathbf{X}) \leq r\}$. We emphasize that this definition of \mathcal{M} is similar to that provided in Equation (78), with the key difference that the constraints $\|\mathcal{P}_{\mathbf{V}^* \perp} \mathcal{P}_{\mathbf{X}}\| \leq 4\sqrt{r}\kappa\delta$ and $\|\mathbf{X}\| \leq 2\sqrt{\sigma_1^*}$ are omitted. This simpler formulation of the implicit region is more broadly applicable across various low-rank matrix recovery problems and, notably, does not depend on the specific observation model used (such as the RIP). Even within the aforementioned matrix sensing setting, we have observed in practice that the omitted constraints do not become active. In other words, $\mathbf{X}_t^\sharp = \mathcal{P}_{\mathcal{M}}(\mathbf{X}_t)$ automatically satisfies $\|\mathcal{P}_{\mathbf{V}^* \perp} \mathcal{P}_{\mathbf{X}_t^\sharp}\| \leq 4\sqrt{r}\kappa\delta$ and $\|\mathbf{X}_t^\sharp\| \leq 2\sqrt{\sigma_1^*}$ for almost all iterations t .

In the asymmetric case, the target rank- r matrix $\mathbf{M}^* \in \mathbb{R}^{n_1 \times n_2}$ is assumed to be potentially indefinite and rectangular. In this setting, it is common to employ a two-factor model $\mathbf{M}^* = \mathbf{X}\mathbf{Y}^\top$, where $\mathbf{X} \in \mathbb{R}^{n_1 \times r'}$ and $\mathbf{Y} \in \mathbb{R}^{n_2 \times r'}$ with $r' \geq r$, and, as in the symmetric case, to directly optimize the lifted loss $f(\mathbf{X}, \mathbf{Y}) = L(\mathbf{X}\mathbf{Y}^\top)$. Correspondingly, the implicit region generalizes to $\mathcal{M} = \{(\mathbf{X}, \mathbf{Y}) \in \mathbb{R}^{n_1 \times r'} \times \mathbb{R}^{n_2 \times r'} \mid \text{rank}(\mathbf{X}) \leq r, \text{rank}(\mathbf{Y}) \leq r\}$. To promote balancedness in the obtained solution, it is also common to include an additional regularization term, $\|\mathbf{X}^\top \mathbf{X} - \mathbf{Y}^\top \mathbf{Y}\|_F^2$ [42, 61].

In addition to the matrix sensing, we consider the following observation models:

- *Matrix completion* [62, 63]: Here, the goal is to recover a rank- r matrix \mathbf{M}^* based on a limited number of observed entries. In the symmetric variant, the recovery is performed by minimizing the objective function

$$f(\mathbf{X}) = \sum_{(i,j) \in \Omega} ((\mathbf{X}\mathbf{X}^\top)_{i,j} - \mathbf{M}^*_{i,j})^2, \quad (123)$$

where $\Omega \subseteq [n] \times [n]$ denotes the set of observed indices. Given an observation probability $0 < p < 1$, we generate Ω randomly as a uniformly selected subset of $[n] \times [n]$ with $|\Omega| = np$. In all of our experiments, we set $p = 0.8$. For the asymmetric variant, we replace the symmetric factorization with the two-factor model and incorporate the balancing regularization term.

- *1-bit matrix completion* [64]: This is a generalization of the classical matrix completion problem, where we observe the entries of \mathbf{M}^* only through 1-bit (binary) measurements. Specifically, each measurement equals 1 with probability $\sigma(\mathbf{M}^*_{i,j})$ and 0 with probability $1 - \sigma(\mathbf{M}^*_{i,j})$, where $\sigma(x) = (1 + e^{-x})^{-1}$ is the logistic (sigmoid) function. Let α_{ij} denote the fraction of measurements for entry (i, j) that are observed as 1. The objective is to minimize

$$f(\mathbf{X}) = \sum_{i,j=1}^N \left(\log \left(1 + \exp \left([\mathbf{X}\mathbf{X}^\top]_{i,j} \right) \right) - \alpha_{ij} [\mathbf{X}\mathbf{X}^\top]_{i,j} \right), \quad (124)$$

In our experiments, we set α_{ij} to its population expectation, i.e., $\alpha_{ij} = \sigma(\mathbf{M}_{i,j}^*)$. For the asymmetric case, we replace the symmetric factorization with the two-factor model and include the balancing regularization, following the same approach as in the previous task.

In all of our experiments, we set $n_1 = n_2 = n = 20$, $r' = 20$ (corresponding to a fully over-parameterized setting), and $r = 3$. For the symmetric variants, the ground-truth matrix is constructed as $\mathbf{M}^* = \mathbf{U}^* \mathbf{\Sigma}^* \mathbf{U}^{*\top}$, where $\mathbf{U}^* \in \mathbb{R}^{n \times r}$ is a randomly generated orthogonal matrix, and $\mathbf{\Sigma}^* \in \mathbb{R}^{r \times r}$ is a diagonal matrix with diagonal entries 10, 5, and 1. Similarly, for the asymmetric variants, the ground-truth matrix is constructed as $\mathbf{M}^* = \mathbf{U}^* \mathbf{\Sigma}^* \mathbf{V}^{*\top}$, where $\mathbf{U}^* \in \mathbb{R}^{n_1 \times r}$ and $\mathbf{V}^* \in \mathbb{R}^{n_2 \times r}$ are randomly generated orthogonal matrices, and $\mathbf{\Sigma}^*$ is the same diagonal matrix as in the symmetric case. In all experiments, the initial points are initialized as all-zero matrices. The perturbation radius is set to $\gamma = 1 \times 10^{-15}$, and the gradient norm threshold is set to $G = 1 \times 10^{-7}$. We use $F = 1 \times 10^{-10}$ and $T_{\text{escape}} = 50$ in all settings. The step size is set to $\eta = 10^{-1}$ for matrix sensing and 1-bit matrix completion, and to $\eta = 2 \times 10^{-2}$ for matrix completion.

Figure 4 illustrates the behavior of IPGD+ (Algorithm 2) applied to the symmetric and asymmetric variants of matrix sensing, matrix completion, and 1-bit matrix completion. Our first key observation is that IPGD+ not only stays close to the defined implicit region \mathcal{M} —as evidenced by the consistently small residual norm—but also efficiently converges to a ground-truth solution in $\mathcal{X}_{\mathcal{M}}$. Notably, the final distance to $\mathcal{X}_{\mathcal{M}}$ precisely matches the residual norm across all instances considered. This phenomenon indicates that our signal-residual decomposition provides an accurate characterization of the IPGD+ trajectory. Moreover, a closer examination of Figure 4 reveals that the deviation rate $r(\cdot)$ (Definition 5) ultimately governs the final residual norm. Specifically, it suggests that a larger cumulative deviation rate, quantified as $\bar{r}_T = \sum_{t=0}^{T-1} r(\mathbf{x}_t)$, leads to a faster growth in the residual norm. This observation aligns with the bound established in Equation (13). Later in this section, we provide a more detailed analysis of the relationship between the cumulative deviation rate and the final residual norm.

Sparse recovery

In this problem, the goal is to recover a s -sparse vector $\boldsymbol{\theta}^* \in \mathbb{R}^d$ from a dataset $\{(\mathbf{x}_i, y_i)\}_{i=1}^N$, where $y_i = \langle \boldsymbol{\theta}^*, \mathbf{x}_i \rangle$. We model the ground-truth vector as a two-layer decomposition, $\boldsymbol{\theta}^* = \mathbf{u} \odot \mathbf{u} - \mathbf{v} \odot \mathbf{v}$, and minimize the objective function

$$f(\mathbf{u}, \mathbf{v}) = \sum_{i=1}^N (y_i - \langle \mathbf{u} \odot \mathbf{u} - \mathbf{v} \odot \mathbf{v}, \mathbf{x}_i \rangle)^2. \quad (125)$$

Notably, under the decomposition $\boldsymbol{\theta}^* = \mathbf{u} \odot \mathbf{u} - \mathbf{v} \odot \mathbf{v}$, the positive entries of $\boldsymbol{\theta}^*$ are represented solely by the first layer $\mathbf{u} \odot \mathbf{u}$, while the negative entries are captured only by the second layer $-\mathbf{v} \odot \mathbf{v}$. Based on this observation, we define the implicit region as $\mathcal{M} = \{(\mathbf{u}, \mathbf{v}) \mid \mathbf{u}_i = 0 \ \forall i \notin \mathcal{S}_+, \ \mathbf{v}_i = 0 \ \forall i \notin \mathcal{S}_-\}$, where $\mathcal{S}_+ = \{i \mid \boldsymbol{\theta}_i^* > 0\}$ and $\mathcal{S}_- = \{i \mid \boldsymbol{\theta}_i^* < 0\}$ collect the indices of the positive and negative entries of $\boldsymbol{\theta}^*$.

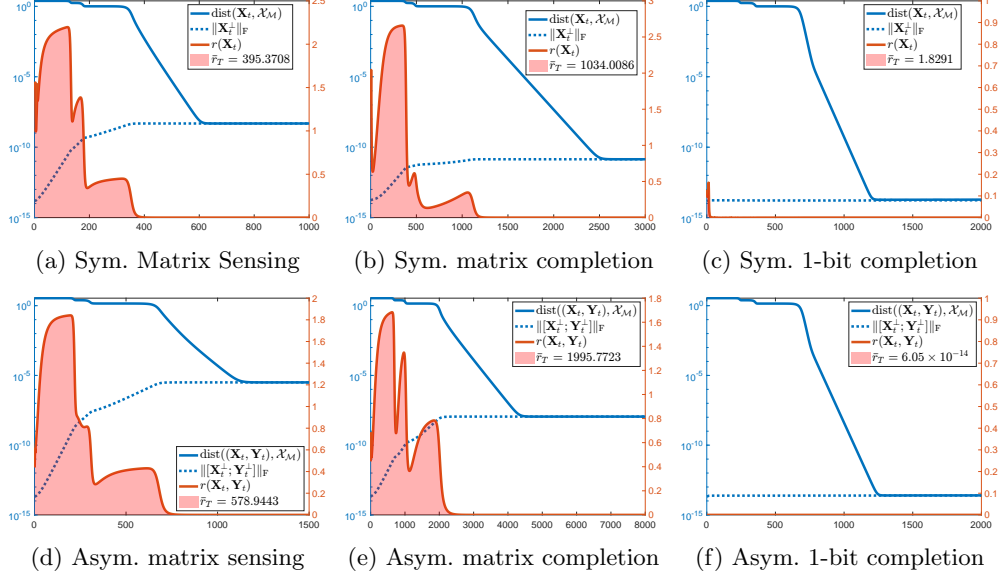


Fig. 4: Behavior of IPGD+ on low-rank matrix recovery. The deviation rate (denoted as $r(\cdot)$) and its cumulative counterpart (shown as \bar{r}_T) serve as strong indicators of whether IPGD+ converges to the ground truth. A large value of \bar{r}_T suggests that the residual norm grows significantly, indicating that IPGD+ is directing the iterations away from the implicit region \mathcal{M} . Conversely, a small value of \bar{r}_T implies that the residual norm remains small, thereby keeping the iterations close to the implicit region \mathcal{M} .

In our experiments, we set $d = 150$, $N = 300$, and $k = 5$. The ground-truth vector is set to an all-zero vector, except for its first five entries, which are set to 10, -5 , 3, -2 , and 1, respectively. The entries of $\{\mathbf{x}_i\}_{i=1}^N$ are independently drawn from a standard normal distribution. As in previous case studies, the initialization is set to an all-zero vector, with a perturbation radius of $\gamma = 1 \times 10^{-15}$. We set the step size to $\eta = 1 \times 10^{-2}$, the gradient norm threshold to $G = 1 \times 10^{-7}$, the escape time to $T_{\text{escape}} = 50$ and the termination threshold to $F = 1 \times 10^{-10}$.

Figure 5 shows the performance of IPGD+ on a sparse recovery instance. Similar to the low-rank matrix recovery, the final solution produced by IPGD+ lies in close proximity to the ground truth, with an error matching the residual norm. Notably, the observed cumulative deviation rate is larger compared to the instances of low-rank matrix recovery considered, leading to a rapid 10^5 -fold increase in the residual norm during the early iterations of the algorithm. Nonetheless, despite this steep rise, the final residual norm remains below 10^{-8} , coinciding with the final error of the recovered solution.

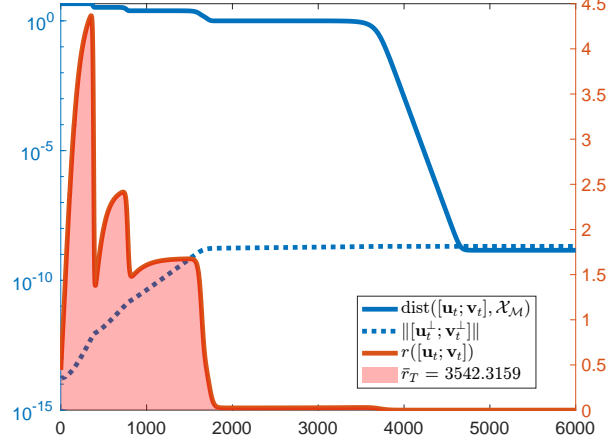


Fig. 5: Behavior of IPGD+ on sparse recovery. Despite the rapid growth of the residual norm during the early iterations of IPGD+, driven by the large cumulative deviation rate, the residual norm eventually stabilizes at approximately 10^{-9} , resulting in a final solution error of the same magnitude.

Effect of the deviation rate on the empirical growth of the residual norm

In our experiments, we observed that a faster growth rate of the residual norm is strongly correlated with a larger cumulative deviation rate. This observation is also supported by our analysis, and in particular by Equation (13), which yields

$$\log \left(\frac{\|\mathbf{x}_T^\perp\|}{\|\mathbf{x}_0^\perp\|} \right) \leq \frac{\eta}{2} \left(\sum_{t=0}^{T-1} r(\mathbf{x}_t) \right) + \frac{\eta\rho}{2} \left(\sum_{t=0}^{T-1} \|\mathbf{x}_t^\perp\| \right) = \frac{\eta}{2} \cdot \bar{r}_T + \frac{\eta\rho}{2} \left(\sum_{t=0}^{T-1} \|\mathbf{x}_t^\perp\| \right), \quad (126)$$

where \bar{r}_T denotes the cumulative deviation rate. We note that the above inequality provides only an upper bound on the growth rate of the residual norm. This naturally raises the follow-up question: how tight is this bound in practice? Figure 6 plots the values of $\log \left(\frac{\|\mathbf{x}_T^\perp\|}{\|\mathbf{x}_0^\perp\|} \right)$ against $\eta\bar{r}_T$ for different instances of low-rank matrix recovery and sparse recovery. Empirically, we observe that the cumulative deviation rate and the empirical growth rate of the residual norm follow the relationship

$$\log \left(\frac{\|\mathbf{x}_T^\perp\|}{\|\mathbf{x}_0^\perp\|} \right) \approx \frac{\eta}{3} \bar{r}_T, \quad (127)$$

indicating that Equation (126) is tight up to a factor of 1.5, modulo the additional term $\frac{\eta\rho}{2} \left(\sum_{t=0}^{T-1} \|\mathbf{x}_t^\perp\| \right)$, which remains negligible as $\|\mathbf{x}_t^\perp\|$ stays small throughout the iterations of IPGD+. This observation confirms that the deviation rate, identified in our theory as the primary driver of the residual norm growth, also manifests in practice, underscoring the sharpness of our theoretical analysis.

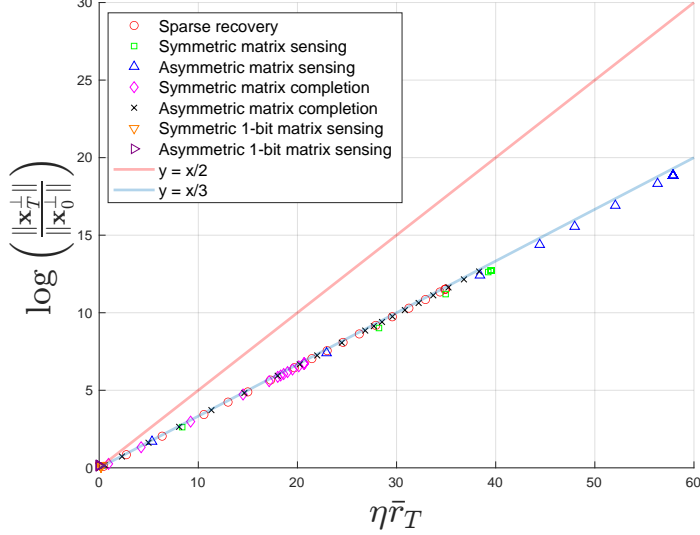


Fig. 6: Cumulative deviation rate vs. empirical growth of the residual norm.

We report the values of $\log\left(\frac{\|\mathbf{x}_T\|}{\|\mathbf{x}_0\|}\right)$ and $\eta \bar{r}_T$ across different values of T and for various objective functions. Specifically, for each experiment discussed above, we select 20 values of T uniformly spaced over the trajectory. The red line labeled $y = x/2$ represents the bound we derive from Equation (126). In practice, the values concentrate around the blue line representing $y = x/3$.

8 Conclusion and Future Directions

In this paper, we study the question of why gradient-based methods in over-parameterized models often yield low-dimensional solutions, even without explicit constraints or regularization. To provide a partial answer to this long-standing question, we study the conditions that enable implicit regularization by investigating when gradient-based methods converge to second-order stationary points (SOSPs) within an implicit low-dimensional region of a smooth and nonconvex function. We identify and formalize the key conditions under which such implicit regularization arises: namely, the combined ability to escape strict saddle points using infinitesimal perturbations and to remain close to an implicit low-dimensional region by controlling the deviation rate. Building on these insights, we introduce *infinitesimally perturbed gradient descent* (IPGD) algorithm and show that it can provably satisfy both conditions. We further study the application of IPGD in the context of over-parameterized matrix sensing. Our theoretical findings are further supported by extensive empirical results, suggesting that these principles extend more broadly across diverse over-parameterized learning settings.

We now discuss two future directions that we believe our proposed framework could potentially address.

Beyond gradient descent with infinitesimal perturbations

While this work focuses on GD with infinitesimal perturbations, a natural follow-up question is whether our framework extends to other widely used variants of GD, such as preconditioned [65–68], accelerated [28, 29], or stochastic gradient descent (SGD) [21]. Take SGD, for instance: unlike IPGD, the perturbations in SGD need not be small; however, they are also not isotropic, meaning they affect the signal and residual norms unevenly. In some cases, such anisotropic perturbations may be advantageous; for example, when they impact the residual norm much less than the signal norm. An intriguing open question is whether the proposed framework, based on the signal-residual decomposition and the deviation rate from the implicit region, can be generalized to encompass such settings. Developing a broader notion of deviation rate could enable direct, principled comparisons between algorithms.

Extension to nonsmooth optimization

One notable limitation of our current framework is its reliance on the gradient and Hessian Lipschitz properties of the objective function within a neighborhood of the implicit region, restricting its applicability to smooth problems. An enticing direction for future work is to explore whether our framework can be extended to nonsmooth settings by leveraging tools from variational analysis. Such an extension would significantly broaden the scope of our framework, encompassing important applications such as robust principal component analysis, robust matrix recovery, and neural networks with nonsmooth activation functions. We emphasize, however, that such an extension is far from trivial, as the challenge of escaping strict saddle points is substantially more delicate in nonsmooth settings. Notably, recent work has shown that even in exactly-parameterized problems, first-order methods such as the stochastic sub-gradient method [69] and proximal methods [18] can only escape *active* strict saddle points. This distinction introduces an additional layer of complexity for developing a theoretical understanding of implicit regularization in nonsmooth regimes.

Acknowledgements

The authors would like to thank Richard Y. Zhang for his thoughtful comments on the initial draft of this paper. This research is supported, in part, by NSF CAREER Award CCF-2337776, NSF Award DMS-2152776, and ONR Award N00014-22-1-2127.

References

- [1] Vaskevicius, T., Kanade, V., Rebeschini, P.: Implicit regularization for optimal sparse recovery. *Advances in Neural Information Processing Systems* **32** (2019)
- [2] Zhao, P., Yang, Y., He, Q.-C.: Implicit regularization via hadamard product over-parametrization in high-dimensional linear regression. *arXiv preprint arXiv:1903.09367* **2**(4), 8 (2019)

- [3] Ma, J., Fattahi, S.: Blessing of depth in linear regression: Deeper models have flatter landscape around the true solution. *Advances in Neural Information Processing Systems* **35**, 34334–34346 (2022)
- [4] Woodworth, B., Gunasekar, S., Lee, J.D., Moroshko, E., Savarese, P., Golan, I., Soudry, D., Srebro, N.: Kernel and rich regimes in overparametrized models. In: *Conference on Learning Theory*, pp. 3635–3673 (2020). PMLR
- [5] Li, Y., Ma, T., Zhang, H.: Algorithmic regularization in over-parameterized matrix sensing and neural networks with quadratic activations. In: *Conference On Learning Theory*, pp. 2–47 (2018). PMLR
- [6] Stöger, D., Soltanolkotabi, M.: Small random initialization is akin to spectral learning: Optimization and generalization guarantees for overparameterized low-rank matrix reconstruction. *Advances in Neural Information Processing Systems* **34**, 23831–23843 (2021)
- [7] Soltanolkotabi, M., Stöger, D., Xie, C.: Implicit balancing and regularization: Generalization and convergence guarantees for overparameterized asymmetric matrix sensing. In: *The Thirty Sixth Annual Conference on Learning Theory*, pp. 5140–5142 (2023). PMLR
- [8] Wang, X., Wu, C., Lee, J.D., Ma, T., Ge, R.: Beyond lazy training for over-parameterized tensor decomposition. *Advances in Neural Information Processing Systems* **33**, 21934–21944 (2020)
- [9] Tong, T., Ma, C., Prater-Bennette, A., Tripp, E., Chi, Y.: Scaling and scalability: Provable nonconvex low-rank tensor estimation from incomplete measurements. *Journal of Machine Learning Research* **23**(163), 1–77 (2022)
- [10] Belkin, M., Hsu, D., Ma, S., Mandal, S.: Reconciling modern machine-learning practice and the classical bias–variance trade-off. *Proceedings of the National Academy of Sciences* **116**(32), 15849–15854 (2019)
- [11] Yang, Z., Yu, Y., You, C., Steinhardt, J., Ma, Y.: Rethinking bias-variance trade-off for generalization of neural networks. In: *International Conference on Machine Learning*, pp. 10767–10777 (2020). PMLR
- [12] Arora, S., Cohen, N., Hazan, E.: On the optimization of deep networks: Implicit acceleration by overparameterization. In: *International Conference on Machine Learning*, pp. 244–253 (2018). PMLR
- [13] Huh, M., Mobahi, H., Zhang, R., Cheung, B., Agrawal, P., Isola, P.: The low-rank simplicity bias in deep networks. *arXiv preprint arXiv:2103.10427* (2021)
- [14] Neyshabur, B., Tomioka, R., Srebro, N.: In search of the real inductive bias: On the role of implicit regularization in deep learning. *arXiv preprint arXiv:1412.6614*

- (2014)
- [15] Neyshabur, B.: Implicit regularization in deep learning. arXiv preprint arXiv:1709.01953 (2017)
 - [16] Ma, J., Fattahi, S.: Global convergence of sub-gradient method for robust matrix recovery: Small initialization, noisy measurements, and over-parameterization. *Journal of Machine Learning Research* **24**(96), 1–84 (2023)
 - [17] Ma, J., Guo, L., Fattahi, S.: Behind the scenes of gradient descent: A trajectory analysis via basis function decomposition. *International Conference on Learning Representations* (2023)
 - [18] Davis, D., Drusvyatskiy, D.: Proximal methods avoid active strict saddles of weakly convex functions. *Foundations of Computational Mathematics* **22**(2), 561–606 (2022)
 - [19] Ge, R., Huang, F., Jin, C., Yuan, Y.: Escaping from saddle points—online stochastic gradient for tensor decomposition. In: *Conference on Learning Theory*, pp. 797–842 (2015). PMLR
 - [20] Jin, C., Ge, R., Netrapalli, P., Kakade, S.M., Jordan, M.I.: How to escape saddle points efficiently. In: *International Conference on Machine Learning*, pp. 1724–1732 (2017). PMLR
 - [21] Fang, C., Lin, Z., Zhang, T.: Sharp analysis for nonconvex sgd escaping from saddle points. In: *Conference on Learning Theory*, pp. 1192–1234 (2019). PMLR
 - [22] Shub, M.: *Global Stability of Dynamical Systems*. Springer, ??? (2013)
 - [23] Jin, C., Netrapalli, P., Ge, R., Kakade, S.M., Jordan, M.I.: On nonconvex optimization for machine learning: Gradients, stochasticity, and saddle points. *Journal of the ACM (JACM)* **68**(2), 1–29 (2021)
 - [24] Levy, K.Y.: The power of normalization: Faster evasion of saddle points. arXiv preprint arXiv:1611.04831 (2016)
 - [25] Du, S.S., Jin, C., Lee, J.D., Jordan, M.I., Singh, A., Poczos, B.: Gradient descent can take exponential time to escape saddle points. *Advances in neural information processing systems* **30** (2017)
 - [26] Nesterov, Y., Polyak, B.T.: Cubic regularization of newton method and its global performance. *Mathematical Programming* **108**(1), 177–205 (2006)
 - [27] Curtis, F.E., Robinson, D.P., Samadi, M.: A trust region algorithm with a worst-case iteration complexity of $\mathcal{O}(\epsilon^{-3/2})$ for nonconvex optimization. *Mathematical Programming* **162**(1), 1–32 (2017)

- [28] Carmon, Y., Duchi, J.C., Hinder, O., Sidford, A.: Accelerated methods for nonconvex optimization. *SIAM Journal on Optimization* **28**(2), 1751–1772 (2018)
- [29] Agarwal, N., Allen-Zhu, Z., Bullins, B., Hazan, E., Ma, T.: Finding approximate local minima faster than gradient descent. In: *Proceedings of the 49th Annual ACM SIGACT Symposium on Theory of Computing*, pp. 1195–1199 (2017)
- [30] Carmon, Y., Duchi, J.: Gradient descent finds the cubic-regularized nonconvex newton step. *SIAM Journal on Optimization* **29**(3), 2146–2178 (2019)
- [31] Lee, J.D., Panageas, I., Piliouras, G., Simchowitz, M., Jordan, M.I., Recht, B.: First-order methods almost always avoid strict saddle points. *Mathematical programming* **176**(1), 311–337 (2019)
- [32] Panageas, I., Piliouras, G., Wang, X.: First-order methods almost always avoid saddle points: The case of vanishing step-sizes. *Advances in Neural Information Processing Systems* **32** (2019)
- [33] Dixit, R., Gürbüzbalaban, M., Bajwa, W.U.: Exit time analysis for approximations of gradient descent trajectories around saddle points. *Information and Inference: A Journal of the IMA* **12**(2), 714–786 (2023)
- [34] Dixit, R., Gürbüzbalaban, M., Bajwa, W.U.: Boundary conditions for linear exit time gradient trajectories around saddle points: Analysis and algorithm. *IEEE Transactions on Information Theory* **69**(4), 2556–2602 (2022)
- [35] Jin, C., Netrapalli, P., Jordan, M.I.: Accelerated gradient descent escapes saddle points faster than gradient descent. In: *Conference On Learning Theory*, pp. 1042–1085 (2018). PMLR
- [36] Staib, M., Reddi, S., Kale, S., Kumar, S., Sra, S.: Escaping saddle points with adaptive gradient methods. In: *International Conference on Machine Learning*, pp. 5956–5965 (2019). PMLR
- [37] Gunasekar, S., Woodworth, B.E., Bhojanapalli, S., Neyshabur, B., Srebro, N.: Implicit regularization in matrix factorization. *Advances in neural information processing systems* **30** (2017)
- [38] Arora, S., Cohen, N., Hu, W., Luo, Y.: Implicit regularization in deep matrix factorization. *Advances in Neural Information Processing Systems* **32** (2019)
- [39] Li, Z., Wang, T., Lee, J.D., Arora, S.: Implicit bias of gradient descent on reparametrized models: On equivalence to mirror descent. *Advances in Neural Information Processing Systems* **35**, 34626–34640 (2022)
- [40] Soudry, D., Hoffer, E., Nacson, M.S., Gunasekar, S., Srebro, N.: The implicit bias of gradient descent on separable data. *Journal of Machine Learning Research*

- [41] Bhojanapalli, S., Neyshabur, B., Srebro, N.: Global optimality of local search for low rank matrix recovery. *Advances in Neural Information Processing Systems* **29** (2016)
- [42] Ge, R., Jin, C., Zheng, Y.: No spurious local minima in nonconvex low rank problems: A unified geometric analysis. In: *International Conference on Machine Learning*, pp. 1233–1242 (2017). PMLR
- [43] Sun, J., Qu, Q., Wright, J.: Complete dictionary recovery over the sphere i: Overview and the geometric picture. *IEEE Transactions on Information Theory* **63**(2), 853–884 (2016)
- [44] Sun, J., Qu, Q., Wright, J.: Complete dictionary recovery over the sphere ii: Recovery by riemannian trust-region method. *IEEE Transactions on Information Theory* **63**(2), 885–914 (2016)
- [45] Sun, J., Qu, Q., Wright, J.: A geometric analysis of phase retrieval. *Foundations of Computational Mathematics* **18**, 1131–1198 (2018)
- [46] Brutzkus, A., Globerson, A.: Globally optimal gradient descent for a convnet with gaussian inputs. In: *International Conference on Machine Learning*, pp. 605–614 (2017). PMLR
- [47] Du, S.S., Lee, J.D., Tian, Y.: When is a convolutional filter easy to learn? *arXiv preprint arXiv:1709.06129* (2017)
- [48] Soltanolkotabi, M., Javanmard, A., Lee, J.D.: Theoretical insights into the optimization landscape of over-parameterized shallow neural networks. *IEEE Transactions on Information Theory* **65**(2), 742–769 (2018)
- [49] Chi, Y., Lu, Y.M., Chen, Y.: Nonconvex optimization meets low-rank matrix factorization: An overview. *IEEE Transactions on Signal Processing* **67**(20), 5239–5269 (2019)
- [50] Zhang, R.Y.: Sharp global guarantees for nonconvex low-rank matrix recovery in the overparameterized regime. *arXiv preprint arXiv:2104.10790* (2021)
- [51] Zheng, Q., Lafferty, J.: Convergence analysis for rectangular matrix completion using burer-monteiro factorization and gradient descent. *arXiv preprint arXiv:1605.07051* (2016)
- [52] Nesterov, Y.: *Lectures on Convex Optimization* vol. 137. Springer, ??? (2018)
- [53] Ma, J., Fattahi, S.: Convergence of gradient descent with small initialization for unregularized matrix completion. In: *The Thirty Seventh Annual Conference on Learning Theory*, pp. 3683–3742 (2024). PMLR

- [54] Candes, E.J., Plan, Y.: Tight oracle inequalities for low-rank matrix recovery from a minimal number of noisy random measurements. *IEEE Transactions on Information Theory* **57**(4), 2342–2359 (2011)
- [55] Ma, J., Fattahi, S.: Can learning be explained by local optimality in low-rank matrix recovery? *arXiv preprint arXiv:2302.10963* (2023)
- [56] Rudin, W.: *Principles of Mathematical Analysis*, 3rd edn. McGraw-Hill, New York (1976)
- [57] Chen, Y., Chi, Y., Fan, J., Ma, C., *et al.*: Spectral methods for data science: A statistical perspective. *Foundations and Trends® in Machine Learning* **14**(5), 566–806 (2021)
- [58] Chen, Y.M., Chen, X.S., Li, W.: On perturbation bounds for orthogonal projections. *Numerical Algorithms* **73**(2), 433–444 (2016)
- [59] Tu, S., Boczar, R., Simchowitz, M., Soltanolkotabi, M., Recht, B.: Low-rank solutions of linear matrix equations via procrustes flow. In: *International Conference on Machine Learning*, pp. 964–973 (2016). PMLR
- [60] Jin, J., Li, Z., Lyu, K., Du, S.S., Lee, J.D.: Understanding incremental learning of gradient descent: A fine-grained analysis of matrix sensing. In: *International Conference on Machine Learning*, pp. 15200–15238 (2023). PMLR
- [61] Zhu, Z., Li, Q., Tang, G., Wakin, M.B.: The global optimization geometry of low-rank matrix optimization. *IEEE Transactions on Information Theory* **67**(2), 1308–1331 (2021)
- [62] Johnson, C.R.: Matrix completion problems. In: *Proceedings of Symposia in Applied Mathematics*, vol. 40, pp. 87–169 (1990)
- [63] Candes, E., Recht, B.: Exact matrix completion via convex optimization. *Communications of the ACM* **55**(6), 111–119 (2012)
- [64] Davenport, M.A., Plan, Y., Van Den Berg, E., Wootters, M.: 1-bit matrix completion. *Information and Inference: A Journal of the IMA* **3**(3), 189–223 (2014)
- [65] Zhang, J., Fattahi, S., Zhang, R.Y.: Preconditioned gradient descent for over-parameterized nonconvex matrix factorization. *Advances in Neural Information Processing Systems* **34**, 5985–5996 (2021)
- [66] Zhang, G., Fattahi, S., Zhang, R.Y.: Preconditioned gradient descent for over-parameterized nonconvex burer–monteiro factorization with global optimality certification. *Journal of Machine Learning Research* **24**(163), 1–55 (2023)
- [67] Tong, T., Ma, C., Chi, Y.: Accelerating ill-conditioned low-rank matrix estimation

- via scaled gradient descent. *The Journal of Machine Learning Research* **22**(1), 6639–6701 (2021)
- [68] Xu, X., Shen, Y., Chi, Y., Ma, C.: The power of preconditioning in overparameterized low-rank matrix sensing. *arXiv preprint arXiv:2302.01186* (2023)
- [69] Davis, D., Drusvyatskiy, D., Jiang, L.: Active manifolds, stratifications, and convergence to local minima in nonsmooth optimization. *Foundations of Computational Mathematics*, 1–83 (2025)